8-2014

Investigation of the Flow and Fate of Nitrate in Epikarst at the Savoy Experimental Watershed, Northwest Arkansas

Jozef Laincz
University of Arkansas, Fayetteville

Investigation of the Flow and Fate of Nitrate in Epikarst at the Savoy Experimental Watershed, Northwest Arkansas

Investigation of the Flow and Fate of Nitrate in Epikarst at the Savoy Experimental Watershed, Northwest Arkansas

A dissertation submitted in partial fulfillment
of the requirements for the degree of
Doctor of Philosophy in Environmental Dynamics

by

Jozef Laincz
Comenius University
Bachelor of Science in Geology, 2001
Comenius University
Magister in Mineralogy and Petrology, 2003

August 2014
University of Arkansas

This dissertation is approved for recommendation to the Graduate Council.

Dr. Phillip Hays
Dissertation Director

Dr. Stephen Boss
Committee Member

Dr. Kristofor Brye
Committee Member

Dr. Van Brahana
Committee Member

Dr. Thad Scott
Committee Member

ABSTRACT

Many karst aquifers are at high risk of nitrate (NO_3^-) contamination due to a combination of vulnerable geology characterized by thin soils and conduit flow, and excess inputs of nutrients from animal feeding operations. One zone that is present in many karst regions and could play an important role in NO_3^- attenuation due to properties such as increased residence time and matrix-water contact is the upper, weathered portion of karst, the epikarst. However, the understanding of this role is lacking, and the objective of this dissertation was to elucidate it. The fate of NO_3^- in the epikarst was traced along a hydrologic gradient using a multi-faceted geochemical approach based primarily on concentration and stable isotope composition of the reactants and products of denitrification. In addition, dye-tracing tests were conducted to assess the flow, solute transport and aquifer characteristics of the epikarst system. The study found multiple lines of evidence for denitrification which is spatially and temporally highly variable and can remove up to 33% of NO_3^- along the studied flowpaths. Dissolved organic carbon and dissolved oxygen appear to control denitrification levels, and both in turn appear to be controlled by hydrologic conditions (saturation). However, the most significant agent of NO_3^- attenuation is dilution, decreasing NO_3^- concentration by upwards of 50%. Transport of water and solutes in the epikarst can be relatively fast (up to 2.2 m/h) and involves preferential flowpaths. However, transport of a point-source solute located in the upper epikarst depends on saturation, and the transported mass is likely to be negligible in the short term (weeks-months) under the normal weather pattern. Overall, the results indicate that the epikarst can be an important buffer against potential groundwater contaminants.

ACKNOWLEDGEMENTS

I thank all who helped me complete this work. I especially thank my advisor, Dr. Phil Hays, and the members of my dissertation committee: Dr. Stephen Boss, Dr. Van Brahana, Dr. Kristofor Brye, and Dr. Thad Scott, for professional guidance, assistance, patience and accommodations throughout the years. I also thank Dr. Phil Hays and Dr. Van Brahana for their guidance in social and cultural matters.

TABLE OF CONTENTS

LIST OF FIGURES AND TABLES

1. INTRODUCTION

PROBLEM

High nitrate (NO_3^-) concentrations in water are detrimental to man and the environment alike. Intake of NO_3^- may result in formation of potentially carcinogenic compounds in the human gastric system (Tenovuo, 1986) as well as low oxygen levels in infant blood (methemoglobinemia), a potentially fatal condition and the reason the U.S. Environmental Protection Agency set the maximum contaminant level for NO_3^- in drinking water at 10 mg/L NO_3^--N (Fan and Steinberg, 1996). In aquatic ecosystems excess nitrate concentrations create ecological imbalances. For example, large amounts of NO_3^- discharging from agricultural watersheds have been implicated in the development of hypoxic zones around the world threatening marine biota (Rabalais and others, 1996; Goolsby and Battaglin, 2001).

The problem of groundwater NO_3^- contamination is most often associated with agricultural activity, and one type of landscape especially vulnerable to such contamination is karst (Power and Schepers, 1989; Boyer and Pasquarell, 1996). Here, the typically thin or missing soil cover, direct point-recharge via sinkholes, and rapid, concentrated flow in the conduit network with little microbial remediation and high rates of dispersion offer little protection of aquifers from contamination. A case in point is the area under study, the karst region of NW Arkansas, where intense animal production and associated nutrient generation exceeding the assimilative capacity of the local crop and pasture land (Gollehon and others, 2001) have been linked to elevated NO_3^- concentrations in local springs and wells (Steele and McCalister, 1990; Adamski, 1997; Davis, Brahana, and Johnston, 2000; Laubhan, 2007). Yet, karst aquifers are important sources of

drinking water; as much as one quarter of the world's population obtains its drinking water from karst aquifers (Ford and Williams, 2007).

Many karst systems are mantled by a layer known as regolith or epikarst, generally defined as the dissolutionally weathered, 3-15 m thick, upper portion of the carbonate bedrock (Ford and Williams, 2007). The U.S. karst map (Veni and others, 2001) indicates that more than 50% of U.S. karst is covered by the epikarst.

The epikarst hydrology is distinctly different from the bedrock beneath and could render epikarst conducive to significant microbial activity including denitrification, the most important NO_3^- attenuation process removing NO_3^- from watersheds in the form of gaseous nitrogen. For example, the epikarst has a tendency to detain and delay recharge (Bakalowicz, 1995; Einsiedl, 2005; Aquilina, Ladouche, and Dörfliger, 2006) which translates into increase in residence time, an important denitrification factor (Seitzinger and others, 2006; Green and others, 2009).

At the same time, the epikarst discharge has been found to constitute a significant part of the total discharge of springs or small catchments. During high flow conditions, this contribution can be in the range of 30-35% (Einsiedl, 2005; Perrin, Jeannin, and Zwahlen, 2003), but it can be as high as 55% (Lee and Krothe, 2001). The quality of waters discharging out of karst watersheds is therefore likely to a great degree dictated by biogeochemical processes taking place in the epikarst. This emphasizes the importance of understanding of biogeochemical functioning of the epikarst.

While various physical aspects of epikarst hydrology have been well established, the understanding of its biogeochemical functioning, including the processes of nitrate attenuation, is lacking. A number of studies on this topic have characterized karst systems where the epikarst

was present (Einsiedl, 2005; Lee and Krothe, 2001; Panno and others, 2001), but none focused solely on the epikarst itself.

The objective of this dissertation was to elucidate the biogeochemical functioning of the epikarst with respect to processes affecting NO_3^- and, more specifically, to identify denitrification, its spatial or temporal variation, and any controlling factors. Once NO_3^- dynamics are elucidated, future research can test the impact of concrete nutrient management practices and livestock grazing patterns to determine the conditions of maximum biogeochemical attenuation of NO_3^-. Such findings may ultimately serve to improve the design of nutrient management practices in Northwest Arkansas as well as other regions in the South-Central and Southeast United States where intense animal production occurs in vulnerable karst.

APPROACH

The objective was addressed by conducting a multi-faceted geochemical characterization of the fate of NO_3^- along the hydrologic gradient of an epikarst site located at the Savoy Experimental Watershed, Northwest Arkansas. The methodology primarily involved measuring concentration and stable isotope composition of the reactants and products of the denitrification reaction and their variation across time (seasons) and space (at different points along multiple flowpaths). In addition, as an essential, complementary part of such characterization, dye-tracing experiments were conducted to assess the flow, solute transport and aquifer characteristics of the studied epikarst system, including flow trajectories, travel/residence time, mode of flow, peak concentrations, recovery load, and overall permeability of the epikarst to a dissolved contaminant.

ORGANIZATION

Chapter 1 defined the problem, objective, and approach of this dissertation. Chapter 2 provides an overview of the key concepts that this work builds on, including hydrogeology of karst, nitrogen cycle, denitrification detections methods, principles of dye tracing in hydrologic applications, and relevant up-to-date research conducted at the study site. Chapter 3 describes the initial geochemical study of NO_3^- processing in the interflow zone (epikarst) with an emphasis on NO_3^- concentration, NO_3^- stable isotopes and dissolved organic carbon bioavailability, and variation with seasonality and type of flow (diffuse vs. focused flow). Chapter 4 focuses on physical hydrology of the epikarst; it discusses the results of dye-tracing experiments and their implications for the conceptual model of water and solute (contaminant) transport. Finally, chapter 5 presents the findings of the second geochemical study which traced denitrification through all of the reactants and products participating in the reaction, including the key indicator of denitrification, dissolved N_2.

REFERENCES

Adamski, J., 1997, Nutrients and Pesticides in Ground Water of the Ozark Plateaus in Arkansas, Kansas, Missouri, and Oklahoma: 96-4313

Aquilina, L., Ladouche, B., and Dörfliger, N., 2006, Water storage and transfer in the epikarst of karstic systems during high flow periods: Journal of Hydrology, v. 327, no. 3-4, p. 472-485.

Bakalowicz, M., 1995, La zone d'infiltration des aquifères karstiques. Méthodes d'étude: Structure et fonctionnement.Hydrogéologie, v. 4, p. 3-21.

Boyer, D.G., and Pasquarell, G.C., 1996, Agricultural land use effects on nitrate concentrations in a mature karst aquifer: Journal of the American Water Resources Association, v. 32, no. 3, p. 565-573.

Davis, R.K., Brahana, J.V., and Johnston, J.S., 2000, Groundwater in Northwest Arkansas: Minimizing Nutrient Contamination From Non-Point Sources in Karst Terrane. MSC-288, 69 p.

Einsiedl, F., 2005, Flow system dynamics and water storage of a fissured-porous karst aquifer characterized by artificial and environmental tracers: Journal of Hydrology, v. 312, no. 1, p. 312-321.

Fan, A.M., and Steinberg, V.E., 1996, Health Implications of Nitrate and Nitrite in Drinking Water: An Update on Methemoglobinemia Occurrence and Reproductive and Developmental Toxicity: Regulatory Toxicology and Pharmacology, v. 23, no. 1, p. 35-43.

Ford, D.C., and Williams, P.W., 2007, Karst hydrogeology and geomorphology: Chichester, England, John Wiley & Sons, 576 p.

Gollehon, N., Caswell, M., Ribaudo, M., Kellogg, R., Lander, C., and Letson, D., 2001, Confined Animal Production and Manure Nutrients: USDA Agriculture Information Bulletin, no. AIB771, p. 1-40.

Goolsby, D.A., and Battaglin, W.A., 2001, Long-term changes in concentrations and flux of nitrogen in the Mississippi River Basin, USA: Hydrological Processes, v. 15, no. 7, p. 1209-1226.

Green, M.B., Wollheim, W.M., Basu, N.B., Gettel, G., Rao, P.S., Morse, N., and Stewart, R., 2009, Effective denitrification scales predictably with water residence time across diverse systems: Nature Precedings, accessed June 15, 2013, *http://precedings.nature.com/documents/3520/version/1/html*.

Laubhan, A.C., 2007, A hydrogeologic and water-quality evaluation of the Springfield aquifer in the vicinity of North-Central Washington County, Arkansas: Fayetteville, University of Arkansas, M.S. Thesis, 182 p.

Lee, E.S., and Krothe, N.C., 2001, A four-component mixing model for water in a karst terrain in south-central Indiana, USA. Using solute concentration and stable isotopes as tracers: Chemical Geology, v. 179, no. 1, p. 129-143.

Panno, S.V., Hackley, K.C., Hwang, H.H., and Kelly, W.R., 2001, Determination of the sources of nitrate contamination in karst springs using isotopic and chemical indicators: Chemical Geology, v. 179, no. 1-4, p. 113-128.

Perrin, J., Jeannin, P., and Zwahlen, F., 2003, Epikarst storage in a karst aquifer: a conceptual model based on isotopic data, Milandre test site, Switzerland: Journal of Hydrology, v. 279, no. 1, p. 106-124.

Power, J., and Schepers, J., 1989, Nitrate contamination of groundwater in North America: Agriculture, Ecosystems & Environment, v. 26, no. 3, p. 165-187.

Rabalais, N.N., Turner, R.E., Justic, D., Dortch, Q., Wiseman, W.J., and Sen Gupta, B.K., 1996, Nutrient changes in the Mississippi River and System Responses on the Adjacent Continental Shelf: Estuaries and Coasts, v. 19, no. 2, p. 386-407.

Seitzinger, S., Harrison, J.A., Bohlke, J.K., Bouwman, A.F., Lowrance, R., Peterson, B., Tobias, C., and Van Drecht, G., 2006, Denitrification across landscapes and waterscapes: a synthesis. Ecological Applications, v. 16, no. 6, p. 2064-2090.

Steele, K.F., and McCalister, W.K., 1990, Nitrate concentrations of ground water from limestone and dolomitic aquifers in the Northeastern Washington County area, Arkansas: MSC-68

Tenovuo, J., 1986, The biochemistry of nitrates, nitrites, nitrosamines and other potential carcinogens in human saliva: Journal of oral pathology, v. 15, no. 6, p. 303-307.

Veni, G., DuChene, H., Crawford, N.C., Groves, C.G., Huppert, G.H., Kastning, E.H., Olson, R., and Wheeler, B.J., 2001, Living with Karst: A Fragile Foundation (Environmental Awareness Series ed.), American Geological Institute, 64 p.

2. OVERVIEW OF RELEVANT CONCEPTS

HYDROGEOLOGY OF KARST

The following section describes the main aspects of karst hydrogeology. It is, for the most part, an adaptation of text written by Mull et al. (1988) and White (1988). More complete discussion of the various aspects of karst hydrogeology can be found in these works.

The term karst, derived from Kras – the geographical name of the limestone region northeast of Trieste Bay (Gams, 1993), describes terrains with characteristic hydrology and landforms. The majority of karst terrains are underlain by limestone or dolomite, with the rest being underlain by gypsum, halite, or other relatively soluble rocks. Karst topography is in essence formed by the removal of rock by processes of dissolution. The rock dissolution and a few other geological processes operating through time create characteristic topographic and geologic features, including sinkholes; karst windows; springs; caves; and losing, sinking, gaining, and underground streams. In certain karst terrains, some of these features may dominate. The hydrology of karst aquifers is also unique and markedly different from that of granular or fractured-rock aquifers due to the size, abundance, integration, and heterogeneous character of fissures, pores, channels, conduits and other solutionally enlarged openings typical of karst aquifers.

Davies and LeGrand (1972) estimate that about 15% of the surface or near-the-land-surface geology of conterminous United States consists of limestone, gypsum, or other soluble rock. Karst terrains are especially well develop in these areas (Figure 2-1): (1) Tertiary Coastal Plain of Georgia and Florida, (2) Paleozoic belt of the Appalachian Mountains

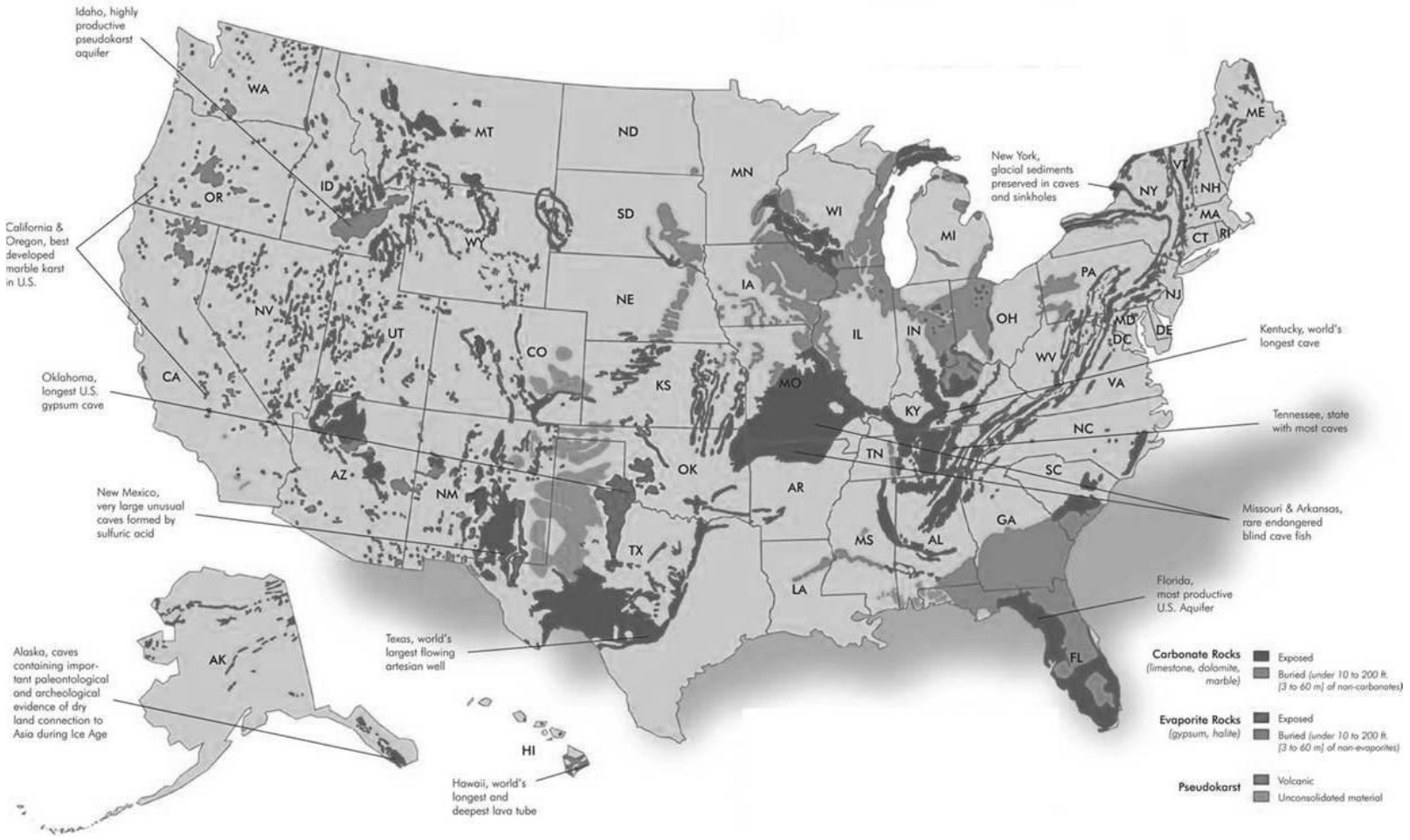

Figure 2-1 Karst map of the USA (from Veni et al., 2001)

stretching from Pennsylvania to Alabama, (3) nearly flat-lying Paleozoic rocks of Alabama, Tennessee, Kentucky, Ohio, Indiana, Illinois, Wisconsin, Minnesota, Arkansas and Missouri, (4) nearly flat-lying Cretaceous carbonate rocks in Texas, (5) nearly flat-lying Permian rocks of New Mexico, and (6) the Paleozoic belt of folded rocks in South Dakota, Wyoming, and Montana (LeGrand, Stringfield, and LaMoreaux, 1976). The subsurface of the Coastal Plain in Alabama and South Carolina for the most part is a karst aquifer, although one exhibiting a minimum of the typical surface karst features.

In order for a groundwater basin to develop in carbonate rocks, the terrain must have (1) an area of intake or recharge, (2) a system of interconnected conduits that transmit water, (3) a discharge point, (4) rainfall, and (5) relief. In case one of these elements is missing, the rock mass will be hydrologically inert, and most likely it cannot function as a groundwater basin.

Groundwater recharge occurs as infiltration through unconsolidated material atop the bedrock or as direct inflow from sinking streams and open swallets. Recharge waters move vertically until they encounter relatively horizontal conduits enlarged by dissolution.

Karst springs are the principal discharge points of the groundwater basin. A karst spring may occur at local or regional base levels or at a point where the land surface intersects the water table or water-bearing cavities. Underlying impervious bedrock can cause springs at the interface of the karst aquifer and the bedrock. Springs can occur either in valley bottoms or at sharp breaks in slope. Karst springs may occur at any point where impermeable rock and faults or other structural features impede groundwater flow and thus restrict the formation or continuity of conduits in the soluble bedrock. Karst springs can occur high, along valley sides, without obvious topographic or geologic cause. This may be caused by rapid down cutting of the main

valley which has exceeded the downward development of solutionally enlarged openings sufficient to lower the karst spring outlets to the local base level (Jennings, 1985).

Adequate rainfall is essential for the solution of limestone to occur. Karst development tends to be absent if precipitation totals less than 10-12 inches per year. Maximum karstification occurs in regions that experience heavy precipitation and regions characterized by seasons of heavy precipitation and drought (Sweeting, 1973).

Most of the karst areas are underlain by carbonate rocks that have varying amounts of fractures. Fractures offer an initiation point for dissolution by migrating water and are typically enlarged by solution where they are in the zone of groundwater circulation. The enlargement of the fractures is controlled, in part, by geologic structure and lithology. These solutionally enlarged fractures present a unique problem for water managers in karst watersheds because of the velocity of groundwater flow and the likelihood that relatively little attenuation of potential contamination occurs while water transits through the karst aquifers. Groundwater velocities in conduits can be as high as 7,500 ft/hr where the potentiometric gradient reaches the steepness of 1:4 (Ford, 1967). Under typical groundwater gradients of 0.5 to 100 ft/mi, velocities within the same conduit range from 30 ft/hr during base flow to 1,300 ft/hr during flood flow (Quinlan and others, 1983). Under such conditions, contaminants can impact water quality further than 10 miles away in just one week during base flow (Vandike, 1982) and much sooner under flood flow conditions.

Where fractures within a bedrock aquifer are well developed and groundwater flow converges to major springs via a well-developed network of conduits, the aquifer is considered mature. In general, mature carbonate aquifers are found beneath mature karst terrain, in which well-developed sinkholes collect and drain surface runoff directly into the subsurface conduit

system. Streams can also drain to the subsurface through a swallet in the stream bed or they can disappear into a swallet at the end of a valley.

In mature karst terrains, springs in a given area tend to have similar flow and water-quality parameters. Spring discharge is generally flashy, responding rapidly to rainfall. Flow is most often turbulent and turbidity, discharge, and temperature are highly variable. Hardness is usually low but also highly variable. Springs that have these characteristics are the outlets for conduit-flow systems (Shuster and White, 1972) that generally drain a discrete groundwater basin. Flow in a conduit system is similar to flow in a surface stream in that both are convergent through a system of tributaries and both receive diffuse (non-concentrated) flow through the adjacent bedrock or sediment.

If the karst aquifer is less mature, water moves through small bedrock openings with only limited solutional enlargement. Flow velocities are low and travel time through a few tens of feet of carbonate bedrock may be on the order of months (Friederich, 1981; Friederich and Smart, 1981). Discharge from springs fed by such slow-moving water in less mature karst is non-flashy, responds slowly to storms, and is relatively uniform. Flow tends to be laminar, turbidity is very low, and water temperature closely approximates the mean annual surface-water temperature. These characteristics are typically associated with groundwater outlets from diffuse-flow systems (Shuster and White, 1972).

Quinlan and Ewers (1985) proposed that the majority of groundwater movement in a diffuse-flow (i.e. less mature karst) system is also conducted through a tributary network of conduits. Truly diffuse flow is only encountered in the headwaters of a groundwater basin and the area adjacent to a conduit. Inspections in quarries and caves indicate that microscopically small solutional enlargements of bedding planes and joints act as tributary conduits (Quinlan and

Ewers, 1985). The authors also described conduit and diffuse flow in carbonate aquifers as end members of a flow continuum. While most carbonate aquifers are characterized by both types of flow (Atkinson, 1977), one type of flow usually dominates. Flow in massive karst aquifers tends to be either predominantly diffuse or predominantly conduit; which one it is depends on the degree of karstic solutional development (Smart and Hobbs, 1986).

Karst features

The most direct and obvious evidence of karstification is the presence of landforms characteristic of karst regions. Karst landforms are generally the direct result of dissolution of soluble carbonate bedrock and form in areas that have vertical and horizontal underground drainage. Although certain karst landforms, such as sinkholes, may develop within a relatively thick layer of unconsolidated regolith on top of the bedrock, the development of these landforms is ultimately controlled by the presence of solutionally enlarged openings in the bedrock. The most common karst features include sinkholes; karst windows; regolith (epikarst); caves; springs; and losing, gaining, sinking, and underground streams. A detailed description of various karst features can be found in White (1988), Jennings (1985), Milanovic (1981), and Sweeting (1973).

Occurrence and movement of groundwater

Groundwater flow in karst terrain occurs both in the upper, unconsolidated sediment layer and in the bedrock, which often constitute a complex, interconnected hydrologic system. The nature of groundwater movement in karst terrain is characterized by considerable spatial variability. In general, two types of flow are encountered: diffuse flow (slow, laminar) and conduit flow (rapid, turbulent). The majority of groundwater flow in a mature karst aquifer is conduit flow, which predominantly occurs in secondary openings and can be described by pipe

and channel flow equations (Gale, 1984). Diffuse flow occurs mostly in primary openings, and it can be described by equations for Darcian flow. Components of groundwater flow in a mature karst aquifer are shown in the generalized block diagram (Gunn, 1986), Figure 2-2.

Groundwater in the unconsolidated surficial material overlying bedrock is generally thought to occur in intergranular (primary) openings and thus tend to be diffuse, behaving according to the theories of groundwater movement in porous media. Although this is generally true, evidence indicates that concentrated flow also occurs in enlarged openings (macropores) in the unconsolidated material (Beven and Germann, 1982). Quinlan and Aley (1987) stated that concentrated flow in macropores (root channels, fissures, animal burrows, and textural transitions) is commonly several orders of magnitude more rapid than in the adjacent unconsolidated sediment.

The occurrence and movement of groundwater in the bedrock of karst terrain differs from that in the bedrock underlying non-karst terrain, chiefly due to the karst bedrock containing conduits that permit relatively rapid, focused transmission of groundwater. The two most common types of rock in karst terrains are limestone and dolomite. These rocks may be relatively impervious except for situations where fractures and bedding planes have been enlarged by groundwater circulation. The circulating water dissolves the carbonate bedrock and enlarges the openings. The enlarged openings may be vertical or horizontal, ranging in size from millimeters to several meters. Water that constitutes conduit flow can enter the subsurface through discrete points of recharge, including sinking streams and sinkholes.

Groundwater in karst terrain, as in all other environments, moves in response to hydraulic gradients from points of recharge to points of discharge following the path of least resistance. The horizontal gradient of the groundwater table, the general shape of the groundwater table, and

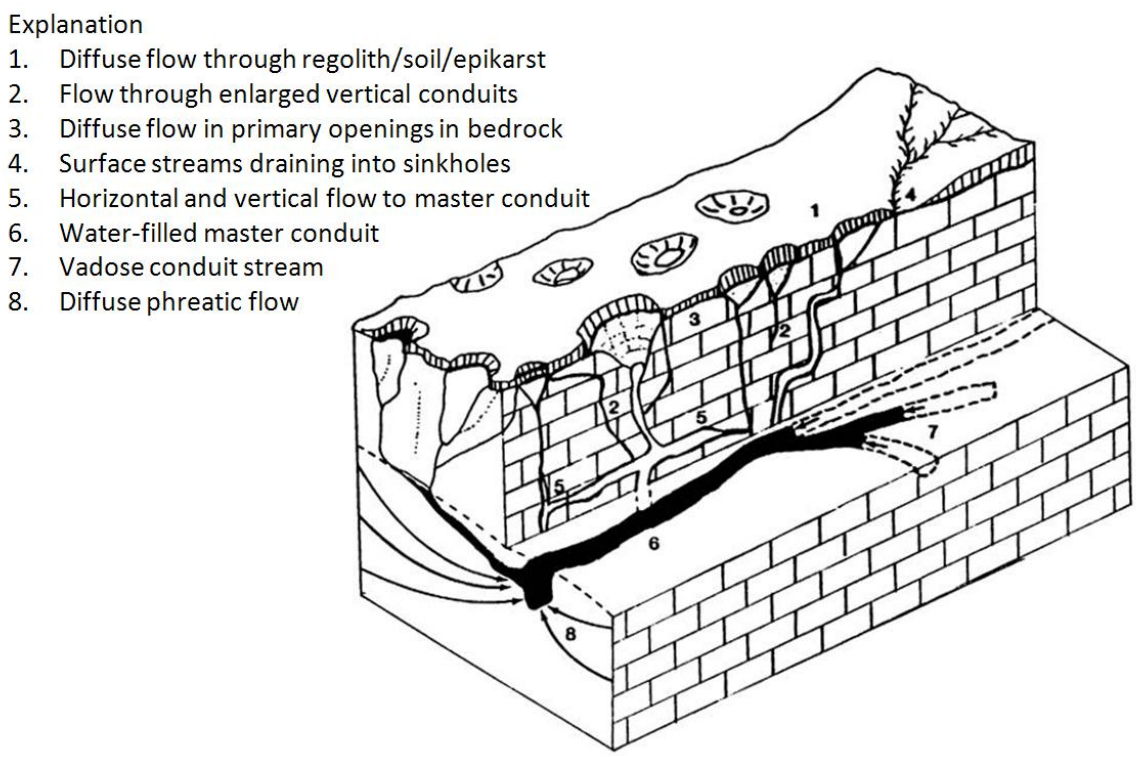

Figure 2-2 Components of groundwater flow in karst (modified from Gunn, 1986)

the direction of movement can be determined from a water-level contour or potentiometric map. The contours are based on the altitude of the water level as measured in wells, springs, and streams. The general direction of groundwater movement can be estimated by drawing flow lines perpendicular to the water-level contours. The direction of groundwater movement determined from a water-level contour map can be confirmed by dye tracing. Dye tracing can also be used to estimate velocity or the rate of groundwater movement, which in karst typically varies both in space and with changing hydrologic conditions.

Vulnerability of karst aquifers to contamination

Groundwater in karst terrain can be highly vulnerable to contamination. This vulnerability depends on multiple factors including the nature (persistence) of the contaminant, present karst features, degree of karst development or maturity, occurrence of groundwater in karst terrain, the

predominant type of flow, the degree of contact of infiltrating water with the soil zone, and the opportunity for transported pollutants to enter the deeper aquifer system.

Dissolved contaminants in aquifers dominated by conduit-flow can be readily transported under all flow conditions. Examples of dissolved contaminants include various industrial organic compounds, herbicides, nutrients, and trace metals.

Contaminants that are associated with suspended material generally require more energy (corresponding with high velocities and turbulence) for transport. The energy required for transport depends on the size, shape, and density of suspended particles. Chemical contaminants may include sediment with attached insecticides, nutrients, and heavy metals. In diffuse-flow conditions, contaminants bound to suspended material can be mechanically filtered out by the small pore openings in the aquifer matrix. In contrast, in the large, well-developed solutional openings with focused flow, contaminants bound to even relatively large-size sediment or other particulate material can be readily transported. Contaminants may enter this type of system from a sinkhole or a sinking stream, rapidly move through the network of conduits, and exit at a spring or well.

Biological contaminants such as viruses, bacteria, other microorganisms, and also some larger organisms, may be readily transported in karst aquifers in a manner similar to the transport of chemical contaminants (Ting, 2005). The biological contaminants may be transported freely or bound to other suspended matter. The transport of larger organisms and aggregates of organisms with suspended particles requires large openings and high flow velocities similar to those that are typical of groundwater movement in karst terrains.

Almost all of recharge into a groundwater flow system percolates through the soil zone. The soil zone can substantially improve the quality of percolating water by filtration, various

physical and chemical processes (dissolution, precipitation, oxidation-reduction reactions, ion exchange, adsorption and desorption, etc.), and biogeochemical transformations such as denitrification.

In karst settings, however, infiltrating water may have minimal or no contact with the soil zone, and contaminant attenuation is therefore minimal. The water recharge relatively quickly enters the subsurface drainage system of solutionally enlarged openings situated below the soil zone or sinkholes. These enlarged openings serve as avenues for rapid introduction of contaminants to groundwater. In karst aquifers, groundwater moves primarily through open conduits and, as a result, it typically moves much faster than it does in other aquifers; velocities may be on the order of kilometers per day. Therefore, any surface contaminant that enters the groundwater system, such as one carried by surface runoff, can be rapidly transported and spread through the system.

Compounding the problem of karst vulnerability, many karst areas are home to intensive animal production which generates large volumes of manure rich in potential groundwater contaminants, organic N compounds (NO_3^- precursors) (Figure 2-3). These areas often do not have sufficient crop and pasture land to assimilate the N generated (Gollehon and others, 2001).The large volumes of manures are typically applied to pastures with extremely thin soils that have a limited nutrient bioremediation capacity, creating potential for leaching of contaminants to groundwater.

Epikarst structure and hydrology

The epikarst, also referred to as the epikarstic zone or subcutaneous zone, is generally defined as the near-surface, dissolutionally weathered portion of the bedrock in carbonate terrains. The epikarst is located at the top of the vadose zone, immediately beneath the soil, or

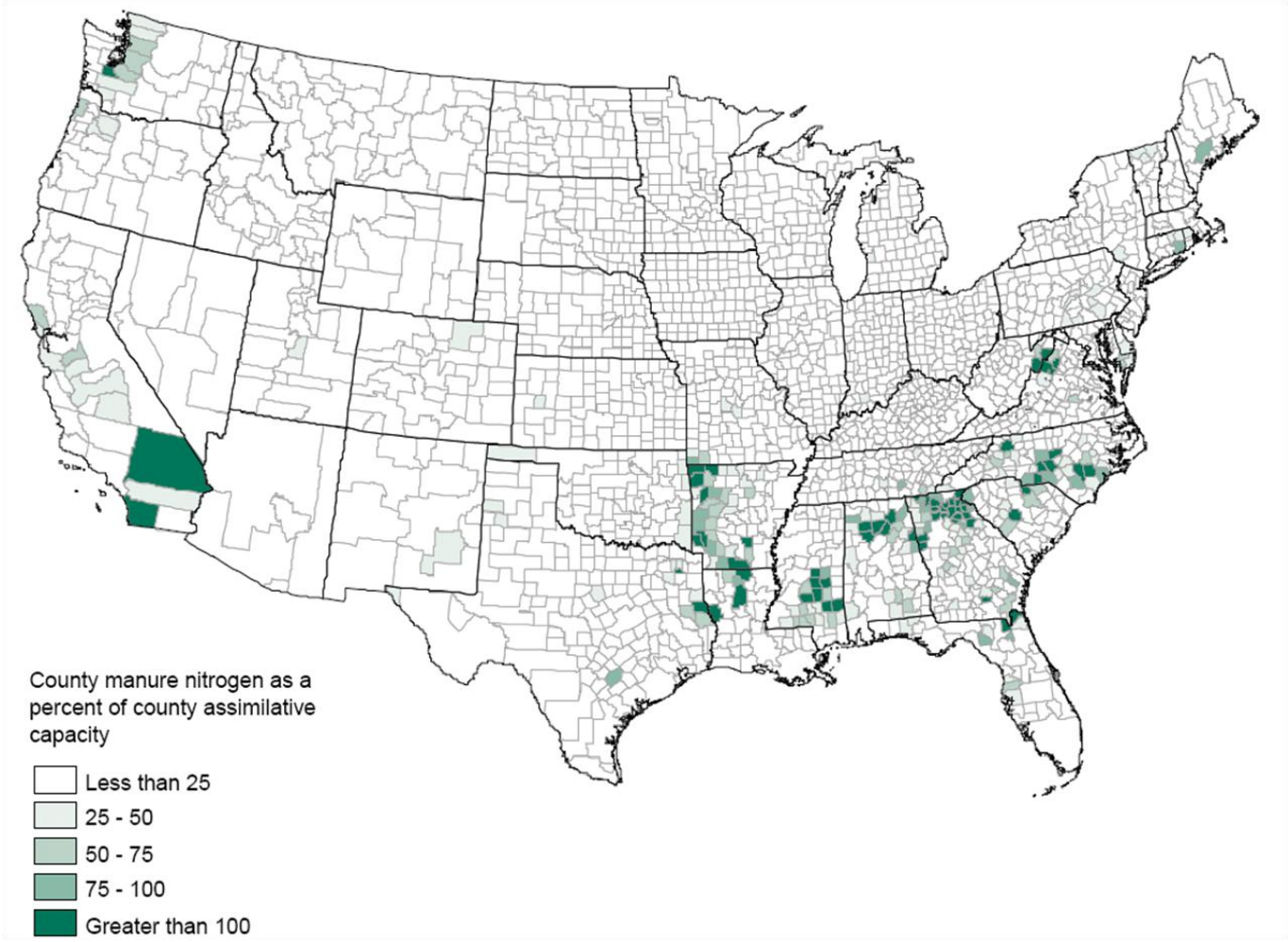

Figure 2-3 Excess manure nitrogen as a share of county assimilative capacity, 1997 (from Gollehon et al., 2001)

exposed at the surface. Epikarst thickness is typically 3-10 meters but can be more than 30 meters (Ford and Williams, 2007). The intensity of epikarstic development, indicated by the percentage of bedrock removed by dissolution, varies from 1 to >50% and routinely decreases with increasing depth below the surface (Aley, 1997). Voids within the weathered bedrock are variably filled with sediments. The percentage of the void volume filled with sediments ranges from <5 to >95% (Aley, 1997). The U.S. karst map (Veni and others, 2001) classifies more than 50% of U.S. karst as buried, i.e., covered by the epikarst.

Hydrogeologic behavior of the epikarst is controlled by the fact that infiltration into epikarst tends to be faster than drainage out of it (Klimchouk, 2004). Porosity, permeability, and consequently hydraulic conductivity within the epikarst diminish with depth; this permeability contrast causes water to accumulate at the epikarst base in the form of an epikarstic aquifer, first described by Mangin (1975). Thus, the epikarst is recognized as an important storage system in which storage can be more significant than in the phreatic zone (Perrin, Jeannin, and Zwahlen, 2003). The storage ability of epikarst varies. Alley (1997) classifies epikarst types based on the storage ability as 1) rapidly draining – with water saturation in the epikarstic zone for a maximum of a few hours at a time, 2) seasonally saturated – with the saturation period lasting for several weeks or months, and 3) perennially saturated – with most of the epikarstic zone constantly saturated.

At the same time, hydraulic behavior of the epikarst is considerably heterogeneous. Klimchouk (2004) describes several flow components within the epikarst (shaft or conduit flow, vertical vadose flow, and lateral vadose seepage) and further notes that while the epikarst generally accounts for recharge retardation and considerable mixing, the epikarst also provides for quick hydraulic response at shaft flow and springs in many systems. In addition, tracing

studies have found the co-existence of pathways of varying flow velocity. For example, Bottrell and Adkinson (1992) studying the Peninn epikarst in England identified three separate flow components with residence times of approximately 3 days, 30 to 70 days, and 160 or more days. Similarly, a study of epikarst in Slovenia found flowpaths of differing velocities, including rapid (0.5-2 cm/s), slower (around 0.1 cm/s), and the slowest (<0.001 cm/s) (Kogovšek and Šebela, 2004a). Tracer experiments conducted in the epikarst of the Swiss Jura mountains found faster (preferential) and slower pathways and also indicated the ability of epikarst to attenuate reactive solutes and particulate contaminants (Sinreich and Flynn, 2011). Flow through the epikarst can occur as diffuse seepage through the primary porosity, through secondary porosity of fissures and joints, and through conduit flow such as cave streams (Gillieson, 1996; Klimchouk, 2000). In addition, Al-Rashidy (1999) studying epikarstic springs described the occurrence of shifting spring basin boundaries with changing hydrologic conditions, producing the phenomenon of overflow spring.

The epikarst has been shown to exhibit chemical heterogeneity, although the evidence is not conclusive. Some evidence points to the epikarst being a heterogeneous, imperfectly mixed system (Friederich and Smart, 1981; Sinreich and Flynn, 2011; Tooth and Fairchild, 2003) while other studies suggest that the epikarst operates as a mixed, homogeneous reservoir producing similar chemical signatures at various discharge sites, with homogenization likely happening in the soil zone (Goede, Green, and Harmon, 1982; Aquilina, Ladouche, and Dörfliger, 2006).

BIOGEOCHEMICAL CYCLING OF NITROGEN

Nitrogen (N) is a non-metallic element with an atomic number of 7 and an atomic weight of 14.0067. Its terrestrial abundance is 50 ppm by mass. The largest N reservoir is the atmosphere where N is almost 80% of the mass. N also occurs in solid earth as partially decayed

organic matter in soils and ocean sediments, and as nitrogen ions in soil water or inclusions of silicate minerals. Despite its low terrestrial abundance, nitrogen is the fourth most abundant element in organic matter. Nitrogen is important to all biota on earth, being incorporated in amino acids, the building blocks of most proteins. N occurs in nature in 6 oxidation states, ranging from +5 to -3. In the pE-pH range of most earth environments, the most stable state of N is +5 (NO_3^-). In water, the stable oxidation states are -3, 0, and +5, with 0 (N_2) being the most stable one. Organic N is nearly always in the -3 oxidation state which is often thermodynamically unstable and thus requires energy for its production and maintenance (Chameides and Perdue, 1997).

Biogeochemical cycling of N on earth (Figure 2-4), the following summary of which is adapted from Chameides & Perdue (1997), essentially consists of transformations between the three oxidation states which are stable in water.

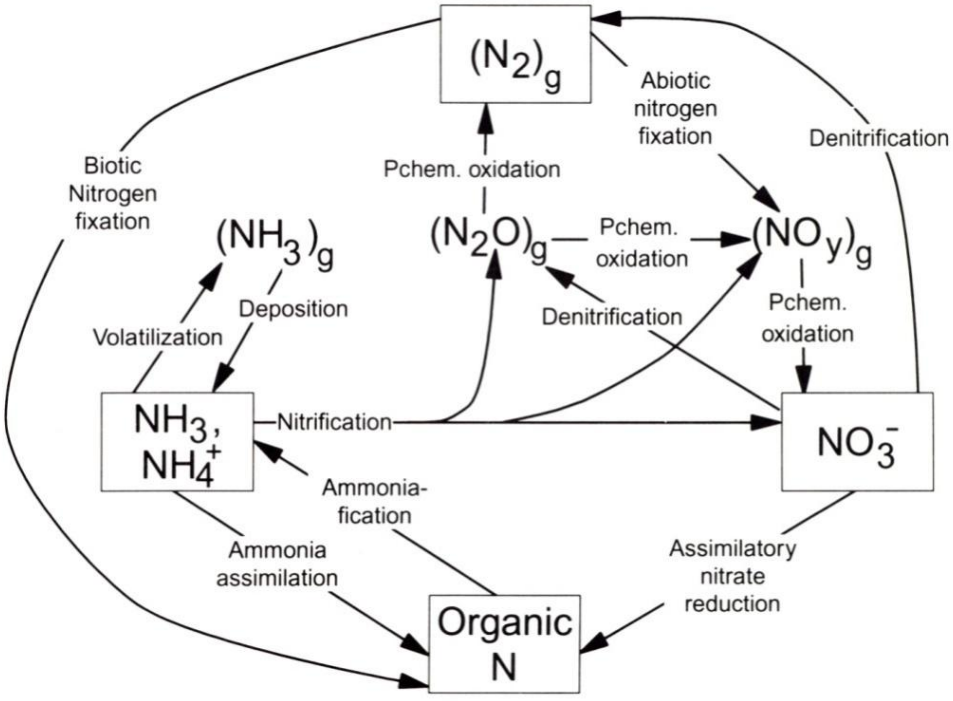

Figure 2-4 Major biogeochemical pathways of the N cycle (from Chameides & Perdue, 1997)

The cycle begins with fixation or conversion of relatively non-reactive atmospheric N_2 to other, utilizable N forms either by lightning or by certain free-living and symbiotic microbes. These microbes contain the enzyme nitrogenase, which catalyzes cleavage of the triple bond in N_2 molecule to produce fixed nitrogen (usually ammonia):

$$N_2 + 5H_2O \rightarrow NH_4^+ + 2OH^- + 1½O_2 \quad \text{(R1.1)}$$

In contrast to microbial fixation which ultimately produces organic N, abiotic fixation by lightning produces nitric oxide gas (NO).

Fixed nitrogen is incorporated into biomass by autotrophs which use it to build complex biomolecules. This can be achieved directly via ammonia assimilation which can be represented by the photosynthesis reaction for continents:

$$830CO_2 + 600H_2O + 9NH_3 + H_3PO_4 + \text{light energy} \rightarrow C_{830}H_{1230}O_{604}N_9P + 830O_2 \quad \text{(R1.2)}$$

Alternatively, if the fixed N source is NO_3^-, NO_3^- is first reduced to ammonia which is then assimilated. Ammonia is again released during the breakdown of organic matter which can be represented by the reverse of the photosynthesis reaction. Ammonia is thermodynamically unstable in oxidizing environments. Nitrifying bacteria, genus Nitrosomonas, catalyze its oxidation to NO_2^-:

$$NH_4^+ + {}^3/_2(O_2)_g \rightarrow NO_2^- + 2H^+ + H_2O$$

which genus Nitrobacter oxidizes to NO_3^-:

$$NO_2^- + ½(O_2)_g \rightarrow NO_3^-$$

Nitrification in general, however, is not 100% efficient. Some fraction of the N being nitrified oxidizes to less oxidized gaseous species such as NO, NO_2, and N_2O. An alternative fate of ammonium ions (NH_4^+) is their conversion to gaseous form (ammonia), especially under alkaline conditions:

$$NH_4^+ + OH^- \rightarrow (NH_3)_g + H_2O$$

When this reaction takes place in a natural environment such soil pore water or the ocean, the ammonia gas produced volatilizes into the atmosphere, transferring fixed N in the -3 oxidation state from the lithosphere or ocean to the atmosphere.

The final, closing step in the biogeochemical cycle of N is denitrification which converts fixed N back into its molecular form, N_2. Denitrification is typically defined as a microbial oxidation of organic matter in which NO_3^- or NO_2^- serves as an electron acceptor and the end product is N_2. Denitrification is predominantly a heterotrophic process of anaerobic respiration carried out by facultative anaerobic bacteria (e.g. Paracoccus denitrificans, Pseudomonas denitrificans). It can be expressed by the following redox reaction (Clark and Fritz, 1997):

$$NO_3^- + {}^5/_4CH_2O \rightarrow \tfrac{1}{2}N_2^- + HCO_3^- + \tfrac{1}{4}H^+ + \tfrac{1}{2}H_2O$$

Denitrification occurs widely in terrestrial, freshwater, and marine systems under special conditions. These generally include depletion of O_2, a more energetically favorable electron acceptor than NO_3^-; availability of NO_3^-/NO_2^- as an electron acceptor; and sufficient quantity of bioavailable organic substrate (Sylvia and others, 1999). Oxygen depletion zones conducive to denitrification can exist in otherwise aerobic soil profiles. Such zones were documented in saturated soil aggregates (Sexstone and others, 1985). In addition, because most denitrifying bacteria couple organic carbon oxidation with the reduction of NO_3^-, rates of denitrification may

often be driven by organic carbon availability (Knowles, 1982). In fact, limits on N cycling set by carbon are an important feature of soils and groundwater, and NO_3^- concentrations have been found to be less important than organic carbon content for determining levels of denitrification (Knowles, 1982; Starr and Gillham, 1993; Drury, McKenney, and Findlay, 1991; Groffman and Tiedje, 1989). Further, within aquatic systems, water residence time has been recognized as an important control on denitrification rates (Montgomery, Coyne, and Thomas, 1997; Dettmann, 2001). Other factors such as pH and temperature may occasionally be limiting factors to denitrification. The presence of denitrifiers, which make up a reasonable fraction of soil bacteria, is seldom a limitation (Sylvia and others, 1999).

Apart from the classical respiratory denitrification, numerous alternative microbial metabolic pathways of N_2 production have been identified. These pathways include production of N_2 from the anaerobic oxidation of NH_4^+ with NO_2^- (anammox) (Kuypers and others, 2003); an aerobic denitrification pathway (Robertson and others, 1995), and pathways utilizing reduced Fe, Mn, and S as reducing agents have been documented as well (Kölle, Strebel, and Böttcher, 1985; Postma and others, 1991; Luther III and others, 1997). This variety of denitrification pathways is not limited to bacteria only – molecular studies have shown that denitrifiers are an extremely diverse group of organisms including bacteria, archea, and fungi (Zumft, 1992). The composition of denitrifying communities in a given environment is complex and apparently subject to large fluctuations, both in time and in space (Groffman and others, 2006).

Spatial and temporal fluctuation of the controls of denitrification, environmental conditions and microbial community composition responding to these conditions, causes denitrification to fluctuate as well. Short term changes in denitrification rates, which can vary more than 100-fold from one day to the next, are often associated with precipitation, irrigation, or nutrient additions

(Sylvia and others, 1999). Seasonal responses, largely due to precipitation patterns or temperature, are also observed. For example, denitrification rates in the Pacific Northwest U. S. are highest in the fall when both soil temperature and water content are relatively high, while low rates are found in the winter, because of low soil temperatures, and in the summer, because of dry soil conditions (Sylvia and others, 1999). Parkin (1987) documented spatial variability of denitrification by showing that 85% of the active denitrification in a soil column could be attributed to less than 0.1% of the soil mass, associated with a small piece of decaying vegetation.

Biogeochemical N cycle also includes various atmospheric processes involving gases released into the atmosphere during the reactions listed previously, such as photochemical oxidation of NO and NO_2, photolysis of N_2O, atmospheric oxidation of ammonia, or denitrification. These atmospheric reactions and their environmental effects are described in Chameides and Perdue (1997) and other references therein.

DENITRIFICATION DETECTION METHODS

Denitrification is the most important natural attenuation mechanism for groundwater NO_3^- contamination. Unlike other potential natural attenuation processes, vegetative uptake and dilution with waters that have a low NO_3^- content, denitrification represents a long-term sink for N since it removes NO_3^- from the watershed in the form of N gases (NO, N_2O, and N_2) which escape to the atmosphere (Martin and others, 1999). Denitrification is also a longer term sink for N relative to microbial immobilization processes that lead to generation of organic N which may later be subjected to remobilization.

Accurate measurement of denitrification is problematic for a variety of reasons including often unavoidable methodological disturbance of the physical setting of the denitrification

process or high background concentration in the environment of the dominant end product (N_2) (Groffman and others, 2006). Also, the notorious high temporal and spatial variation of denitrification (Sylvia and others, 1999) makes the process difficult to quantify.

Notwithstanding the difficulty in measurement, denitrification has been measured in a wide range of terrestrial and aquatic environments using a variety of methods recently reviewed in Groffman and others (2006). These include (1) acetylene methods based on the inhibition of the reduction of N_2O to N_2 using acetylene (C_2H_2) (Yoshinari and Knowles, 1976; Balderston, Sherr, and Payne, 1976) and subsequent quantification of N_2O as the terminal product of denitrification, (2) ^{15}N tracer methods which most typically involve the addition of ^{15}N labeled NO_3^- and NH_4 into the system under investigation followed by direct measurement of ^{15}N-labeled denitrification gases (Myrold and Hall, 1990), (3) direct quantification of N_2 and N_2O denitrification emissions from mixed or intact soil cores enclosed in gas-tight incubation vessels (Scholefield, Hawkins, and Jackson, 1997; Butterbach-Bahl, Willibald, and Papen, 2002), (4) direct N_2 measurements in aquatic systems measuring either N_2 flux in water above sediment in an enclosure (Kana and others, 1998; Cornwell, Kemp, and Kana, 1999) or N_2 in water samples taken from the environment in question, commonly accompanied by measurements of Ar as a conservative tracer (Vogel, Talma, and Heaton, 1981; Bohlke and Denver, 1995), (5) traditional mass balance approaches which generally quantify N inputs and outputs and attribute the difference to denitrification, frequently assuming negligible change in storage within the system (David and Gentry, 2000; David and others, 2001), (6) stochiometric approaches which determine denitrification in aquatic environments from the difference between expected and observed amounts of dissolved inorganic N, with the expected amount calculated from a known elemental ratio of decomposed organic matter (Redfield, Ketchum, and Richards, 1963; Cline

and Richards, 1972), (7) stable isotope abundances of elements such as N and O in NO_3^-, NO_2^-, nitrous oxide (N_2O), of which perhaps the most commonly analyzed are $\delta^{15}N$ and $\delta^{18}O$ in NO_3^-, which increase exponentially with decreasing NO_3^- concentration due to denitrification, with the change in $\delta^{15}N$ about twice the change in $\delta^{18}O$ (Mariotti, Landreau, and Simon, 1988; Bottcher and others, 1990; Kendall and McDonnell, 1998), (8) approaches to determine denitrification rates using analyses of anthropogenic atmospheric constituents including ^3H, ^3He, CFC's, SF_6, and others, as indicators of groundwater age (Cook and Herczeg, 2000), (9) molecular approaches based on characterizing microbial denitrifiers through the functional genes involved in the denitrification pathway (Bothe and others, 2000). The methods applied in this study include geochemical mass balance, stable isotopes of NO_3^-, and direct dissolved N_2/Ar measurements. These methods are briefly reviewed in the following sections.

Geochemical mass-balance approach

The mass-balance approach has been widely used to study denitrification in systems of various scales, from lab columns (Reddy, Patrick Jr, and Lindau, 1989) to marine systems (Emery, Orr, and Rittenberg, 1955; Nielsen, Nielsen, and Rasmussen, 1995). In order to accurately estimate denitrification by mass balance, all N fluxes and changes in the storage need to be known; however, the change in storage is often assumed as negligible, and only inputs and outputs are quantified, with the difference attributed to denitrification. For example, David and Gentry (2000) and David and others (2001) quantified denitrification in a watershed by calculating the difference between net anthropogenic N inputs (fertilizer N, biological fixation, atmospheric deposition) and outputs (animal/grain export, riverine losses) while assuming zero net soil mineralization during the study period. Pribyl and others (2005) estimated denitrification flux (D) in a reach of the South Platte River from NO_3^- transport and transformation fluxes as:

$$O = I + S + N - D$$

where NO_3^--N input fluxes include groundwater (S), surface inflow (tributary stream, I) and nitrification (N), and NO_3^--N output flux consists of river outflow (O). Other similar examples of denitrification studies applying the output-input mass balance approach are in Sjodin and others (1997) and Smith and others (1991). The mass-balance method is useful in a wide range of scales where inputs, outputs, and storages can be well constrained, and for all systems it can provide at least some insight into the potential importance of denitrification. In pristine terrestrial systems, however, N inputs and outputs are small, and the method usually lacks the sensitivity to pick up small but important denitrification fluxes (Groffman and others, 2006).

Stable isotope abundances

Denitrification can potentially have large effects on groundwater geochemistry such as changes in speciation and stable isotopic composition of carbon and nitrogen-containing compounds which participate in the denitrification process (Smith, Howes, and Duff, 1991). Stable isotopic composition changes occur during chemical reactions as a result of different reaction rates of molecules with different masses which lead to isotope partitioning or fractionation described by Urey (1947). For example, as nitrogen compounds are chemically altered within a system, stable isotopes of NO_3^-, ^{15}N and ^{14}N, may undergo isotopic fractionation whereby one of the nitrogen isotopes is either incorporated into or depleted from the system, changing the nitrogen isotope ratio of a compound.

Stable isotope composition is measured as the ratio of the two most abundant isotopes of a given element and typically expressed using the delta (δ) notation which relates the measured isotopic ratio of the sample to that of the reference or standard. For nitrogen, δ is expressed as:

$$\delta^{15}N = \frac{\left(\frac{^{15}N}{^{14}N}\right)_{sample}}{\left(\frac{^{15}N}{^{14}N}\right)_{VSMOW}} - 1 \ * 1000‰$$

where VSMOW is the name of the reference used (Vienna Standard Mean Ocean Water) for which δ equals 0‰ by consensus. A δ-‰ value that is positive, e.g. +10‰ signifies that the sample contains 10 permil or 1% more of the heavier isotope (e.g. ^{15}N) than the reference, or is enriched in the heavy isotope by 10 ‰.

Denitrification can cause changes in the concentrations and isotopic compositions of many different aqueous species and solids in aquatic systems, for example: (1) the $\delta^{15}N$ and $\delta^{18}O$ values of the residual NO_3^- increase exponentially with decreasing NO_3^- concentration (Figure 2-5), with the change in $\delta^{15}N$ about twice the change in $\delta^{18}O$ (Figure 2-6) (Mariotti, Landreau, and Simon, 1988; Bottcher and others, 1990; Amberger and Schmidt, 1987), (2) the $\delta^{15}N$ value of N_2 may decrease or increase as a result of adding denitrification product N_2 to other components of N_2 in the system (Vogel, Talma, and Heaton, 1981), (3) the $\delta^{34}S$ value of sulfate or the $\delta^{13}C$ value of DIC may change as oxidation products of reduced S or C compounds are added to the existing pools during denitrification (Smith, Howes, and Duff, 1991; Strebel, Bottcher, and Fritz, 1990; Nascimento, Atekwana, and Krishnamurthy, 1997), and (4) the $\delta^{13}C$, $\delta^{15}N$, and $\delta^{34}S$ values of organisms (and derivative sediments and soils) may change as a result of changes in the isotopic compositions of their C, N, and S sources during denitrification (Altabet and others, 1999) (for N isotope changes).

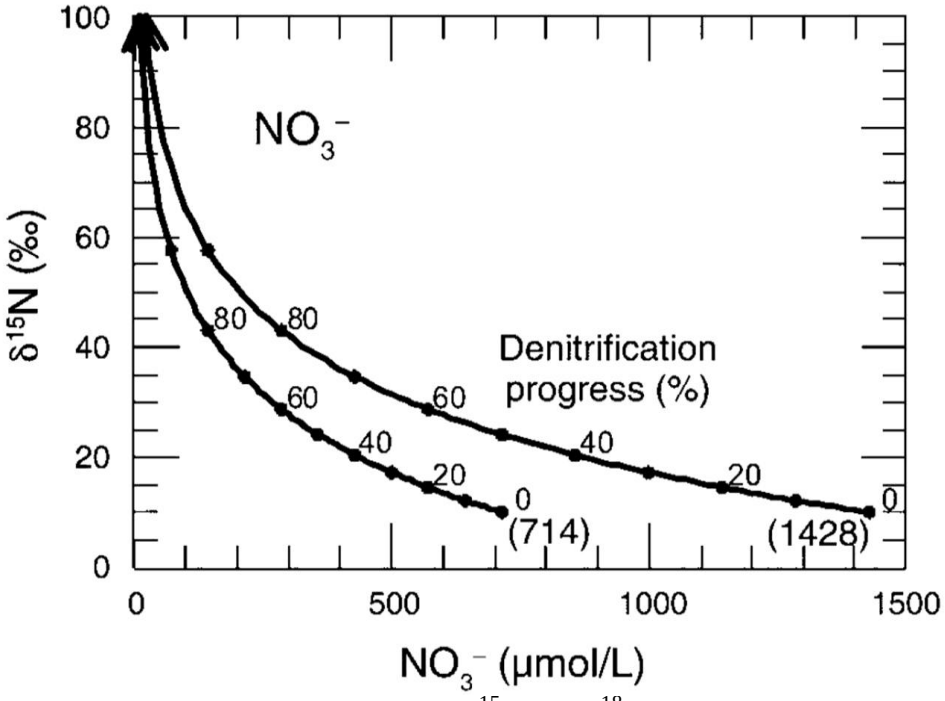

Figure 2-5 Denitrification causes $\delta^{15}N$ and $\delta^{18}O$ values of the residual NO_3^- to increase exponentially with decreasing NO_3^- concentration (modified from Böhlke et al., 2002)

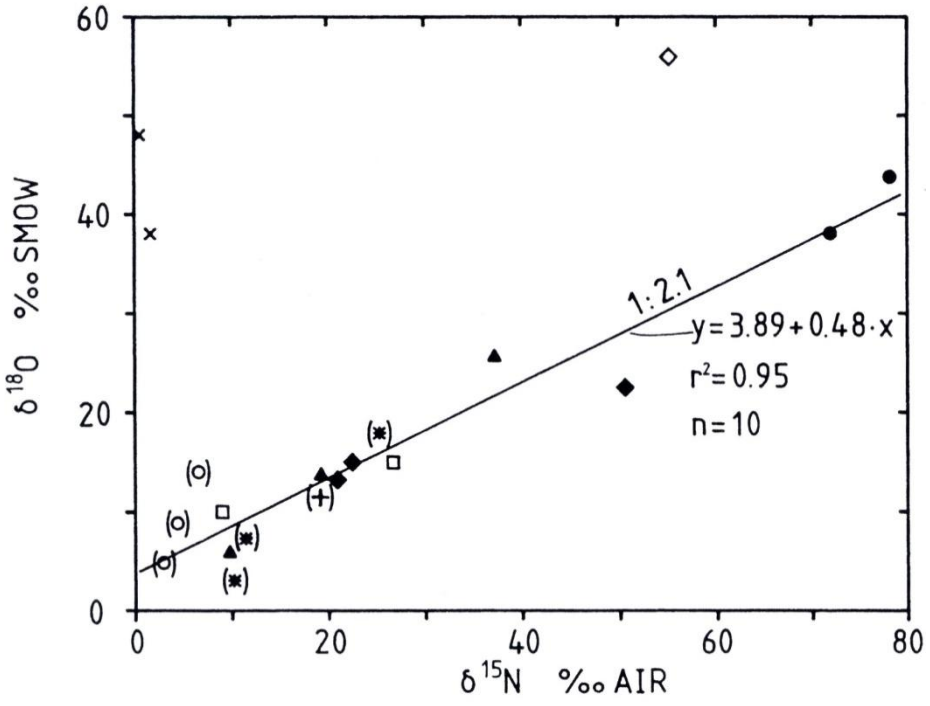

Figure 2-6 Denitrification produces NO_3^- isotopic enrichment which is typically twice as great for $\delta^{15}N$ as for $\delta^{18}O$. $\delta^{15}N$ and $\delta^{18}O$ values plot on a line with 0.5 slope (from Bottcher et al., 1990).

Dissolved N_2 and Ar method

A number of studies indicated that denitrification in groundwater can be identified by analyses of dissolved gases, including N_2 and Ar, based on the principle that in groundwater N_2 accumulates as the principle denitrification product while Ar remains virtually constant. Therefore, any increase in the dissolved N_2/Ar ratio with time or along the flow-path is a sign of microbial denitrification.

Denitrification was in most studies calculated as excess N_2 above the background N_2 concentration – the concentration in water equilibrated with the atmosphere during recharge – which can be calculated based on temperature during recharge which, in turn, can be estimated from Ar concentration (Vogel, Talma, and Heaton, 1981; Bohlke and Denver, 1995; Smith, Howes, and Duff, 1991; Heaton and Vogel, 1981; Dunkle and others, 1993). Some of these studies found that excess air was introduced in the percolating groundwater and contributed additional N_2, the amount of which, however, was quantified and subtracted from the measured total N_2 concentrations (Vogel, Talma, and Heaton, 1981; Bohlke and Denver, 1995; Smith, Howes, and Duff, 1991; Heaton and Vogel, 1981; Dunkle and others, 1993). In several studies, which investigated denitrification in systems with relatively shallow flow-paths, <2 m below the ground surface, and where excess air incorporation was not a complicating factor, denitrification N_2 was calculated as a simple increase in N_2 along a flow-path, from one sampling point to another (Blicher-Mathiesen, McCarty, and Nielsen, 1998; Mookherji, McCarty, and Angier, 2003). In these shallow systems, N_2 production-driven degassing occurred along the flow-path. The N_2 loss due to degassing was calculated from the difference in the groundwater Ar concentrations between sampling points and the ratio of partial pressures of N_2 and Ar. The

amount of degassed N_2 was then added to the measured N_2 concentrations (Blicher-Mathiesen, McCarty, and Nielsen, 1998).

FLUORESCENT DYE TRACING

Principles of dye tracing

Water tracing is a fundamental investigative tool in hydrogeology, providing information on water discharge, trajectory, velocity and dispersivity. Tracer material is typically introduced as a spike of high concentration, which moves via advection and dispersion in tandem with water which is sampled at some point downgradient. Over time the tracer spike becomes attenuated by dispersion, and tracer adsorption may significantly retard the tracer. As a result, groundwater tracing is most effective where groundwater travel times are relatively short and dispersion limited, for example in linking recharge from sinking streams to focused-flow discharge points such as springs in karst aquifers. However, tracing is also a suitable technique for vadose zone investigations (Flury and Wai, 2003; Kogovšek and Šebela, 2004b), frequently used to characterize preferential flow paths (Kung, 1990; Larsson and others, 1999; Al-Qinna, 2003; Mortensen and others, 2004).

Fluorescent dyes are widely used hydrologic tracers because of their wide availability, low cost, and low toxicity. In addition, fluorescent dyes can be routinely detected at parts-per-trillion levels, although unequivocal detection above background levels usually requires higher concentrations. Reviews on the properties and applications of fluorescent dyes can be found in Smart and Laidlaw (1977), Davis and others (1980), Mull and others (1988), or Quinlan (1991).

At its simplest level, tracing can identify point-to-point connections between discrete recharge areas and discharge points such as springs or wells. This simply requires positive identification of a tracer indicated by concentrations above background. Fluorescent dyes can be

visually detected at parts-per-billion levels. Sub-visible tracing may be undertaken by accumulating dye on in-situ charcoal detectors, subsequently eluted, to obtain an integrated indicator of exposure to dye. The dye concentration in the elutant can be quantified, but since the adsorption and elution are not quantitative, such traces are treated as qualitative (Smart and others, 1998).

Quantitative traces involve monitoring of the concentration of dye in water samples over time at groundwater discharge points such as springs or wells. In addition, determination of the mass of dye recovered requires injecting a known quantity of dye and measuring discharge. Water samples are collected, usually with automatic samplers, during passage of the dye cloud, and the dye content of each sample is measured. The dye concentrations are plotted against time to generate time-concentration breakthrough curves which allow the determination of the sequence of tracer arrival at multiple points. Well defined time-concentration curves provide robust evidence of a successful trace and allow estimation of hydraulic parameters such as hydraulic conductivity and dispersivity (Domenico and Schwartz, 1990). However, the elaborate logistics associated with quantitative tracing precludes its widespread use.

Quantitative characteristics for dye tracing

The development of quantitative information from dye traces is based primarily on the analysis of breakthrough curves which are plots of concentration, corresponding to specific sampling locations, versus elapsed time since injection. These curves are also known as dye-recovery, dye-response, or time-concentration curves. The concentrations versus time data typically plot as a skewed curve with the rising limb steeper than the falling limb. The shape and magnitude of dye-recovery curves are primarily affected by the amount of dye injected, the velocity and magnitude of flow, the mixing characteristics within the flow system, adsorption,

the sampling interval, and whether the discharge is diluted by non-dyed waters (Mull, Smoot, and Liebermann, 1988).

Some quantitative characteristics of the dye trace, such as elapsed time to peak dye concentration, may be read directly from the measured data, while others, such as mean travel time and normalized dye concentration, are calculated from the measured data. Still other characteristics, particularly the dispersion coefficient, may be estimated from the data only when simplifying assumptions are made. The following, adapted from Mull and others (1988), describes the primary quantitative characteristics for dye tracing.

The mass of dye recovered is summed from the time-concentration data for a dye trace by the following equation:

$$M_{out} = 0.1019 \sum_{i=1}^{n} Q_i \; C_i' - C_0' \; \Delta t_i$$

where M_{out} represents the mass of dye recovered, 0.1019 is a unit conversion factor, n is the number of sampling intervals equal to the total number of samples minus one, i is the i^{th} sampling interval, Q_i is mean discharge during the i^{th} sampling interval (ft^3/s), $C_i^{'}$ is the mean measured dye concentration during the i^{th} interval equal to the mean of the two samples taken at the beginning and end of the interval (mg/L), $C_0^{'}$ is background dye concentration measured at time of injection (mg/L), and Δt_i is the duration of the i^{th} sampling interval (hr).

Measured dye-recovery concentration needs to be adjusted for background concentration and reasonable dye loss by:

$$C'' = (C' - C_0') \frac{M_{in}}{M_{out}}$$

where C'' is adjusted concentration (mg/L), C' is measured concentration (mg/L), and M_{in} represents the mass of dye injected (kg).

Because the quantity or mass of injected dye may be different for different dye traces, dye concentrations for each trace are normalized to give the concentration that would have occurred if a standard mass of one kilogram of dye had been injected. Normalized dye concentrations are calculated as:

$$C = (C' - C_0')\frac{1}{M_{out}}$$

where C stands for normalized dye concentration in milligrams per liter per kilogram of dye injected.

When comparing multiple traces conducted between the same sites but under varying hydrologic conditions, the effects of discharge, and hence dilution, variation on the dye recovery curves of normalized concentration, can be removed by converting normalized dye concentrations to normalized dye loads. The normalized dye load, or mass flux, is the amount of dye per kilogram injected passing the sampling point at a given time. Normalized load is normalized concentration times discharge, calculated as:

$$L = 28.32\ C\ Q$$

where L is normalized dye load in milligrams per second per kilogram of dye injected, 28.32 is a unit conversion factor, C is normalized dye concentration in (mg/L)/kg, and Q is discharge in ft^3/s.

Time of travel is the time required for the dye cloud to move from the injection point to the sampling point. For quantitative analysis, the time of travel for the bulk of the dye cloud is

represented by the centroid/mass-weighted mean of the dye-recovery curve. The time of travel of the centroid of the dye mass, or simply the mean travel time, is computed as:

$$t = \frac{\sum_{i=1}^{n} t_i C_i \Delta t_i Q_i}{\sum_{i=1}^{n} C_i \Delta t_i Q_i}$$

where t is mean travel time (hr), t_i is elapsed time since injection during the i^{th} sampling interval (hr), and C_i is normalized dye concentration during the i^{th} sampling interval, in (mg/L)/kg.

Calculation of the apparent velocity of groundwater follows directly from the mean travel time:

$$u = \frac{d}{3600t}$$

where u is mean flow velocity (ft/s), d is map distance of the trace (ft), and 3600 is a unit conversion factor.

The standard deviation of the time of travel of the dye mass is a temporal measure of the amount of dispersion of the dye mass that occurred during the dye trace. It indicates how much the dye cloud has spread out in time, between the injection point and the sampling site. It is related to the time of travel and the rate of dispersion, and is calculated as:

$$\sigma_t = \left(\frac{\sum_{i=1}^{n} (t_i - t)^2 C_i \Delta t_i Q_i}{\sum_{i=1}^{n} C_i \Delta t_i Q_i} \right)^{0.5}$$

where σ_t is the standard deviation of the travel time of the dye mass (hr).

The skewness coefficient (γ) is a measure of the lateral asymmetry of the time-concentration curve. It is a non-dimensional statistical parameter computed as:

$$\gamma = \frac{\sum_{i=1}^{n}(t_i - t)^3 C_i \Delta t_i Q_i}{n\sigma_t^3 \sum_{i=1}^{n} C_i \Delta t_i Q_i}$$

Dispersion describes the spreading of the dye mass that results both in increasing persistence and decreasing concentration over time. It is caused by simple molecular diffusion, known as hydrodynamic dispersion, and the turbulence of the water body. Application of dispersion to groundwater flow is in karst terrains is presently limited to conceptual use in interpretation and comparison of repeated dye traces under differing hydrologic conditions. The dispersion coefficient computation is based on equations presented by Fischer (1968), with the assumptions of constant velocity and uniform flow characteristics between the injection and sampling points for the entire duration of the dye trace. The first, more general equation is based on the definition of dispersion coefficient from a slug injection of dye:

$$D_1 = \frac{3600}{2} u^2 \frac{\sigma_t^2}{t}$$

where D_1 is the first dispersion coefficient (ft^2/s). The second equation is based on the further assumption that the dye-response curve is normally distributed, with zero skew along the flow path. When sampled at the peak of the dye-recovery curve,

$$C_{peak} = \frac{588.5}{A\sqrt{4\pi D_2 t_{peak}}}$$

where C_{peak} is the peak of the normalized concentration curve (mg/L/kg), 588.5 is a unit conversion factor, A is the effective cross-sectional area of the flow medium (ft^2), estimated as discharge divided by mean flow velocity, and D_2 is the second dispersion coefficient (ft^2/s). On

the basis of the last equation, the second estimate of the dispersion coefficient may be computed as:

$$C_{peak} = \frac{346{,}400}{4\pi t_{peak}(C_{peak}A)^2}$$

where 346,400 is a unit conversion factor.

SUMMARY OF RELEVANT UP-TO-DATE RESEARCH AT THE SEW

A large amount of relevant data related to soils, subsurface-geophysics, hydrology and groundwater chemistry have been collected in the SEW plot area up to date, providing a basis for a hydrogeologic conceptual model of the study site.

Six soils are present in Basin 1 with the Clarksville cherty silt loam (12-60% slope, Loamy-skeletal, siliceous, semiactive, mesic Typic Paleudults) and Nixa cherty silt loam (3-8% slope, Loamy-skeletal, siliceous, active, mesic Glossic Fragiudults) dominating and comprising 49 and 30%, respectively, of the watershed area. These soils formed from cherty limestone residuum and contain chert fragments in excess of 35% of the soil volume (Sauer & Logsdon, 2002). The other soils are Pickwick silt loam (3-8% slope. Fine-silty, mixed, semiacive, thermic, Typic Paleudults), Razort silt loam (Fine-loamy, mixed, active, mesic Mollic Hapludalfs) and Razort gravelly silt loam (Sauer and Logsdon, 2002). Two principal soil series within the plot include Captina silt loam (3-6% slope, Fine-silty, siliceous, active, mesic Typic Fragiudults) and Nixa cherty silt loam. Soils of the Nixa cherty silt loam typically have low-permeability fragipans developed at 36-60 cm depth (Harper, Phillips, and Haley, 1969).

The stones and coarse fragments characteristic of the soils in Basin 1 create preferential flow paths that accelerate water and solute movement to the groundwater (Al-Qinna, 2003). The

significant gravel content in the soil profile markedly affects the soil hydraulic properties by disrupting the continuity of soil pore system and providing a random distribution of large voids among coarse fragments that have no direct contact with fine soil textural fractions. Solute transport in these soils is dominated by convective flow. Water and solute tracing experiments indicated that the soils exhibit unique structure where water and solute flow rapidly through the large pores, channels, root holes, and worm holes (Al-Qinna, 2003).

The subsurface of the plot contains a highly fractured and weathered stratified carbonate unit (bedrock) starting 0.1-1.0 meter deep in the upper half of the plot and deeper in the lower half as revealed by ground-penetrating radar (GPR) and electrical resistivity surveys (Ernenwein and Kvamme, 2004). This unit is composed of abundant contrasting material (limestone, chert, weathered zones with clay) whereas the lower half of the plot is more homogenous, indicating a weathered and transported regolith. Drilling and excavating verified this subsurface structure of the plot and also confirmed its continuation down from the plot where the depth to bedrock is approximately 1.5 meter (Winston, 2006; Laincz, 2007).

Two major storm runoff mechanisms occurring in the plot are infiltration excess runoff and saturation excess runoff. On average, infiltration excess runoff dominates and occurs in 58% of the total plot area while saturation excess runoff, generated over saturated surfaces, occurs in 26% of the plot area; 16% of the plot area contributes no runoff (Leh, 2006). Data also indicate that only 2-8% of precipitation volume runs off the plot during January runoff-producing storm events (Leh, 2006). Sauer and Logsdon (2002) measured water balance parameters in an Ozark Highlands setting similar to that of the SEW plot. This study found the amount of total runoff from a 0.4 ha watershed in 13 months was only 2.6% of precipitation, although 3 winter storm events accounting for this runoff had runoff amounts of 9, 19, and 53% of precipitation. Other

storm events of comparable or greater intensity during other seasons failed to produce runoff, likely due to dry soil conditions and taller grass canopy. Drainage through the root zone occurred primarily in the winter and accounted for 9.9% of precipitation. The water balance was dominated by evaporation which accounted for 91% of precipitation.

Three tracer tests were conducted to delineate hydrologic flow-paths at the site. Two initial sodium bromide tracer tests conducted in the summer 2005 and 2006 failed to produce expected results. In both instances no tracer was recovered from the seeps within 2 weeks after its surface application inside the plot, likely due to insufficient quantity of water to flush the tracer and the summer timing of these tests when high evapo-transpiration rates limited downward movement of water and the tracer through the vadose zone. Brahana and others (2006) found evapotranspiration during the summer season causing substantial loss of water from the epikarst shallow groundwater system manifested in extreme diurnal fluctuation of the interflow zone seeps discharge. A qualitative dye tracer test conducted in January 2007, involving introduction of fluorescein into two small trenches inside the plot under high antecedent moisture conditions, revealed that the seeps J2-J5 and the interceptor trench are hydrologically connected with the plot (Laincz, 2007). The tracer travel times from the plot to these multiple sampling points varied and ranged from 10-40 hours. These travel times indicated a faster vadose zone transport than can be ascribed to matrix flow, thus indicating the presence of macropores. No dye arrived at seep J1, suggesting none or very limited hydrologic connection with the plot.

Water quality was monitored at the plot from June 2004 until June 2005 (Winston, 2006). Only 3 out of 8 sampling events conducted, however, were storm-flow events that produced flow in the interceptor trench, making it possible to obtain water samples from this sampling point and evaluate interflow zone NO_3^- transport and processing (July 3rd, 2004; December 1st, 2004;

December 7th, 2004). Results from these 3 events showed that dilution was a prominent process in the interflow zone, reducing concentrations of solutes by 53-87% between the trench and the seeps (up-gradient and terminal interflow zone sampling point, respectively). NO_3^- concentrations in the trench ranged from 22.3-48.0 mg/L, decreasing toward the seeps, where they ranged from 1.4-8.0 mg/L. After correcting the seeps NO_3^- concentrations for the effect of dilution, mass balance revealed that between 1 and 33% of NO_3^- is being removed along the interflow zone flow-paths as a result of processes other than dilution or mixing, e.g. microbial denitrification and immobilization. The isotopic composition of the interflow zone NO_3^- fell between two potential sources of NO_3^- origin: soil organic matter and manure. NO_3^- $\delta^{15}N$ and $\delta^{18}O$ of the seeps water samples ranged from 0.4-5.3 ‰ and 3.8-5.3 ‰, respectively. An isotopic data analysis suggested these $\delta^{15}N$ and $\delta^{18}O$ values of the seeps water samples (residual NO_3^- pool) were isotopically enriched by 0.2-5.9 ‰ and 0.3-1.9 ‰, respectively, relative to modeled values which could be expected if dilution had been the only process affecting the NO_3^- concentration and isotopic composition. DOC analysis indicated a correlation between DOC concentration and the degree of NO_3^- processing for the interflow zone seeps. In addition, DOC bioavailability assays showed that DOC was more bioavailable in the interflow zone seeps than in focused-flow dominated flow-paths of the watershed (springs Langle and Copperhead). In summary, preliminary NO_3^- mass balance and isotopic composition data combined with DOC concentration and bioavailability data suggested that the interflow zone is a potential zone of NO_3^- processing (Winston, 2006).

Studies of the basin-scale SEW hydrogeology concluded that a stream piracy is a frequent local phenomenon. Permeability contrasts within the soil, interflow-zone, and within the bedrock concentrate flow and distribute flow down gradient along the flow-paths of least resistance.

These are a reflection of purity of limestone and are a dominant control on the hydrology. Springs in the basin represent an interception of these flow paths with the land surface and range from intermittent to continuous. Hydraulic gradients of the groundwater, following the tilt of the rock formations, act independently from surface water bodies where confinement by chert layers is effective (Al-Qinna, 2003; Brahana, 1995; Brahana, 1997; Brahana and others, 1999). Tracer studies in the focused-flow zone of the basin indicated high solute/bacterial transport in this zone which can be 500 meters per 15 hours (Ting, 2005; Whitsett, 2002), emphasizing the importance of the interflow zone as a contaminant bioremediation zone.

In summary, up-to-date research suggests that runoff events at SEW are rare and tend to occur during winter months. Further, precipitation generally quickly infiltrates the regolith mantle (epikarst) where water moves bimodally via diffuse and macropore flow in both vertical and lateral directions; lateral movement – interflow – occurs due to permeability contrasts presented by chert ledges and the bedrock surface. Macropores including root channels, worm holes, and pores created by the loose contact between chert fragments and soil matrix are abundant in the regolith mantle and greatly accelerate water and solute flow through the mantle. At the study site, interflow paths begin in the upland area underneath a thin (30-75 cm) soil horizon relatively rich in organics and terminate on the side slope down-gradient as 5 springs (seeps). During wet antecedent conditions the time of travel of a solute from the upland plot area to these seeps (through the interflow zone) can range from 10 to 40 hours.

REFERENCES

Aley, T., 1997, Groundwater tracing in the epikarst: The Engineering Geology and Hydrogeology of Karst Terranes—Proceedings of the 6th multidisciplinary conference on sinkholes and the engineering and environmental impacts of karst, Springfield, MO, April 6-9, 1997, p. 6-9.

Al-Qinna, M.I., 2003, Measuring and modeling soil water and solute transport with emphasis on physical mechanisms in karst topography: Fayetteville, University of Arkansas, Ph.D. Dissertation, 273 p.

Al-Rashidy, S.M., 1999, Hydrogeologic controls of groundwater in the shallow mantled karst aquifer, Copperhead Spring, Savoy Experimental Watershed, northwest Arkansas: Fayetteville, University of Arkansas, M.S. Thesis, p.96

Altabet, M.A., Pilskaln, C., Thunell, R., Pride, C., Sigman, D., Chavez, F., and Francois, R., 1999, The nitrogen isotope biogeochemistry of sinking particles from the margin of the Eastern North Pacific: Deep Sea Research Part I: Oceanographic Research Papers, v. 46, no. 4, p. 655-679.

Amberger, A., and Schmidt, H.L., 1987, Naturliche isotopen-gehalte von nitrat als indikatoren fur dessen herkunft: Geochimica et Cosmochimica Acta, v. 51, p. 2699-2705.

Aquilina, L., Ladouche, B., and Dörfliger, N., 2006, Water storage and transfer in the epikarst of karstic systems during high flow periods: Journal of Hydrology, v. 327, no. 3-4, p. 472-485.

Atkinson, T.C., 1977, Diffuse Flow and Conduit Flow in Limestone Terrain in the Mendip Hills, Somerset (Great Britain): Journal of Hydrology, v. 35, no. 1/2, p. 93-110.

Balderston, W.L., Sherr, B., and Payne, W.J., 1976, Blockage by acetylene of nitrous oxide reduction in Pseudomonas perfectomarinus. Applied and Environmental Microbiology, v. 31, no. 4, p. 504-508.

Beven, K., and Germann, P., 1982, Macropores and water flow in soils: Water Resources Research, v. 18, no. 5, p. 1311-1325.

Blicher-Mathiesen, G., McCarty, G.W., and Nielsen, L.P., 1998, Denitrification and degassing in groundwater estimated from dissolved dinitrogen and argon: Journal of Hydrology, v. 208, no. 1-2, p. 16-24.

Bohlke, J.K., and Denver, J.M., 1995, Combined Use of Groundwater Dating, Chemical, and Isotopic Analyses to Resolve the History and Fate of Nitrate Contamination in Two Agricultural Watersheds, Atlantic Coastal Plain, Maryland: Water Resources Research, v. 31, no. 9, p. 2319-2339.

Bothe, H., Jost, G., Schloter, M., Ward, B.B., and Witzel, K., 2000, Molecular analysis of ammonia oxidation and denitrification in natural environments: FEMS microbiology reviews, v. 24, no. 5, p. 673-690.

Bottcher, J., Strebel, O., Voerkelius, S., and Schmidt, H.L., 1990, Using isotope fractionation of nitrate-nitrogen and nitrate-oxygen for evaluation of microbial denitrification in a sandy aquifer: Journal of Hydrology, v. 114, no. 3-4, p. 413-424.

Bottrell, S.H., and Atkinson, T.C., 1992, Tracer study of flow and storage in the unsaturated zone of a karstic limestone aquifer: Tracer hydrology: Rotterdam, Balkema, p. 207-211.

Brahana, J.V., 1995, Controlling influences on ground-water flow and transport in the shallow karst aquifer of northeastern Oklahoma and northwestern Arkansas: Proceedings of the Arkansas Water Resources Center 1994 Research Conference, Fayetteville, Arkansas, p. 25.

Brahana, J.V., 1997, Rationale and methodology for approximating spring-basin boundaries in the mantled karst terrane of the Springfield Plateau, northwestern Arkansas, *in* Beck, B.F., Stephenson, J.B. eds. The engineering geology and hydrogeology of karst terranes: United States (USA), AA Balkema, Rotterdam, p. 77-82.

Brahana, J.V., Hays, P.D., Kresse, T.M., Sauer, T.J., and Stanton, G.P., 1999, The Savoy Experimental Watershed—Early lessons for hydrogeologic modeling from a well-characterized karst research site, *in* Palmer, A.N., Palmer, M.V. and Sasowsky, I.D. eds. Karst Modeling: Special Publication No. 5: Charlottesville, VA, Karst Water Institute, p. 247-254. at http://www.karstwaters.org/publications/curpubslist.htm

Brahana, J.V., Killingbeck, J.J., Stielstra, C., Leh, M.D.K., Murdoch, J.F., and Chaubey, I., 2006, Elucidating flow characteristics of epikarst springs using long-term records that encompass extreme hydrogeologic stresses: Geological Society of America Abstracts with Programs, Philadelphia, Pennsylvania, v. 38, p. 196.

Butterbach-Bahl, K., Willibald, G., and Papen, H., 2002, Soil core method for direct simultaneous determination of N2 and N2O emissions from forest soils: Plant and Soil, v. 240, no. 1, p. 105-116.

Chameides, W.L., and Perdue, E.M., 1997, Biogeochemical cycles: New York, New York, Oxford University Press, 224 p.

Clark, I.D., and Fritz, P., 1997, Environmental Isotopes in Hydrogeology: Boca Raton, Florida, CRC Press LLC, 328 p.

Cline, J.D., and Richards, F.A., 1972, Oxygen Deficient Conditions and Nitrate Reduction in the Eastern Tropical North Pacific Ocean: Limnology and Oceanography, v. 17, no. 6, p. 885-900.

Cook, P.G., and Herczeg, A.L., 2000, Environmental Tracers in Subsurface Hydrology: Boston, Massachusetts, USA, Kluwer Academic Publishers

Cornwell, J.C., Kemp, W.M., and Kana, T.M., 1999, Denitrification in coastal ecosystems: methods, environmental controls, and ecosystem level controls, a review: Aquatic Ecology, v. 33, no. 1, p. 41-54.

David, M.B., McIsaac, G.F., Royer, T.V., Darmody, R.G., and Gentry, L.E., 2001, Estimated historical and current nitrogen balances for Illinois: Scientific World, v. 1, p. 597-604.

David, M.B., and Gentry, L.E., 2000, Anthropogenic Inputs of Nitrogen and Phosphorus and Riverine Export for Illinois, USA: J Environ Qual, v. 29, no. 2, p. 494-508.

Davies, W.E., and LeGrand, H.E., 1972, Karst of the United States, *in* Herak, M., Stringfield, V.T. eds. Karst—Important karst regions of the northern hemisphere: Holland, Elsevier, p. 467-505.

Davis, S.N., Thompson, G.M., Bentley, H.W., and Stiles, G., 1980, Ground-Water Tracers-A Short Review: Ground Water, v. 18, no. 1, p. 14-23.

Dettmann, E.H., 2001, Effect of water residence time on annual export and denitrification of nitrogen in estuaries: A model analysis: Estuaries and Coasts, v. 24, no. 4, p. 481-490.

Domenico, P.A., and Schwartz, F.W., 1990, Physical and Chemical Hydrology: New York, John Wiley and Sons, 824 p.

Drury, C.F., McKenney, D.J., and Findlay, W.I., 1991, Relationships between denitrification, microbial biomass and indigenous soil properties: Soil Biology & Biochemistry, v. 23, no. 8, p. 751-755.

Dunkle, S.A., Plummer, L.N., Busenberg, E., Phillips, P.J., Denver, J.M., Hamilton, P.A., Michael, R.L., and Copen, T.B., 1993, Chlorofluorocarbons (CCl_3F and CCl_2F_2) as dating tools and hydrologic tracers in shallow groundwater of Delmarva Peninsula, Atlantic Coastal Plain, United States: Water Resources Research, v. 29, no. 12, p. 3837-3860.

Emery, K.O., Orr, W.L., and Rittenberg, S.C., 1955, Nutrient budgets in the ocean, *in* Essays in the natural sciences in honor of Captain Alan Hancock: Los Angeles, CA, USA, University of Southern California Press, p. 299-309.

Ernenwein, E.G., and Kvamme, K.L., 2004, Geophysical Investigations For Subsurface Fracture Detection In The Savoy Experimental Watershed, Arkansas: Unpublished report, Department of Biological and Agricultural Engineering, University of Arkansas, 24 p.

Fischer, H.B., 1968, Dispersion Predictions in Natural Streams: American Society of Civil Engineers, Journal of the Sanitary Engineering Division, v. 94, no. SA5, p. 927-943.

Flury, M., and Wai, N.N., 2003, Dyes as tracers for vadose zone hydrology: Reviews of Geophysics, v. 41, no. 1, p. 1002.

Ford, D.C., 1967, Sinking Creeks of Mt. Tupper: A Remarkable Groundwater System in Glacier National Park: Canadian Geographer, v. 11, p. 49-52.

Ford, D.C., and Williams, P.W., 2007, Karst hydrogeology and geomorphology: Chichester, England, John Wiley & Sons, 576 p.

Friederich, H., 1981, The hydrochemistry of recharge in the unsaturated zone, with special reference to the Carboniferous limestone aquifer of the Mendip Hills: Bristol, England, University of Bristol, Ph.D. Dissertation, p.93

Friederich, H., and Smart, P.L., 1981, Dye tracer studies of the unsaturated zone: recharge of the Carboniferous Limestone aquifer of the Mendip Hills, England: Proceeding of the 8th International Speleological Congress, Bowling Green, Kentucky, USA, p. 283-286.

Gale, S.J., 1984, The hydraulics of conduit flow in carbonate aquifers: Journal of Hydrology, v. 70, no. 1, p. 309-327.

Gams, I., 1993, Origin of the term "karst", and the transformation of the classical karst (kras): Environmental Geology, v. 21, no. 3, p. 110-114.

Gillieson, D., 1996, Caves: Processes, Development, Management: Oxford, Blackwell, 324 p.

Goede, A., Green, D., and Harmon, R., 1982, Isotopic composition of precipitation, cave drips and actively forming speleothems at three Tasmanian cave sites: Helictite, v. 20, no. 1, p. 17-28.

Gollehon, N., Caswell, M., Ribaudo, M., Kellogg, R., Lander, C., and Letson, D., 2001, Confined Animal Production and Manure Nutrients: USDA Agriculture Information Bulletin, no. AIB771, p. 1-40.

Groffman, P.M., and Tiedje, J.M., 1989, Denitrification in North Temperate Forest Soils: Relationships between Denitrification and Environmental Factors at the Landscape Scale: Soil Biology & Biochemistry, v. 21, no. 5, p. 621-626.

Groffman, P.M., Alatabet, M.A., Bohlke, J.K., Butterbach-Bahl, K., David, M.B., Firestone, M.K., Giblin, A.E., Kana, T.M., Nielsen, L.P., and Voytek, M.A., 2006, Methods For Measuring Denitrification: Diverse Approaches To a Difficult Problem: Ecological Applications, v. 16, no. 6, p. 2091-2122.

Gunn, J., 1986, A conceptual model for conduit flow dominated karst aquifers: Proceedings of the International Symposium on Karst Water Resources. IAHS publication no. 161, Ankara, 1985, v. 161, p. 587-596.

Harper, M.D., Phillips, W.W., and Haley, G.J., 1969, Soil Survey, Washington County, Arkansas: Washington, DC, USDA-SCS, US Govt. Print. Off.

Heaton, T.H.E., and Vogel, J.C., 1981, "Excess air" in groundwater: Journal of Hydrology, v. 50, p. 201-216.

Jennings, J.N., 1985, Karst Geomorphology: New York, Basil Blackwell Inc., 293 p.

Kana, T.M., Sullivan, M.B., Cornwel, J.C., and & Groszkowski, K.M., 1998, Denitrification in estuarine sediments determined by membrane inlet mass spectrometry: Limnology and Oceanography, v. 43, no. 2, p. 334-339.

Kendall, C., and McDonnell, J.J., 1998, Isotope Tracers in Catchment Hydrology: Amsterdam, Elsevier Science B.V., 839 p.

Klimchouk, A., 2004, Towards defining, delimiting and classifying epikarst: Its origin, processes and variants of geomorphic evolution: Speleogenesis and Evolution of Karst Aquifers, v. 2, no. 1, p. 1-13,

Klimchouk, A., 2000, The formation of epikarst and its role in vadose speleogenesis: Speleogenesis: Evolution of Karst Aquifers, National Speleological Society: Huntsville, p. 91-99.

Knowles, R., 1982, Denitrification: Microbiology and Molecular Biology Reviews, v. 46, no. 1, p. 43-70.

Kogovšek, J., and Šebela, S., 2004a, Water tracing through the vadose zone above Postojnska Jama, Slovenia: Environmental Geology, v. 45, no. 7, p. 992-1001.

Kogovšek, J., and Šebela, S., 2004b, Water tracing through the vadose zone above Postojnska Jama, Slovenia: Environmental Geology, v. 45, no. 7, p. 992-1001.

Kölle, W., Strebel, O., and Böttcher, J., 1985, Formation of sulfate by microbial denitrification in a reducing aquifer: Water Supply, v. 3, no. 1, p. 35-40.

Kung, K.J.S., 1990, Preferential flow in a sandy vadose zone: 1. Field observation: Geoderma, v. 46, no. 1-3, p. 51-58.

Kuypers, M.M., Sliekers, A.O., Lavik, G., Schmid, M., Jorgensen, B.B., Kuenen, J.G., Sinninghe Damste, J.S., Strous, M., and Jetten, M.S., 2003, Anaerobic ammonium oxidation by anammox bacteria in the Black Sea: Nature, v. 422, no. 6932, p. 608-611.

Laincz, J., 2007, Qualitative dye tracer test at the Savoy Experimental Watershed plot : Unpublished Report.

Larsson, M.H., Jarvis, N.J., Torstensson, G., and Kasteel, R., 1999, Quantifying the impact of preferential flow on solute transport to tile drains in a sandy field soil: Journal of Hydrology, v. 215, no. 1-4, p. 116-134.

LeGrand, H., Stringfield, V., and LaMoreaux, P., 1976, Hydrologic Features of United States Karst Regions: Karst Hydrology and Water Resources, Proceedings of US-Yugoslavian Symposium, Dubrovnik, June 2-7, 1975, June 2-7, 1975

Leh, M.D.K., 2006, Quantification of rainfall-runoff mechanisms in a pasture dominated watershed: Fayetteville, University of Arkansas, M.S. Thesis, 101 p.

Luther III, G.W., Sundby, B., Lewis, B.L., Brendel, P.J., and Silverberg, N., 1997, The interaction of manganese with the nitrogen cycle in continental margin sediments: alternative pathways for dinitrogen formation: Geochimica et Cosmochimica Acta, v. 61, p. 4043-4052.

Mangin, A., 1975, Contribution à l'étude hydrodynamique des aquifères karstiques: Dijon, France, Université de Dijon, Ph.D., p.124

Mariotti, A., Landreau, A., and Simon, B., 1988, N-15 isotope biogeochemistry and natural denitrificatiion process in groundwater: Application to the chalk aquifer in Northern France: Geochimica et Cosmochimica Acta, v. 52, p. 1869-1878.

Martin, T.L., Kaushik, N.K., Trevors, J.T., and Whiteley, H.R., 1999, Review: Denitrification in temperate climate riparian zones: Water, Air, & Soil Pollution, v. 111, no. 1, p. 171-186.

Milanovic, P.T., 1981, Karst hydrogeology: Colorado, Water Resources Publications, 434 p.

Montgomery, E., Coyne, M.S., and Thomas, G.W., 1997, Denitrification can cause variable NO_3^- concentrations in shallow groundwater: Soil Science, v. 162, no. 2, p. 148-156.

Mookherji, S., McCarty, G.W., and Angier, J.T., 2003, Dissolved gas analysis for assessing the fate of nitrate in wetlands: Journal of the American Water Resources Association, v. 39, no. 2, p. 381-387.

Mortensen, A.P., Jensen, K.H., Nilsson, B., and Juhler, R.K., 2004, Multiple Tracing Experiments in Unsaturated Fractured Clayey Till: Vadose Zone Journal, v. 3, no. 2, p. 634-644.

Mull, D.S., Liebermann, T.D., Snoot, J.L., and Woosley, L.H., 1988, Application of dye-tracing techniques for determining solute transport characteristics of ground water in karst terranes: Atlanta, GA, US EPA, EPA904/6-88-001

Mull, D.S., Smoot, J.L., and Liebermann, T.D., 1988, Dye Tracing Techniques Used to Determine Ground-Water Flow in a Carbonate Aquifer System Near Elizabethtown, Kentucky: 87-4174, 95 p.

Myrold, D.D., and Hall, S.A., 1990, Measuring denitrification in soils using 15N techniques, *in* Revsbech, N.P., Sorensen, J. eds. Denitrification in Soil and Sediment: New York, USA, Plenum Press, p. 181-198.

Nascimento, C., Atekwana, E.A., and Krishnamurthy, R.V., 1997, Concentrations and isotope ratios of dissolved inorganic carbon in denitrifying environments: Geophysical Research Letters, v. 24, no. 12, p. 1511-1514.

Nielsen, K., Nielsen, L.P., and Rasmussen, P., 1995, Estuarine nitrogen retention independently estimated by the denitrification rate and mass balance methods: a study of Norsminde Fjord, Denmark: Marine Ecology Progress Series, v. 119, p. 275-283.

Parkin, T.B., 1987, Soil Microsites as a Source of Denitrification Variability: Soil Science Society of America Journal, v. 51, no. 5, p. 1194-1199.

Perrin, J., Jeannin, P., and Zwahlen, F., 2003, Epikarst storage in a karst aquifer: a conceptual model based on isotopic data, Milandre test site, Switzerland: Journal of Hydrology, v. 279, no. 1, p. 106-124.

Postma, D., Boesen, C., Kristiansen, H., and Larsen, F., 1991, Nitrate Reduction in an Unconfined Sandy Aquifer: Water Chemistry, Reduction Processes, and Geochemical Modeling: Water Resources Research, v. 27, no. 8, p. 2027-2045.

Pribyl, A.L., Mccutchan, J.H., Lewis, W.M., and Saunders III, J.F., 2005, Whole-system estimation of denitrification in a plains river: a comparison of two methods: Biogeochemistry, v. 73, no. 3, p. 439-455.

Quinlan, J.F., 1991, Use of dyes for tracing ground water: aspects of regulation: Proceedings of the Third Conference on the Hydrogeology, Ecology, Monitoring and Management of Ground Water in Karst Terranes, Nashville, Tennessee, p. 687-696.

Quinlan, J.F., and Aley, T., 1987, Discussion of "A new approach to the disposal of solid waste on land," by Heath R. C. and Lehr J. H. Ground Water, v. 25, no. 5, p. 615-616.

Quinlan, J.F., and Ewers, R.O., 1985, Ground Water Flow in Limestone Terranes: Strategy Rationale and Procedure for Reliable, Efficient Monitoring of Ground Water Quality in Karst Areas: Proceedings of the Fifth National Symposium and Exposition on Aquifer Restoration and Ground Water Monitoring, Columbus, Ohio, p. 197-234.

Quinlan, J.F., Ewers, R.O., Ray, J.A., Powell, R.L., and Krothe, N.C., 1983, Groundwater Hydrology and Geomorphology of the Mammoth Cave Region, Kentucky, and of the Mitchell Plain, Indiana, *in* Shaver, R.H., Sunderman, J.A. eds. Field Trips in Midwestern Geology: Bloomington, Indiana, Geological Society of American and Indiana Geological Survey, p. 1-85.

Reddy, K.R., Patrick Jr, W.H., and Lindau, C.W., 1989, Nitrification-denitrification at the plant root-sediment interface in wetlands: Limnology and Oceanography, v. 34, no. 6, p. 1004-1013.

Redfield, A.C., Ketchum, B.H., and Richards, F.A., 1963, The influence of organisms on the composition of sea-water, *in* Hill, M.N. ed. The Sea. Volume 2.: New York, USA, John Wiley & Sons, p. 26-77.

Robertson, L.A., Dalsgaard, T., Revsbech, N.P., and Kuenen, J.G., 1995, Confirmation of 'aerobic denitrification' in batch cultures, using gas chromatography and ^{15}N mass spectrometry: FEMS microbiology ecology, v. 18, no. 2, p. 113-120.

Sauer, T.J., and Logsdon, S.D., 2002, Hydraulic and Physical Properties of Stony Soils in a Small Watershed: Soil Science Society of America Journal, v. 66, no. 6, p. 1947-1956.

Scholefield, D., Hawkins, J.M.B., and Jackson, S.M., 1997, Development of a helium atmosphere soil incubation technique for direct measurement of nitrous oxide and dinitrogen fluxes during denitrification: Soil Biology and Biochemistry, v. 29, no. 9-10, p. 1345-1352.

Sexstone, A.J., Revsbech, N.P., Parkin, T.B., and Tiedje, J.M., 1985, Direct Measurement of Oxygen Profiles and Denitrification Rates in Soil Aggregates: Soil Science Society of America Journal, v. 49, no. 3, p. 645.

Shuster, E.T., and White, W.B., 1972, Source areas and climatic effects in carbonate groundwaters determined by saturation indices and carbon dioxide pressures: Water Resources Research, v. 8, no. 4, p. 1067-1073.

Sinreich, M., and Flynn, R., 2011, Comparative tracing experiments to investigate epikarst structural and compositional heterogeneity: Speleogenesis and Evolution of Karst Aquifers, no. 10, p. 253-258,

Sjodin, A.L., Lewis, W.M., and Saunders III, J.F., 1997, Denitrification as a component of the nitrogen budget for a large plains river: Biogeochemistry, v. 39, no. 3, p. 327-342.

Smart, C.C., Zabo, L., Alexander, E.C., and Worthington, S.R.H., 1998, Some Advances in Fluorometric Techniques for Water Tracing: Environmental monitoring and assessment, v. 53, no. 2, p. 305-320.

Smart, P.L., and Hobbs, S.L., 1986, Characterization of carbonate aquifers: a conceptual base: Environmental Problems in Karst Terranes and Their Solutions Proceedings, Bowling Green, Kentucky, USA, p. 1-14.

Smart, P.L., and Laidlaw, I.M.S., 1977, An evaluation of some fluorescent dyes for water tracing: Water Resources Research, v. 13, no. 1, p. 15-33.

Smith, R.L., Howes, B.L., and Duff, J.H., 1991, Denitrification in nitrate-contaminated groundwater: Occurrence in steep vertical geochemical gradients: Geochimica et Cosmochimica Acta, v. 55, p. 1815-1825.

Starr, R.C., and Gillham, R.W., 1993, Denitrification and Organic Carbon Availability in Two Aquifers: Ground Water, v. 31, no. 6, p. 934-947.

Strebel, O., Bottcher, J., and Fritz, P., 1990, Use of isotope fractionation of sulfate-sulfur and sulfate-oxygen to assess bacterial desulfurication in a sandy aquifer: Journal of Hydrology, v. 121, no. 1, p. 155-172.

Sweeting, M.M., 1973, Karst Landforms: New York, Columbia University Press, 362 p.

Sylvia, D.M., Fuhrmann, J.J., Hartel, P.G., and Zuberer, D.A., 1999, Principles and Applications of Soil Microbiology: Upper Saddle River, New Jersey, Prentice Hall, 550 p.

Ting, T., 2005, Assessing bacterial transport, storage and viability in mantled Karst of northwest Arkansas using clay and Escherichia coli labeled with lanthanide series metals: Fayetteville, University of Arkansas, Ph.D. Dissertation, p.279

Tooth, A.F., and Fairchild, I.J., 2003, Soil and karst aquifer hydrological controls on the geochemical evolution of speleothem-forming drip waters, Crag Cave, southwest Ireland: Journal of Hydrology, v. 273, no. 1, p. 51-68.

Urey, H.C., 1947, The thermodynamic properties of isotopic substances: Journal of the Chemical Society, v. 1947, p. 562-581.

Vandike, J., 1982, The effects of the November 1981 liquid-fertilizer pipeline break on groundwater in Phelps County, Missouri: 75

Veni, G., DuChene, H., Crawford, N.C., Groves, C.G., Huppert, G.H., Kastning, E.H., Olson, R., and Wheeler, B.J., 2001, Living with Karst: A Fragile Foundation (Environmental Awareness Series ed.), American Geological Institute, 64 p.

Vogel, J.C., Talma, A.S., and Heaton, T.H.E., 1981, Gaseous nitrogen as evidence for denitrification in groundwater: Journal of Hydrology, v. 50, p. 191-200.

White, W.B., 1988, Geomorphology and Hydrology of Karst Terrains: New York, Oxford University Press, 464 p.

Whitsett, K.S., 2002, Sediment and bacterial tracing in mantled karst at Savoy Experimental Watershed, northwest Arkansas: Fayetteville, University of Arkansas, M.S. Thesis, 66 p.

Winston, B.A., 2006, The biogeochemical cycling of nitrogen in a mantled karst watershed: Fayetteville, University of Arkansas, M.S. Thesis, p.88

Yoshinari, T., and Knowles, R., 1976, Acetylene inhibition of nitrous oxide reduction by denitrifying bacteria: Biochemical and Biophysical Research Communications, v. 69, no. 3, p. 705-710.

Zumft, W.G., 1992, The denitrifying prokaryotes, *in* Dworkin, M., Falkow, S., Rosenberg, E., Schleifer, K.H. and Stackebrandt, E. eds. The Prokaryotes: an evolving electronic resource

for the microbiological community: New York, New York, USA, Springer-Verlag, p. 554-582. at http:/141.150.157.117:8080/prokPUB/index.htm

3. INVESTIGATION OF NITRATE PROCESSING IN THE INTERFLOW ZONE OF MANTLED KARST, NORTHWEST ARKANSAS

ABSTRACT

Anthropogenic nitrate contamination of groundwater is a common problem in vulnerable terrains dominated by karst topography. Elucidation of in-situ nitrate dynamics is important to the design of sustainable land-management practices in these terrains. A field-scale study was conducted at a manure-amended, mantled karst site in the Ozark Highlands to characterize multiple potential sources and processes affecting nitrate in the interflow zone. Increased water residence time and water-matrix contact may favor nitrate attenuation processes, such as denitrification, in the interflow zone, which is situated between the soil and focused-flow (bedrock) zones. Groundwater samples were collected along the hydrologic gradient in and below the study plot and analyzed for reactive species concentration (nitrate), conservative species concentration (chloride), nitrate isotopic compositions ($\delta^{15}N$ and $\delta^{18}O$), and dissolved organic carbon concentration and bioavailability. Nitrate $\delta^{15}N$ and $\delta^{18}O$ indicated a mixed soil organic matter/manure origin of nitrate. Mass-balance calculations indicated that although mixing was the primary process decreasing nitrate concentration along flowpaths through the interflow zone, up to 33 percent of nitrate moving through the interflow zone may have been removed through microbial processing. The magnitude of this processing varied spatially and temporally. Nitrate $\delta^{15}N$ and $\delta^{18}O$ at the seeps exhibited a positive relationship, a possible indication of denitrification. Dissolved organic carbon bioavailability was elevated in the interflow zone relative to the focused-flow zone while dissolved organic carbon concentration was lower in the interflow zone than in the focused flow zone. This suggests that, compared to

the focused-flow zone, the interflow zone has a greater quality and greater utilization of carbon substrate, and consequently has greater potential for denitrification. Overall, the observations suggest that the interflow zone may be important for nitrate attenuation in karst systems.

INTRODUCTION

High nitrate (NO_3^-) concentrations in water are detrimental to man and the environment. High intake of NO_3^- may result in formation of potentially carcinogenic compounds in the human gastric system (Tenovuo, 1986) as well as low oxygen levels in blood of infants, a potentially fatal condition and the reason for the U.S. Environmental Protection Agency to regulate NO_3^- in drinking water by establishing maximum contaminant level of 10 mg/L NO_3^- as nitrogen (N) (Fan and Steinberg, 1996). Large amounts of NO_3^- discharging from agricultural watersheds have been implicated in the development of hypoxic zones around the world including in the Gulf of Mexico (Rabalais and others, 1996; Goolsby and Battaglin, 2001).

Intensive animal production in Northwest Arkansas generates large volumes of manure rich in NO_3^- precursors – organic N compounds. Counties in Northwest Arkansas are among 2% of U.S. counties which together generate 12% of the Nation's total manure N (Gollehon and others, 2001). With the mass of manure generated, these counties do not have sufficient crop and pasture land to assimilate the N generated (Gollehon and others, 2001). Moreover, these large volumes of manures are typically applied to pastures with soils which often are, as is the case in Northwest Arkansas, extremely thin with limited nutrient bioremediation potential. To accentuate problems further, Northwest Arkansas is underlain by karst; a carbonate rock terrain made up of interconnected and hierarchically enlarged fractures, conduits and large voids which can readily transport manure-derived contaminants into the deeper subsurface with little chance for attenuation. Unsurprisingly, numerous studies reported NO_3^- contamination in springs and

wells throughout Northwest Arkansas (Steele and McCalister, 1990; Adamski, 1997; Davis, Brahana, and Johnston, 2000; Laubhan, 2007) where demand for water is rapidly increasing, with the region being the sixth most dynamically growing Metropolitan Statistical Area in the country (U.S. Census Bureau, 2001).

To protect groundwater in this vulnerable landscape, effective manure management practices need to be designed that take into account the capacity of the local mantled karst environment to attenuate NO_3^-. That goal, in turn, requires elucidation of in-situ NO_3^- attenuation processes among which primarily are vegetative uptake, dilution with waters low in NO_3^-, and denitrification, i.e. microbial reduction of NO_3^- to N gases (NO, N_2O, N_2). Denitrification is the most important NO_3^- attenuation process in as much as it removes NO_3^- from the watershed in the form of N gases (Martin and others, 1999). These gases represent a longer term sink for N relative to N immobilization processes that lead to generation of organic N which may later be subjected to remobilization. Denitrification has been successfully measured using a range of methods in a wide range of terrestrial, marine, and freshwater environments (see review by Groffman and others, 2006). The occurrence of denitrification generally requires a set of conditions including NO_3^- and/or NO_2^- availability, presence of denitrifiers, low O_2 concentrations, sufficiently long residence time, and a supply of bioavailable organic matter (Seitzinger and others, 2006).

Karst environments are considered unfavorable to denitrification because of high flow velocities and low nutrient supply; however, many karst terrains, including Northwest Arkansas, are mantled by regolith (epikarst) containing impermeable layers such as relict insoluble chert ledges and fragipan. These along with the surface of the underlying limestone bedrock divert infiltrating groundwater laterally (Al-Rashidy, 1999; Little, 2001), creating a hydrologic

compartment known as the interflow zone. The interflow zone increases residence time, delays the movement of water into the deeper, less biogeochemically active, focused-flow compartment of the system, and facilitates contact between water and soil or rock where NO_3^- utilizing microbes reside. In addition, the interflow zone may contain surface-derived bioavailable dissolved organic matter as an energy source for denitrifiers. Thus the interflow zone may be an important zone of NO_3^- attenuation. However, this topic has been investigated by few studies, and the potential of the interflow zone for NO_3^- attenuation remains unclear. This study aimed to investigate this potential, including the occurrence of denitrification and other biogeochemical as well as physical processes affecting the fate of NO_3^- in the interflow zone, using a mass balance approach involving reactive (NO_3^-) and conservative (Cl^-) species, NO_3^- $\delta^{15}N$ and $\delta^{18}O$ isotopic composition, and dissolved organic carbon concentration (DOC) and bioavailability. This study hypothesized that the interflow zone, compared to the other compartments of karst, is a site of increased biogeochemical activity, including microbial processing of NO_3^-, enabled by favorable biogeochemical and hydrologic characteristics.

METHODOLOGY

Site

The study was conducted at the Savoy Experimental Watershed (SEW), near the town of Savoy, Arkansas. The area is typical of the mantled karst setting of the Springfield Plateau of the Ozarks where regolith covers the underlying chert-rich limestone. Topography is ridge and valley with elevation in the watershed ranging from 317 to 376 m. Land cover consists of hardwood forest (57%) and pasture (43%). The study focused on and around an instrumented plot in Basin 1 (Figure 3-1), which is drained by an ephemeral stream that flows towards the southwest and discharges into the Illinois River. Average annual rainfall for the area is 1,119 mm

with mean January and July air temperatures of 1.1 and 25.9°C, respectively (Owenby and Ezell, 1992).

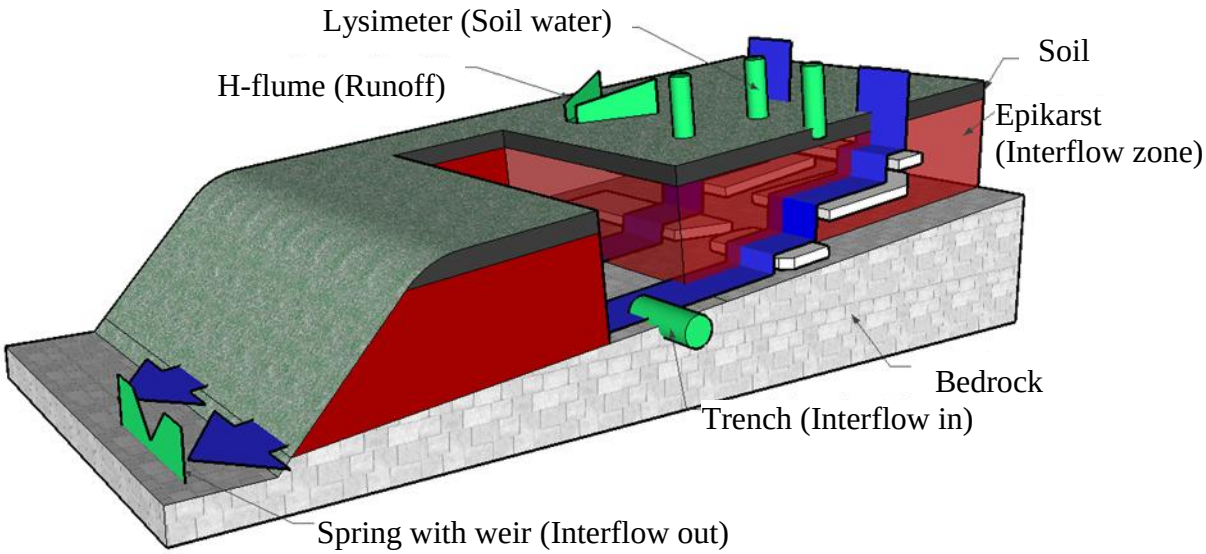

Figure 3-1 Diagram of study plot illustrating hydrogeologic components and sampling instruments. Langle and Copperhead Springs are located about 500 yards W from the site.

Sampling

The fate of NO_3^- was studied across a hydraulic gradient; from an infiltration area within and in the vicinity of an instrumented plot located on a ridge-top pasture (15% slope) in Basin 1, through the subsurface interflow zone, to the main drainage points of the basin – Langle and Copperhead Spring; special attention was given to the interflow zone. Hydrogeology of the system was established by previous research focusing on various aspects such as runoff and infiltration mechanisms (Sauer and others, 2000; Sauer and Logsdon, 2002; Leh, 2006), regolith and bedrock geophysics (Ernenwein and Kvamme, 2004), water and solute movement in the regolith mantle (Al-Qinna, 2003; Brahana and others, 2005; Brahana and others, 2006; Laincz,

2007) as well as saturated-flow characteristics and controls in the underlying bedrock (Brahana, 1995; Brahana, 1997; Brahana and others, 1999; Whitsett, 2002; Ting, 2005)(Brahana and others, 2005; Brahana, 1997). In summary, this research has shown that runoff events are rare, and rainfall tends to quickly infiltrate into the regolith mantle where water moves via diffuse and macropore flow both vertically and laterally; lateral movement – interflow – occurs owing to permeability contrasts presented by chert ledges, the bedrock surface, and soil features such as fragipans. Macropores including root channels, worm holes, and pores created by the loose contact between chert fragments and soil matrix are abundant and greatly accelerate water and solute flow through the mantle. At the study site, interflow paths begin in the upland area underneath a thin (30-75 cm) soil horizon relatively rich in organics. These emerge on the side slope down-gradient as springs. During wet antecedent conditions the time of travel of a solute from the upland plot area to these springs (through the interflow zone) can range from 10 to 40 hours. Downgradient of the emergence points, the flow forms a losing stream, with the water entering focused-flow dominated bedrock to emerge after approximately 500 meters at Langle and Copperhead Springs. The time of travel for this focused flow for a conservative tracer can be approximately 11.5 hours with the peak concentration arriving 15-19 hours after tracer injection (Whitsett, 2002; Ting, 2005).

Three distinct hydrologic components or zones of the system were characterized: diffuse flow (soil water), interflow (epikarstic flow), and focused flow (Figure 3-1). Diffuse flow was sampled by 8 suction-cup lysimeters installed 75 cm deep in the ground inside the plot; these samples required compositing owing to low-volume yield of individual lysimeters. The interflow zone was sampled at an upper and lower point on the flowpath in order to evaluate NO_3^- evolution along flow paths within this zone. The upper point (referred to as ‘interflow in’) was

an interceptor trench similar in design to the one in Smettem and others (1991) and constructed at the down-slope boundary of the plot. The second point (interflow out) consisted of three seeps (J2, J2b, J3) on the slope side, downgradient from the plot and the trench, representing the terminus of the interflow zone flowpaths. Finally, focused-flow sampling points included two main springs draining Basin 1, Copperhead and Langle, and one smaller spring adjacent to the plot area, J1. Dye tracing (Laincz, 2007) confirmed that J1 has no hydrologic connection to the plot area, and distinct physical and chemical parameters of its water suggest that it is dominated by focused flow. In addition, surface runoff was collected for three events. Discharge and field parameters including pH, conductivity, temperature, and dissolved oxygen were measured. Sampling was conducted for seven events between July 2004 and June 2005, three of which were conducted under storm flow and four under base-flow conditions. The plot area was amended with chicken litter in June and October 2004 at a rate of 5 tons per acre to simulate common agricultural practices in terms of NO_3^- loading and to increase NO_3^- signal.

Analysis

Samples were analyzed for major anions and cations using ion chromatography (EPA method 300.0) and ICP (EPA method 200.7), respectively. Stable isotopes of NO_3^- ($\delta^{15}N$ and $\delta^{18}O$) were analyzed using the Denitrifier Method (Sigman and others, 2001; Casciotti and others, 2002). The method precision and accuracy for $\delta^{15}N$ were 0.35‰ and 0.43‰, respectively, and for $\delta^{18}O$ they were 0.66‰ and 0.78‰, respectively. DOC concentration was determined using high-temperature combustion with a Shimadzu TOC5050 (Benner and Strom, 1993). Bioavailability of DOC was measured as groundwater community respiration normalized to DOC concentration and bacterial abundance, which was determined using epifluorescent microscopy (Porter and Feig, 1980). Details pertaining to bioavailability measurement as well as

to all of the above mentioned sampling and analytical procedures can be found in Winston (2006). Data analysis including analysis of variance, correlation and linear regression were performed using JMP version 8 (SAS Institute Inc., Cary, NC).

RESULTS AND DISCUSSION

DOC concentration and DOM bioavailability

DOC constituted 80% of total organic carbon in SEW water samples, providing the necessary substrate for microbial processes. DOC concentration ranged from 0.14 to 22.44 mg/L with overall median of 1.43 mg/L (Table 3-1). The median for high-flow events was slightly higher (3.03 mg/L) compared to low-flow events (1.10 mg/L), and DOC concentration of high-flow events also exhibited greater variability. Mean DOC concentrations for the July and December 2004 events were elevated relative to the other events sampled. DOC concentrations tended to decrease downgradient (Figure 3-2) suggesting possible utilization for microbial metabolic processes. Importantly, mean DOC concentrations were significantly different between the samples representing the trench (interflow in) and those of the interflow zone exit points, the seeps ($p = 0.0412$), indicating DOC loss along the flowpaths of the interflow zone.

DOM bioavailability was determined for only 12 samples all of which were collected from the higher discharge sites – J1, J2, Copperhead Spring and Langle Spring – due to difficulty obtaining sufficient representative sample volumes from the other sampling sites. In addition, no one sampling event included all of the four sites, and the July 2004 event was not sampled for bioavailability at all. Nevertheless, the available data indicate seasonal and spatial variation of DOM quality. DOM bioavailability in the interflow and focused-flow zones was lower during fall events relative to spring events (Figure 3-3), suggesting a relatively more refractory DOC pool during fall and influx of labile organic carbon from growing plants and microbial exudates

during spring. Spatially, comparing the individual sampling points, bioavailability was elevated in J2 and Langle Spring relative to J1 and Copperhead Spring. The sites representing the interflow zone exhibited about 2.6 times greater bioavailability than the focused-flow zone sites (Figure 3-4), indicating that the former has a more utilizable carbon substrate and increased potential for NO_3^- microbial processing.

Table 3-1 Field, chemical, isotopic, bacterial and DOC bioavailability parameters of the samples (Site acronyms: SUR = surface, LYS = lysimeters, TRE = trench, Jx = springs, LAN = Langle Spring, COP = Copperhead Spring)

Date/flow	Site	Temp. (°C)	pH	Specific Conduct. (uS/cm)	O_2 (mg/L)	Alkal. (mg/L)	Cl^-	NO_3^- /NO_2^--N (mg/L)	$\delta^{15}N$ (‰)	sd
3-Jul-04	SUR	-	-	-	-	41.3	1.49	1.6	2.15	0.23
high	LYS	-	-	-	-	54.4	20.5	0.64	9.66	0.12
	TRE	-	-	-	-	4.8	22.4	22.3	5.14	0.1
	J1	15.6	6.58	143	-	49.6	3	1.67	2.95	0.17
	J2	16.2	6.99	188	-	84.7	5.04	2	3.89	0.21
	J2B	16.6	6.93	166	-	68.3	10.6	2.42	4.22	0.06
	J3	17.2	6.23	141	-	65.5	4.72	1.4	3.59	0.15
	LAN	15.9	6.42	136	-	46.6	9.86	1.45	3.22	0.17
	COP	17	6.48	130	-	46.8	5.86	1.48	3.57	0.42
25-Sep-04	SUR	-	-	-	-	-	-	-	-	-
low	LYS	-	-	-	-	-	-	-	-	-
	TRE	-	-	-	-	-	-	-	-	-
	J1	15.2	7.17	295	8.1	117	4.81	3.64	-	-
	J2	16.7	7.05	293	6.7	119	4.89	3.37	-	-
	J2B	16.7	7.22	292	6.8	119	4.87	3.38	-	-
	J3	17	7.4	291	7.1	120	4.86	3.13	-	-
	LAN	16.4	7.14	345	8.4	127	6.55	5.55	-	-
	COP	15.5	7.48	388	7.7	135	6.48	7.86	-	-
1-Nov-04	SUR	-	-	-	-	-	-	-	-	-
high	LYS	-	-	-	-	-	-	-	-	-
	TRE	-	-	-	-	-	-	-	-	-
	J1	15.5	7.01	297	8.02	107	11.73	3.53	-	-
	J2	16.4	7.06	296	6.6	116	6.59	3.29	-	-
	J2B	16.4	7.01	295	6.72	-	5.67	3.41	-	-
	J3	16.7	7.19	293	7.17	113	7.55	2.91	-	-
	LAN	16.4	6.59	374	8.21	116	13.08	2.79	-	-
	COP	16.5	6.75	331	8.55	138	9.08	6.63	-	-
1-Dec-04	SUR	-	-	-	-	-	-	-	-	-

Date/flow	Site	Temp. (°C)	pH	Specific Conduct. (uS/cm)	O_2 (mg/L)	Alkal. (mg/L)	Cl^-	NO_3^- /NO_2^--N (mg/L)	$\delta^{15}N$ (‰)	sd
low	LYS	12.1	7.8	123	9.07	38.4	22.6	11.2	6.81	0.33
	TRE	8	7.71	770	11.8	48.2	37.5	48	5.04	0.44
	J1	12.2	7.73	290	9.39	-	4.37	3.12	4.12	0.66
	J2	12.9	7.44	295	8.14	30.8	4.8	3.26	4.36	0.12
	J2B	12.7	7.49	292	7.83	38.2	5.24	3.42	4.96	0.48
	J3	12.3	7.36	290	8.33	23.6	5.02	2.63	4.56	0.08
	LAN	15.2	7.49	220	9.52	34.5	3.59	1.3	5.53	0.17
	COP	14.9	7.61	233	9.3	76.5	3.82	3.3	6.74	0.14
7-Dec-04	SUR	10.3	7.15	216	6.61	27.4	9.12	5.8	3.35	0.21
high	LYS	12.8	6.76	216	6.33	25.5	31.5	19.4	6.89	0.05
	TRE	11.2	7.56	500	8.52	8.6	18.3	39.5	6.43	0.48
	J1	13.6	7.42	118	7.81	33.6	2.72	2.53	0.35	0.25
	J2	13.4	7.14	220	6.84	72.4	5.01	3.42	3.35	0.29
	J2B	12.8	7.55	228	6.62	47	8	7.96	5.26	0.69
	J3	13.3	7.02	125	7.36	43.6	4.61	1.4	1.04	0.09
	LAN	14	7.4	162	8.11	50.2	5.32	2.85	3.59	0.18
	COP	12.6	7.58	174	8.04	54.9	2.99	3.51	3.83	0.11
21-Mar-05	SUR	-	7.7	43	-	6.7	0.54	1.35	3.55	0.01
low	LYS	-	-	315	-	32.4	26.5	9.6	8.94	0.23
	TRE	-	-	-	-	-	-	-	-	-
	J1	13.9	7.37	297	-	117	4.16	3.43	4.69	0
	J2	12.6	7.39	302	-	116	4.26	3.26	5.02	0.21
	J2B	11.8	7.51	305	-	116	4.23	3.16	4.68	0.06
	J3	12.5	7.37	383	-	117	4.17	2.87	4.76	0.12
	LAN	12.9	7.38	260	-	105	3.75	2	7.89	0.12
	COP	13.9	7.49	342	-	117	5.87	6.72	8.84	0.15
13-Jun-05	SUR	-	-	-	-	-	-	-	-	-
low	LYS	-	-	-	-	-	-	-	-	-
	TRE	-	-	-	-	-	-	-	-	-
	J1	14.5	7.12	264	-	120	4.11	3.44	3.75	0.37
	J2	16.6	7.09	260	-	118	4.19	3.17	4.43	0.32
	J2B	16	7.04	264	-	121	4.18	3.15	4.18	0.44
	J3	16.5	7.27	262	-	122	4.11	2.94	4.19	0.09
	LAN	14.5	6.99	268	8.84	119	4.43	2.84	6.39	2.04
	COP	14.2	6.82	328	8.6	135	8.26	7.46	8.2	0.13

Table 3-1 Cont. Field, chemical, isotopic, bacterial and DOC bioavailability parameters of the samples (Site acronyms: SUR = surface, LYS = lysimeters, TRE = trench, Jx = springs, LAN = Langle Spring, COP = Copperhead Spring)

Date/flow	Site	$\delta^{18}O$ (‰)	sd	DOC-C (mg/L)	DIC-C (mg/L)	Bact. Abund. (10^4 cells/mL)	sd	Relat. Bioav.	sd
3-Jul-04	SUR	5.25	0.52	22.44	7.78	-	-	-	-
high	LYS	2.18	0.55	8.27	11.39	-	-	-	-
	TRE	2.42	0.37	3.77	2.62	-	-	-	-
	J1	4.83	0.34	3.55	24.82	270	21	-	-
	J2	4.82	0.04	2.09	21.86	250	12	-	-
	J2B	4.52	0.85	2.35	17.18	-	-	-	-
	J3	6.27	0.36	3.19	18.84	260	16	-	-
	LAN	3.21	0.53	2.33	17.22	150	18	-	-
	COP	3.08	0.29	2.6	30.85	210	27	-	-
25-Sep-04	SUR	-	-	-	-	-	-	-	-
low	LYS	-	-	-	-	-	-	-	-
	TRE	-	-	-	-	-	-	-	-
	J1	-	-	0.59	25.8	-	-	-	-
	J2	-	-	0.14	24.52	-	-	-	-
	J2B	-	-	1.1	26.71	-	-	-	-
	J3	-	-	0.18	26.24	-	-	-	-
	LAN	-	-	1.03	30.47	-	-	-	-
	COP	-	-	1.03	30.85	-	-	-	-
1-Nov-04	SUR	-	-	-	-	-	-	-	-
high	LYS	-	-	-	-	-	-	-	-
	TRE	-	-	-	-	-	-	-	-
	J1	-	-	0.5	24.37	4.7	0.16	1.5	0.2
	J2	-	-	0.58	24.35	2.3	0.03	-	-
	J2B	-	-	0.6	25.78	3.3	0.06	-	-
	J3	-	-	0.3	24.92	2.2	0.06	-	-
	LAN	-	-	0.76	26.41	5.2	0.47	-	-
	COP	-	-	0.62	27.8	1.5	0.12	1.2	0.9
1-Dec-04	SUR	-	-	-	-	-	-	-	-
low	LYS	4.95	0.56	3.08	6.01	-	-	-	-
	TRE	5.13	0.91	5.48	1.7	-	-	-	-
	J1	4.63	0.32	1.4	8.02	4.6	0.16	0.7	0.2
	J2	5.17	0.41	1.09	19.34	4	0.13	-	-
	J2B	5.27	0.3	4.03	19.27	-	-	-	-
	J3	6.4	0.6	1.48	19.57	3.2	0.22	-	-
	LAN	5.41	0.53	1.7	15.5	4.8	0.13	-	-
	COP	5.58	0.72	1.32	15.24	5.5	0.16	0.8	0.3
7-Dec-04	SUR	-0.89	0.45	22.2	2.62	-	-	-	-
high	LYS	4.72	0.51	4.55	5.33	-	-	-	-
	TRE	3.74	0.93	4.76	0.88	-	-	-	-
	J1	3.93	0.42	4.68	8.02	8.1	0.8	0.1	0.3
	J2	4.26	0.07	3.11	7.78	5.2	0.43	-	-
	J2B	4.04	0.45	2.96	10.32	-	-	-	-
	J3	4.43	0.57	4.07	7.97	5.2	0.37	-	-
	LAN	2.43	0.3	2.17	10.3	17	1.3	-	-

Date/flow	Site	$\delta^{18}O$ (‰)	sd	DOC-C (mg/L)	DIC-C (mg/L)	Bact. Abund. (10^4 cells/mL)	sd	Relat. Bioav.	sd
	COP	11.8	0.53	3.1	10.63	16	0.9	0.24	0.4
21-Mar-05	SUR	19.67	0.44	5.28	5.65	-	-	-	-
low	LYS	7.33	0.28	2.51	8.02	-	-	-	-
	TRE	-	-	-	-	-	-	-	-
	J1	6.53	0.07	0.92	26.54	3.6	0.14	-	-
	J2	8.21	0.36	0.97	24.26	5.4	0.12	19	0.4
	J2B	5.47	0.03	0.95	10.32	5.6	0.41	-	-
	J3	6.5	0.14	0.98	24.66	3.5	0.15	-	-
	LAN	6.92	0.18	1.45	26.81	5.1	0.39	16	0.3
	COP	6.35	0.63	1.36	27.97	4.8	0.32	15	0.3
13-Jun-05	SUR	-	-	-	-	-	-	-	-
low	LYS	-	-	-	-	-	-	-	-
	TRE	-	-	-	-	-	-	-	-
	J1	2.87	0.8	0.48	28.79	3.8	0.33	-	-
	J2	2	0.82	0.84	29.6	2.6	0.4	12	0.4
	J2B	2.22	0.74	1.3	28.48	-	-	-	-
	J3	5.86	0.23	0.86	32.9	2.3	0.33	-	-
	LAN	4.04	0.98	1.1	32.9	4	0.7	20	0.1
	COP	3.49	0.61	1.38	30.13	4.3	0.8	2	0.1

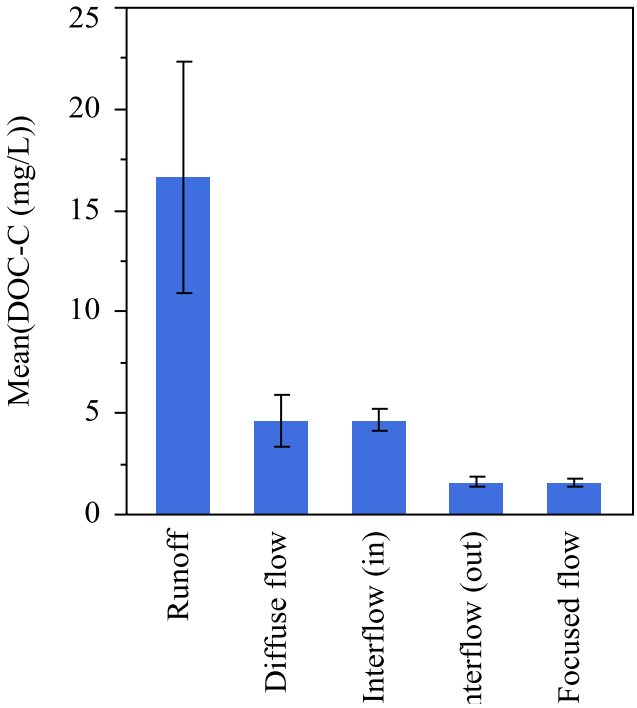

Figure 3-2 Mean (± 1 SE) DOC concentration across the hydrologic gradient

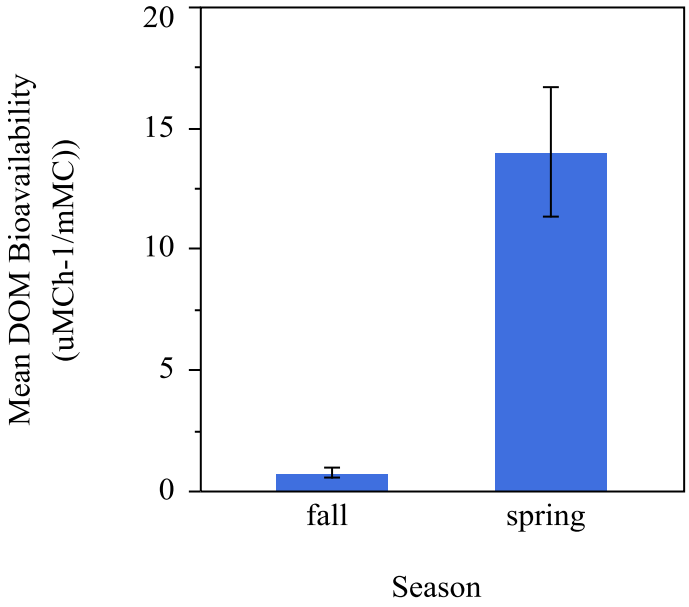

Figure 3-3 Mean (±1 SE) relative bioavailability of DOC by season

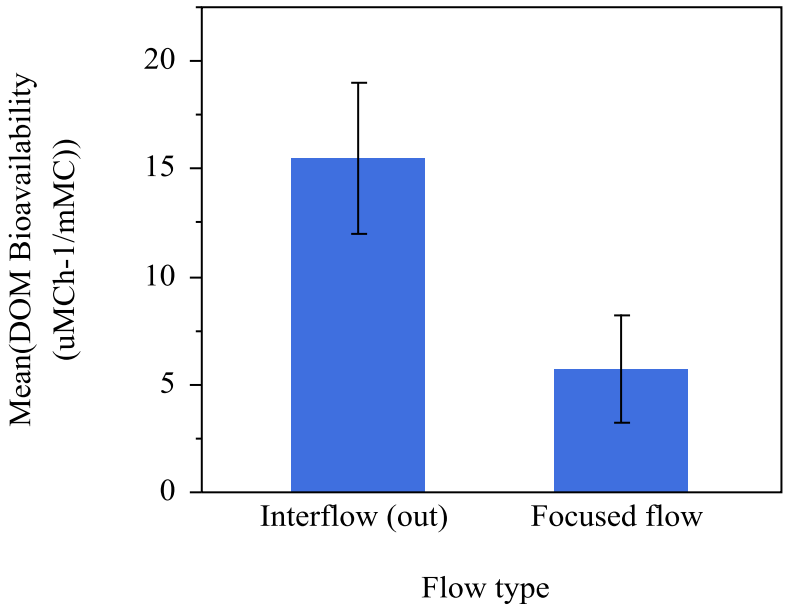

Figure 3-4 Mean (±1 SE) relative bioavailability of DOC by flow type. Focused flow is the mean of average bioavailabilities of seep J1, Langle and Copperhead Springs. Interflow (out) here represents seep J2.

Nitrate concentration and isotopic composition

NO_3^- concentration ranged from 0.64 to 48 mg/L throughout the study with a median of 3.3 mg/L (Table 3-1). Average NO_3^- concentrations were not significantly different among events. Along the gradient, NO_3^- concentration averages for lysimeters, trench, and Copperhead Spring were 10.2, 36.6, and 5.3 mg/L, respectively, which was higher relative to the interflow zone seeps and Langle Spring, where NO_3^- concentration was within a relatively narrow range of 2.8 to 3.4 mg/L. Similar to mean DOC concentration, NO_3^- concentration was significantly different between the trench (interflow in) and the interflow zone exit points, the seeps ($p < 0.0001$), indicating loss of NO_3^- along the interflow zone flowpaths. This loss was evaluated using a mixing model outlined below to determine the magnitude of processing in the interflow zone.

Nitrate $\delta^{15}N$ ranged from 0.35 to 9.66‰ and had a mean of 4.85‰ (Table 3-1). Seasonally, $\delta^{15}N$ values appeared to slightly increase during spring and fall; averages for spring and fall events were elevated relative to the overall mean by about 1.19 and 0.42‰, respectively. Across the flow path, the highest average value was in the diffuse-flow zone (8.08‰) and the lowest in the runoff samples (3.02‰). $\delta^{18}O\text{-}NO_3^-$ values ranged from -0.89 to 19.67‰ with a mean of 5.13‰. Similar to $\delta^{15}N$, $\delta^{18}O$ values also tended to increase during spring and fall. Average values for spring and fall events were elevated relative to the overall mean by about 3.24 and 0.19‰. Across the flow path, runoff had the highest average value (8.01‰) while the 'interflow in' (trench) samples had the lowest (3.76‰). The measured $\delta^{15}N$ and $\delta^{18}O$ values are similar to those published by other authors for groundwater in karst (Panno and others, 2001; Einsiedl, Maloszewski, and Stichler, 2005). Ninety percent of both $\delta^{15}N$ and $\delta^{18}O$ values fell between approximately 2 and 8‰, a range indicative of a mixture of nitrate derived from soil organic matter and animal manure (Clark and Fritz, 1997).

Denitrification is known to cause the $\delta^{15}N$ and $\delta^{18}O$ values of the residual NO_3^- to increase as a result of kinetic isotopic fractionation (Bottcher and others, 1990). In addition to this isotopic enrichment of the remaining NO_3^- pool, the ratio of the enrichment of oxygen to N tends to be close to 1:2 (Kendall and McDonnell, 1998) imparting an additional signal for recognition of denitrification. Nitrate $\delta^{15}N$ and $\delta^{18}O$ of the samples from the interflow zone-draining seeps and the adjacent small spring J1 positively correlate, indicating simultaneous enrichment in the heavy isotopes that could most plausibly be explained as the effect of denitrification (Figure 3-5). The linear relationship with a slope of 0.2 deviates from the 0.5 slope typical of denitrification. In addition, the strength of this correlation is relatively weak ($r^2 = 0.140671$; $p = 0.23$); however, studies of denitrification in natural settings rarely find a perfect fit with the model denitrification relationship, which may be still less likely to be found in a system as dynamic and heterogeneous as karst. The relationship as such could be a valid indication of denitrification.

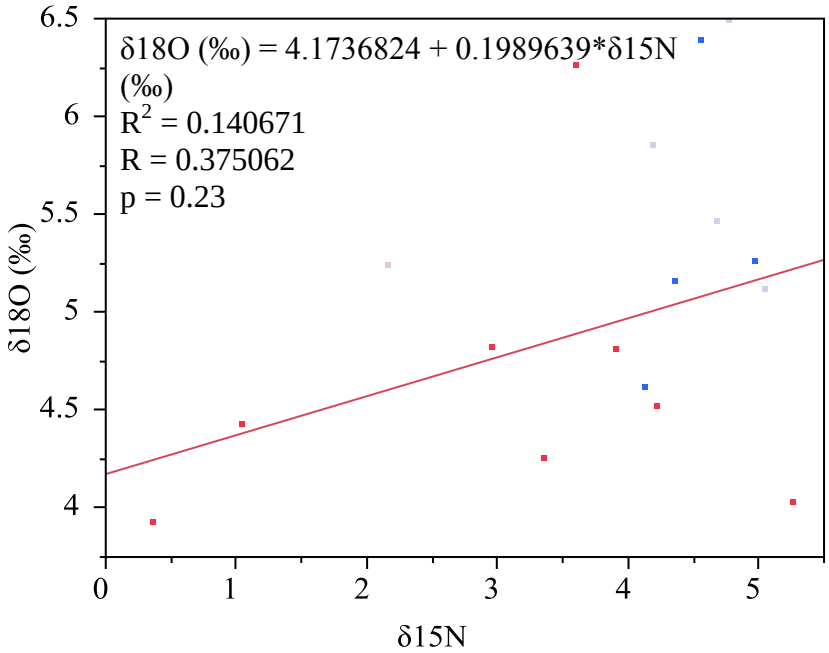

Figure 3-5 Co-linearity between $\delta^{15}N$ and $\delta^{18}O$ of seep and J1 samples

Nitrate processing: a binary mixing model

Three post-storm sampling events (July 3, December 1 and 7, 2004) were conducted under hydrologic conditions wet enough to induce flow in the trench, and these events thus enabled assessing NO_3^- evolution between the trench as an upper interflow zone point and interflow zone exit points – the seeps. Concentrations of solutes in the seeps were lower as compared to the trench. For example, average Cl^- concentration at the seeps was 75% lower than the average concentration at the trench. In addition, for a given trench-seep flowpath, the magnitude of the decrease was unequal between conservative and reactive species; NO_3^- decrease was on average 16% greater than Cl^- decrease. While the decrease in Cl^- indicated dilution or mixing along the interflow zone flowpaths, the greater decrease in NO_3^- concentration indicated the existence of an additional likely mechanism of NO_3^- removal – microbial processing.

The amount of microbial processing was evaluated for the three sampling events by modeling NO_3^- and DOC concentrations expected at the seeps as a result of mixing (dilution) and comparing these model values to measured values, which represent the combined effects of mixing and microbial processes, such as microbial assimilation and denitrification. Microbial processing would have decreased NO_3^- and DOC concentration beyond the decrease resulting from mixing.

The evidence of dilution along the trench-seep flowpaths led us to adopt a flow model that assumed two types of water mixing along these flow paths, producing a mixture discharging out of the seeps; one type infiltrating in and carrying the chemical and isotopic signature of the up-gradient plot, where manure amendment had provided a strong solute source, and another type infiltrating in and carrying the chemical and isotopic signature of the surrounding unamended off-plot area. Based on dye-tracing evidence, the interceptor trench immediately down-gradient

from the plot was considered representative of the plot water, and spring J1 with lack of hydrologic connection to the plot was regarded as representative of off-plot water type.

Nitrate and DOC concentrations expected in the mixtures of plot and off-plot waters were calculated using a common two-component mass-balance equation (Faure and Mensing, 2005; Fry, 2006):

$$X_M = X_P * f_P + X_{OP} * f_{OP}$$

where X_M, X_P, and X_{OP} are the concentrations of DOC or NO_3^- in a seep mixture, plot and off-plot water components, respectively, and *f* represents the mass fractions or mixing proportions of these components. The mass fractions were calculated by solving the equation above for f_P using conservative species (Cl^-) as concentrations. The off-plot mass fraction f_{OP} was then obtained by subtracting f_P from 1.

Table 3-2 lists the mass fractions of plot and off-plot components calculated for each seep mixture, NO_3^- concentrations expected in the seep mixtures from mixing, corresponding measured concentrations, and the difference between calculated and measured. Average calculated NO_3^- concentration in the seep mixture was 6.6 mg/L. Average measured concentration, however, was about 3.1 mg/L, and so the average 3.47 mg of missing NO_3^- in a liter of the seep mixture was possibly denitrified and/or microbially immobilized. Since plant roots at the site do not reach into the interflow zone, assuming that microbial processing is indeed the process responsible for the missing NO_3^- is reasonable. Performing similar calculations with DOC, 0.23 mg/L on average of DOC loss in the interflow zone mixtures could not be accounted for by plot/off-plot mixing and was likely consumed by some DOC-utilizing microbial process. Although the calculated amount of missing DOC appears modest, it may be

underestimated. Other potential inputs of DOC percolating into the interflow zone flow-paths and not accounted for in the mixing equation may have increased the final measured DOC concentration and thus reduced the calculated difference ascribable to processes other than mixing.

Table 3-2 NO_3^- concentration measured and predicted by the binary mixing model, and the difference between the two ascribable to microbial processing

Sampling event	Seep	Endmember fractions		Nitrate, mg/L			Nitrate Processing, %
		Plot (Trench)	Off-plot (J1)	Modeled	Measured	Mod.-Meas.	
3-Jul-04	J2	0.11	0.89	3.84	2	1.84	8
3-Jul-04	J2b	0.39	0.61	9.75	2.42	7.33	33
3-Jul-04	J3	0.09	0.91	3.50	1.4	2.10	9
1-Dec-04	J2	0.01	0.99	3.70	3.26	0.44	1
1-Dec-04	J2b	0.03	0.97	4.30	3.42	0.88	2
1-Dec-04	J3	0.02	0.98	4.00	2.63	1.37	3
7-Dec-04	J2	0.15	0.85	7.96	3.42	4.54	12
7-Dec-04	J2b	0.34	0.66	15.06	7.96	7.10	18
7-Dec-04	J3	0.12	0.88	7.01	1.4	5.61	14

CONCLUSIONS

Mass-balance calculations based on two-component mixing indicated that most of NO_3^- concentration decrease in the interflow zone was caused by dilution. Between 1 and 33%, however, depending on the flowpath, was removed by additional processes, which likely included microbial processing since uptake by vegetation does not occur in the interflow zone. The $\delta^{15}N$ and $\delta^{18}O$ values of this remnant NO_3^- present in the seep samples and the adjacent site J1 exhibited a positive correlation ($r = 0.4$; $p = 0.23$), possibly an indication of denitrification. Nitrate $\delta^{15}N$ and $\delta^{18}O$ also proved useful in accurately pinpointing the source of this nitrate – a

mixture of organic matter and animal manure. DOC concentration generally decreased along the flowpath and mass-balance computation showed that, for the majority of seep samples, dilution could not account for this decrease entirely. As a result, another carbon consuming process, utilization by microbes, likely occurred. Both DOC concentration and DOM bioavailability were elevated in the interflow zone relative to focused-flow paths, giving the former a greater potential for NO_3^- attenuation. Temporally, DOC as well as NO_3^- increased during high-flow conditions, creating favorable conditions for microbial processing of NO_3^-. In the karst watershed as a whole, DOM bioavailability appeared to be influenced by seasonality, with spring having greater DOM bioavailability than fall, suggesting an influx of labile organic matter during spring. Whereas all measured parameters varied considerably in both time and space, the overall evidence from this study have largely confirmed the original hypothesis: the interflow zone appears to be a zone of increased NO_3^- attenuation, including microbial processing and possibly denitrification, enabled by sufficient supply or availability of DOC. It seems that more research in this area is warranted to confirm the occurrence of NO_3^- attenuation mechanisms and, importantly, to determine how they are affected by environmental variables, flow path, and land use.

REFERENCES

Adamski, J., 1997, Nutrients and Pesticides in Ground Water of the Ozark Plateaus in Arkansas, Kansas, Missouri, and Oklahoma: 96-4313

Al-Qinna, M.I., 2003, Measuring and modeling soil water and solute transport with emphasis on physical mechanisms in karst topography: Fayetteville, University of Arkansas, Ph.D. Dissertation, 273 p.

Al-Rashidy, S.M., 1999, Hydrogeologic controls of groundwater in the shallow mantled karst aquifer, Copperhead Spring, Savoy Experimental Watershed, northwest Arkansas: Fayetteville, University of Arkansas, M.S. Thesis, p.96

Benner, R., and Strom, M., 1993, A critical evaluation of the analytical blank associated with DOC measurements by high-temperature catalytic oxidation: Marine Chemistry, v. 41, no. 1, p. 153-160.

Bottcher, J., Strebel, O., Voerkelius, S., and Schmidt, H.L., 1990, Using isotope fractionation of nitrate-nitrogen and nitrate-oxygen for evaluation of microbial denitrification in a sandy aquifer: Journal of Hydrology, v. 114, no. 3-4, p. 413-424.

Brahana, J.V., 1995, Controlling influences on ground-water flow and transport in the shallow karst aquifer of northeastern Oklahoma and northwestern Arkansas: Proceedings of the Arkansas Water Resources Center 1994 Research Conference, Fayetteville, Arkansas, p. 25.

Brahana, J.V., 1997, Rationale and methodology for approximating spring-basin boundaries in the mantled karst terrane of the Springfield Plateau, northwestern Arkansas, *in* Beck, B.F., Stephenson, J.B. eds. The engineering geology and hydrogeology of karst terranes: United States (USA), AA Balkema, Rotterdam, p. 77-82.

Brahana, J.V., Hays, P.D., Kresse, T.M., Sauer, T.J., and Stanton, G.P., 1999, The Savoy Experimental Watershed—Early lessons for hydrogeologic modeling from a well-characterized karst research site, *in* Palmer, A.N., Palmer, M.V. and Sasowsky, I.D. eds. Karst Modeling: Special Publication No. 5: Charlottesville, VA, Karst Water Institute, p. 247-254. at http://www.karstwaters.org/publications/curpubslist.htm

Brahana, J.V., Killingbeck, J.J., Stielstra, C., Leh, M.D.K., Murdoch, J.F., and Chaubey, I., 2006, Elucidating flow characteristics of epikarst springs using long-term records that encompass extreme hydrogeologic stresses: Geological Society of America Abstracts with Programs, Philadelphia, Pennsylvania, v. 38, p. 196.

Brahana, J.V., Ting, T.E., Al-Qinna, M., Murdoch, J.F., Davis, R.K., Laincz, J., Killingbeck, J.J., Szilvagyi, E., Doheny-Skubic, M., Chaubey, I., Hays, P.D., and Thoma, G., 2005, Quantification of hydrologic budget parameters for the vadose zone and epikarst in mantled karst: U. S. Geological Survey Karst Interest Group Proceedings, Rapid City, South Dakota, September 12-15, 2005, September 12-15, 2005, v. U.S. Geological Survey Scientific Investigations Report 2005-5160, p. 144-152.

Casciotti, K.L., Sigman, D.M., Hastings, G.M., Bohlke, J.K., and Hilkert, A., 2002, Measurement of the Oxygen Isotopic Composition of Nitrate in Seawater and Freshwater Using the Denitrifier Method: Analytical Chemistry, v. 74, no. 19, p. 4905-4912.

Clark, I.D., and Fritz, P., 1997, Environmental Isotopes in Hydrogeology: Boca Raton, Florida, CRC Press LLC, 328 p.

Davis, R.K., Brahana, J.V., and Johnston, J.S., 2000, Groundwater in Northwest Arkansas: Minimizing Nutrient Contamination From Non-Point Sources in Karst Terrane. MSC-288, 69 p.

Einsiedl, F., Maloszewski, P., and Stichler, W., 2005, Estimation of denitrification potential in a karst aquifer using the N-15 and O-18 isotopes of NO3−: Biogeochemistry, v. 72, no. 1, p. 67-86.

Ernenwein, E.G., and Kvamme, K.L., 2004, Geophysical Investigations For Subsurface Fracture Detection In The Savoy Experimental Watershed, Arkansas: Unpublished report, Department of Biological and Agricultural Engineering, University of Arkansas, 24 p.

Fan, A.M., and Steinberg, V.E., 1996, Health Implications of Nitrate and Nitrite in Drinking Water: An Update on Methemoglobinemia Occurrence and Reproductive and Developmental Toxicity: Regulatory Toxicology and Pharmacology, v. 23, no. 1, p. 35-43.

Faure, G., and Mensing, T.M., 2005, Isotopes: Principles and Applications (3rd ed.): Hoboken, New Jersey, Wiley, 896 p.

Fry, B., 2006, Stable isotope ecology, Springer, 308 p.

Gollehon, N., Caswell, M., Ribaudo, M., Kellogg, R., Lander, C., and Letson, D., 2001, Confined Animal Production and Manure Nutrients: USDA Agriculture Information Bulletin, no. AIB771, p. 1-40.

Goolsby, D.A., and Battaglin, W.A., 2001, Long-term changes in concentrations and flux of nitrogen in the Mississippi River Basin, USA: Hydrological Processes, v. 15, no. 7, p. 1209-1226.

Groffman, P.M., Alatabet, M.A., Bohlke, J.K., Butterbach-Bahl, K., David, M.B., Firestone, M.K., Giblin, A.E., Kana, T.M., Nielsen, L.P., and Voytek, M.A., 2006, Methods For Measuring Denitrification: Diverse Approaches To a Difficult Problem: Ecological Applications, v. 16, no. 6, p. 2091-2122.

Kendall, C., and McDonnell, J.J., 1998, Isotope Tracers in Catchment Hydrology: Amsterdam, Elsevier Science B.V., 839 p.

Laincz, J., 2007, Qualitative dye tracer test at the Savoy Experimental Watershed plot: Unpublished Report.

Laubhan, A.C., 2007, A hydrogeologic and water-quality evaluation of the Springfield aquifer in the vicinity of North-Central Washington County, Arkansas: Fayetteville, University of Arkansas, M.S. Thesis, 182 p.

Leh, M.D.K., 2006, Quantification of rainfall-runoff mechanisms in a pasture dominated watershed: Fayetteville, University of Arkansas, M.S. Thesis, 101 p.

Little, P.R., 2001, Characterization and development of a conceptual model of groundwater flow and transport in Basin 2, Savoy Experimental Watershed, Northwest Arkansas: Fayetteville, University of Arkansas, M.S. Thesis,

Martin, T.L., Kaushik, N.K., Trevors, J.T., and Whiteley, H.R., 1999, Review: Denitrification in temperate climate riparian zones: Water, Air, & Soil Pollution, v. 111, no. 1, p. 171-186.

Owenby, J.R., and Ezell, D.S., 1992, Monthly station normals of temperature, precipitation, and heating and cooling degree days, 1961-1990, Arkansas. Climatography of the United States No. 81:

Panno, S.V., Hackley, K.C., Hwang, H.H., and Kelly, W.R., 2001, Determination of the sources of nitrate contamination in karst springs using isotopic and chemical indicators: Chemical Geology, v. 179, no. 1-4, p. 113-128.

Porter, K., and Feig, Y., 1980, The use of DAPI for identification and enumeration of bacteria and blue-green algae: Limnol.Oceanogr, v. 25, p. 943-948.

Rabalais, N.N., Turner, R.E., Justic, D., Dortch, Q., Wiseman, W.J., and Sen Gupta, B.K., 1996, Nutrient changes in the Mississippi River and System Responses on the Adjacent Continental Shelf: Estuaries and Coasts, v. 19, no. 2, p. 386-407.

Sauer, T.J., Daniel, T.C., Nichols, D.J., West, C.P., Moore, P.A.,Jr., and Wheeler, G.L., 2000, Runoff Water Quality from Poultry Litter-Treated Pasture and Forest Sites: Journal of Environmental Quality, v. 29, p. 515-521.

Sauer, T.J., and Logsdon, S.D., 2002, Hydraulic and Physical Properties of Stony Soils in a Small Watershed: Soil Science Society of America Journal, v. 66, no. 6, p. 1947-1956.

Seitzinger, S., Harrison, J.A., Bohlke, J.K., Bouwman, A.F., Lowrance, R., Peterson, B., Tobias, C., and Van Drecht, G., 2006, Denitrification across landscapes and waterscapes: a synthesis. Ecological Applications, v. 16, no. 6, p. 2064-2090.

Sigman, D.M., Casciotti, K.L., Andreani, M., Barford, C., Galanter, M., and Bohlke, J.K., 2001, A Bacterial Method for the Nitrogen Isotopic Analysis of Nitrate in Seawater and Freshwater: Analytical Chemistry, v. 73, p. 4145-4153.

Smettem, K.R.J., Chittleborough, D.J., Richards, B.G., and Leaney, F.W., 1991, The influence of macropores on runoff generation from a hillslope soil with a contrasting textural class: Journal of Hydrology, v. 122, no. 1-4, p. 235-252.

Steele, K.F., and McCalister, W.K., 1990, Nitrate concentrations of ground water from limestone and dolomitic aquifers in the Northeastern Washington County area, Arkansas: MSC-68

Tenovuo, J., 1986, The biochemistry of nitrates, nitrites, nitrosamines and other potential carcinogens in human saliva: Journal of oral pathology, v. 15, no. 6, p. 303-307.

Ting, T., 2005, Assessing bacterial transport, storage and viability in mantled Karst of northwest Arkansas using clay and Escherichia coli labeled with lanthanide series metals: Fayetteville, University of Arkansas, Ph.D. Dissertation, p.279

U.S. Census Bureau, 2001, Metropolitan Areas Ranked by Percent Population Change: 1990 to 2000: accessed January 1, 2008, at http://www.census.gov/population/cen2000/phc-t3/tab05.pdf

Whitsett, K.S., 2002, Sediment and bacterial tracing in mantled karst at Savoy Experimental Watershed, northwest Arkansas: Fayetteville, University of Arkansas, M.S. Thesis, 66 p.

Winston, B.A., 2006, The biogeochemical cycling of nitrogen in a mantled karst watershed: Fayetteville, University of Arkansas, M.S. Thesis, p.88

4. CHARACTERIZATION OF EPIKARSTIC FLOW UNDER HIGH-FLOW CONDITIONS AT THE SAVOY EXPERIMENTAL WATERSHED, NORTHWEST ARKANSAS, USING DYE TRACING

ABSTRACT

Epikarst, the weathered, upper portion of karst developed in many karst terrains is a potential site of denitrification and thus may play an important role in nitrate attenuation in these regions. Epikarst denitrification has recently been studied at the Savoy Experimental Watershed, NW Arkansas as documented in other chapters of this dissertation. The goal of this study was to complement these efforts with an in-situ characterization of epikarstic flow using a natural-gradient, quantitative dye tracer test. Uranine dye (3 kg) was injected in post-storm conditions into two trenches situated on a ridge-top pasture. For 16 days with one significant rain event (11.4 cm), water samples were collected at downgradient resurgence points (an interceptor trench and 5 epikarstic springs) and subsequently analyzed for uranine concentration. Rainfall, discharge, water temperature and specific conductance were also measured. The epikarst exhibited a dynamic response to recharge events, with a nearly instantaneous discharge increase, culmination at 60 and 200 times the baseflow level on average, and return to baseflow level in 2-4 hours after rainfall cessation. Dye was positively detected at all of the sites except for one (J1). The breakthrough occurred about 60 hours after injection and was associated with a storm-induced flow pulse. Travel velocities ranged from 1.0 to 2.2 m/h. Both the dynamic hydraulic response and the velocities exceeding the hydraulic conductivity of the epikarst matrix indicated flow through preferential flowpaths. Dye recovery rate was 0.82%. Relatively low temperature indicated deeper flowpaths for J1. Event water dominated the epikarst storm discharge (45-85% of discharge) and steadily decreased to >1% after the storm. All of the measured parameters

varied greatly in space indicating heterogeneity of the system. Overall, the results confirm that the epikarst is a subsystem of karst with unique hydrologic properties. From a contaminant transport standpoint, epikarst transport of a point-source solute can be relatively rapid; however transport is dependent on saturation (flow pulse).Under the normal weather pattern and as long as the solute source does not reach into the deeper, perennially saturated zone, the epikarst appears to have a good ability to contain a point-source contaminant.

INTRODUCTION

Karst aquifers, an important source of drinking water world-wide, are highly vulnerable to contamination, including nitrate (NO_3^-) contamination (Power and Schepers, 1989; Boyer and Pasquarell, 1996). This is due to the typical karst features such as thin or missing soil cover, direct point-recharge via sinkholes, or rapid, concentrated flow in conduits with little microbial remediation and high rates of dispersion. A case in point is the karst region under study in NW Arkansas, where intense animal production and excess nutrient generation have been linked to elevated NO_3^- concentrations in local wells and springs (Adamski, 1997; Steele and McCalister, 1990; Davis, Brahana, and Johnston, 2000; Laubhan, 2007).

Many karst systems, however, contain a zone of potential NO_3^- attenuation via denitrification, i.e., microbial conversion of NO_3^- to N gases. This zone is the epikarst, generally defined as the weathered, typically 3-15 m thick, upper portion of karst (Ford and Williams, 2007). The U.S. karst map (Veni and others, 2001) classifies in excess of 50% of U.S. karst as buried, i.e., containing the epikarst. In addition, significant volumes of discharge from catchments come from the epikarst; during high flow conditions, this contribution can be in the range of 30-35% (Perrin, Jeannin, and Zwahlen, 2003; Einsiedl, 2005), but it can be as high as

55% (Lee and Krothe, 2001). This illustrates the potential impact of the epikarst on the quality of water discharging out of watersheds.

The epikarst could be conducive to denitrification thanks to several distinct hydrologic properties. For example, it has a tendency to detain and delay recharge (Einsiedl, 2005; Bakalowicz, 1995; Aquilina, Ladouche, and Dörfliger, 2006) as porosity and permeability diminish with depth, often leading to formation of the epikarstic aquifer (Mangin, 1975). This translates into increase in residence time, an important denitrification factor (Seitzinger and others, 2006; Green and others, 2009). The decrease in permeability with depth also induces lateral flow (Klimchouk, 2004) which manifests itself as epikarst springs on hillsides and acts to route the flow away from vertical shafts and conduits leading to the phreatic zone in the deeper bedrock. Friedrich and Smart (1981) also noted significant lateral diffusion within the epikarst, with lateral spread as much as 80 m. In addition, studies documented that the epikarst is a chemically reactive zone. Aquilina and others (2006) observed changes in Cl^-, Br^-, oxygen-18 and deuterium composition of the epikarst waters through interaction with soil and biological processes. Similarly, Sinreich and Flynn (2011) demonstrated the attenuation capacity of the epikarst for reactive solutes using organic dye and phosphate tracers.

At the same time, hydraulic behavior of the epikarst is considerably heterogeneous. Klimchouk (2004) describes several flow components within the epikarst (shaft or conduit flow, vertical vadose flow, and lateral vadose seepage) and further notes that while the epikarst generally accounts for recharge retardation and considerable mixing, the epikarst also provides for quick hydraulic response at shaft flow and springs in many systems. In addition, tracing studies have found the co-existence of pathways of varying flow velocity. For example, Bottrell and Adkinson (1992) studying the Peninn epikarst in England identified three separate flow

components with residence times of approximately 3 days, 30 to 70 days, and 160 or more days. Similarly, a study of epikarst in Slovenia found flowpaths of differing velocities, including rapid (0.5-2 cm/s), slower (around 0.1 cm/s), and the slowest (<0.001 cm/s) (Kogovšek and Šebela, 2004). Tracer experiments conducted in the epikarst of the Swiss Jura mountains found faster (preferential) and slower pathways (Sinreich and Flynn, 2011). Flow through the epikarst can occur as diffuse seepage through the primary porosity, through secondary porosity of fissures and joints, and through conduit flow such as cave streams (Gillieson, 1996; Klimchouk, 2000). Locally at the Savoy site, Al-Rashidy (1999) studying a pair of major Basin 1 springs describes the phenomenon of shifting spring basin boundaries with changing hydrologic conditions; separate under low flow while shifting and overlapping under high flow conditions, with one spring (Copperhead) acting as the overflow spring. Al-Rashidy (1999) also notes systematic differences in temperature, pH, specific conductance, and discharge between the springs.

In recent years, intensive research of nitrate attenuation processes in the epikarst has been conducted at an epikarst site in Basin 1 of the Savoy Experimental Watershed (Winston, 2006; Laincz and others, 2009; Laincz, 2011). These studies were accompanied by a rudimentary hydrologic characterization based on qualitative dye tracer tests. However, accurately reconstructing biogeochemical processes in any hydrologic system requires a comprehensive understanding of the system's hydrology which can only be achieved through more sophisticated methods such as quantitative dye tracing. In addition, the heterogeneous nature of the epikarst means that the findings of hydrologic investigations at other locations may not apply, and the complexity of groundwater flow including prominent joint- and fracture-flow precludes simulation using Darcy's law-based models.

Therefore, to complement biogeochemical studies at the Savoy site and, as a secondary goal, to add to the knowledge of hydrologic functioning of the epikarst in general, this study conducted an in-situ hydrologic characterization of the epikarst at the Savoy site using a natural-gradient, quantitative dye-tracing test. This characterization focused primarily on identification of flow trajectories and times of travel; determination of tracer concentrations and tracer recovery loads; and assessment of the overall hydrology of the system from the standpoint of contaminant (NO_3^-) transport and attenuation.

In preparation for this test, four preliminary qualitative tracer tests had been performed at the site between 2005 and 2007 with the purpose of identifying correct sampling locations (hydraulic connections), sampling frequencies, type of tracer dye, tracer load, and other parameters important for designing a successful quantitative tracer test. These efforts provided several useful insights regarding in-situ water and solute movement as well as application of dye tracing in this type of epikarst setting. These tests are therefore summarily described at the beginning of the results and discussion section.

METHODOLOGY

Site description

The study site is located in Basin 1 of the Savoy Experimental Watershed (SEW), near the town of Savoy in Northwestern Arkansas. Geologically, the area is typical of the mantled karst setting of the Springfield Plateau of the Ozarks with regolith covering the underlying chert-rich limestone. Topography of the watershed consists of ridges and valleys with elevation ranging from 317 to 376 m. Land cover consists of hardwood forest (57%) and pasture (43%). Basin 1 is drained by an ephemeral stream that flows towards the southwest and discharges into the Illinois

River. Average annual rainfall for the area is 1,119 mm with mean January and July air temperatures of 1.1 and 25.9°C, respectively (Owenby and Ezell, 1992).

In-situ epikarst description

The studied segment of the epikarst underlies a north-sloping (15%) ridge-top pasture bounded along the north side by an erosional side slope with five epikarstic springs (Figure 4-1). The epikarst profile consists of 0.5-3 m thick cherty soil cover with chert content of up to 60%, sometimes referred to as the regolith, dominated by Clarksville cherty silt loam (Loamy-skeletal, siliceous, semiactive, mesic Typic Paleudults) (Sauer and Logsdon, 2002). An important hydrologic feature of the soil cover are abundant macropores including root channels, worm holes, and pores created by the loose contact between chert fragments and soil matrix that greatly accelerate water and solute flow (Al-Qinna, 2003). The epikarst is located beneath the soil where ground-penetrating radar (GPR) and electrical resistivity surveys revealed a highly fractured and weathered stratified carbonate unit (bedrock) starting about 0.5-1 m deep in the upper half of the site and about 1.5-3 m deep in the lower half toward the side slope (Ernenwein and Kvamme, 2004) (Figure 4-2). This epikarst profile structure was subsequently confirmed during drilling and excavation efforts. Stratigraphically, the epikarst horizon is part of the regional silicic-carbonate Boone formation, which in Basin 1 is approximately 30 to 80 feet thick and underlain by relatively pure limestone of St. Joe formation (Al-Rashidy, 1999) (Figure 4-3).

Principles of quantitative dye tracing

This study employed the technique of quantitative dye tracing, a fundamental tool for determining subsurface water and solute movement, which has been successfully applied in numerous epikarst studies (Al-Qinna, 2003; Stone and others, 1995; Aley, 1997; Kogovšek and Šebela, 2004; Brahana and others, 2006; Petrella, Falasca, and Celico, 2008). The method

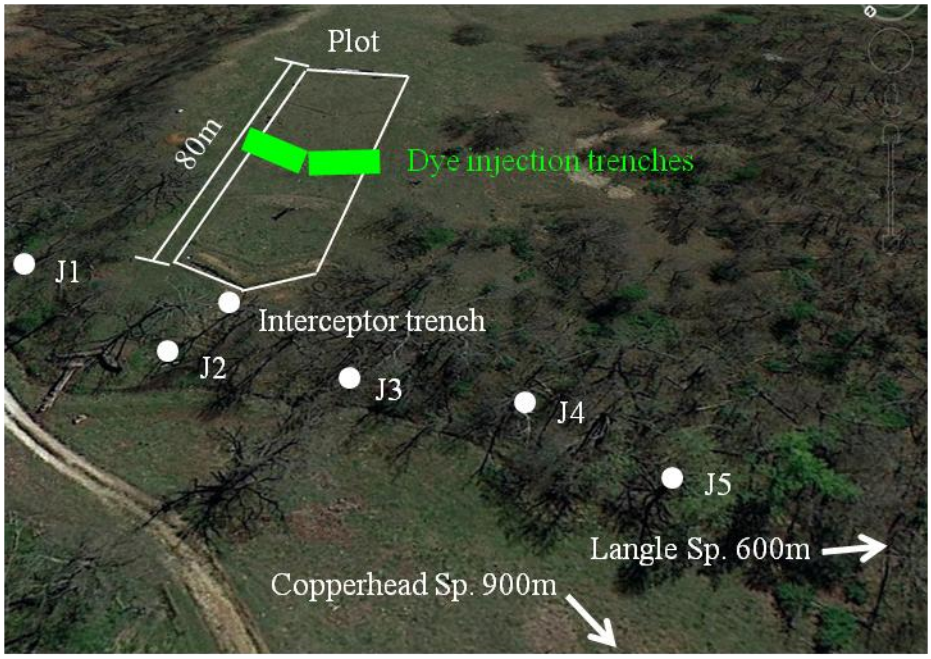

Figure 4-1 Location of the injection trenches, the interceptor trench and epikarstic springs J1, J2, J3, J4 and J5. Distances from the injection trenches to the sampling sites are as follows: J1 = 69 m, J2 = 81 m, J3 = 94 m, J4 = 116, J5 = 137 m, and Interceptor trench = 66 m. (Image from Google Earth)

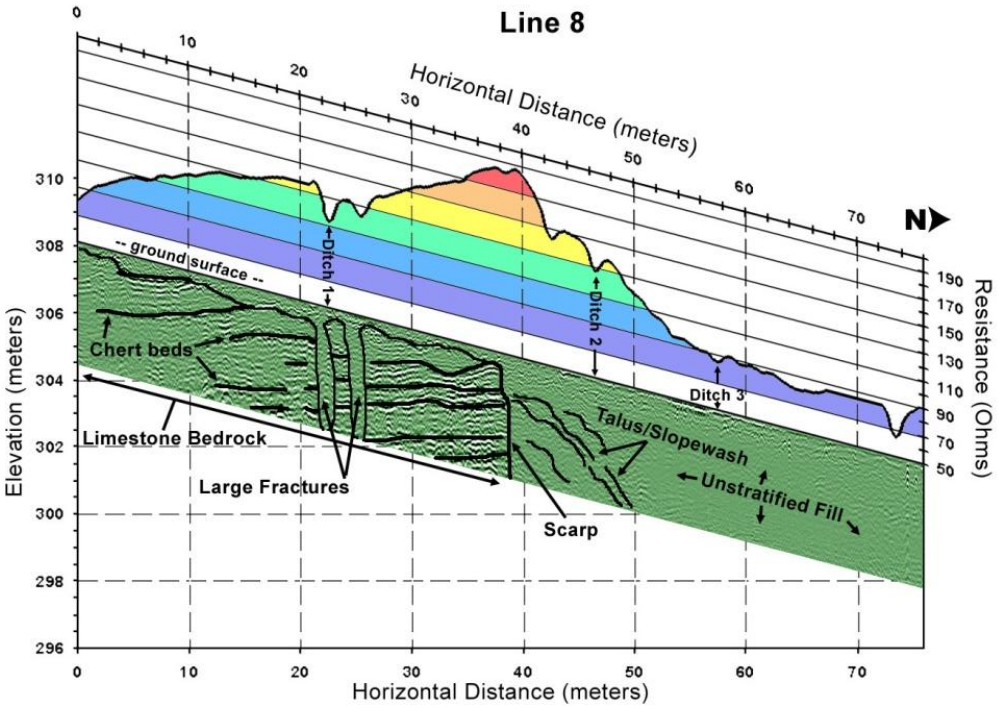

Figure 4-2 Ground penetrating radar profile of epikarst through the middle of the plot lengthwise (plot shown on image above). (Ernenwein and Kvamme, 2004)

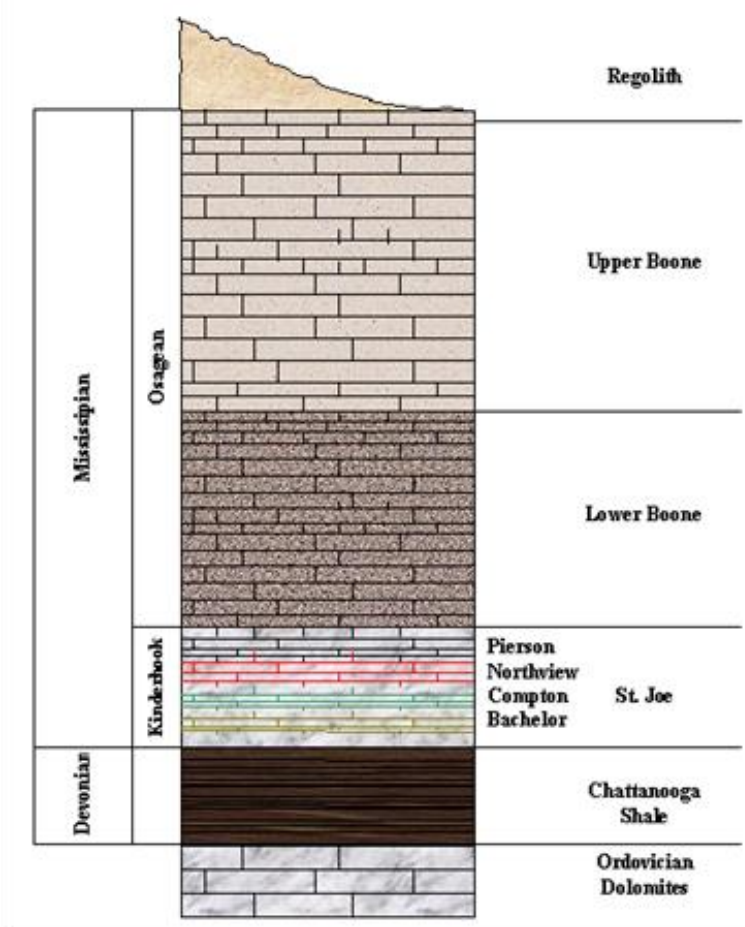

Figure 4-3 Stratigraphic column for the SEW (Bartholmey, 2001)

utilizes the fact that a soluble, nonreactive tracer (e.g., fluorescent dyes) released into water behaves in the same manner as the water particles, and hence tracing the movement of the tracer effectively traces the movement of the carrying fluid (Kilpatrick and Wilson Jr, 1989). Quantitative dye tracing consists of injection of a known quantity of dye and the measurement of the concentration of dye at all points of discharge that are hydraulically connected to the injection site. Determination of total dye recovery also requires the measurement of groundwater discharge. Water samples are typically collected with automatic samplers and analyzed for dye concentration using a properly calibrated fluorometer. These data are plotted against time to obtain a dye hydrograph or tracer breakthrough curve. The breakthrough curve can be used to

determine characteristics such as the rate of travel between the injection site and the recovery site (groundwater flow velocity), peak tracer concentration, tracer dispersion, mixing, tracer persistence or others. It can also be used to estimate a variety of parameters related to geometry and hydraulic properties of the aquifer. A complete description of these calculations along with theoretical background of quantitative dye tracing is provided in Mull and others (1988) or Field (2002); the second publication also includes software for calculation of these parameters. An informative review paper on the use of dyes as tracers in hydrology, including properties and analytical considerations, was published by Flury and Wai (2003).

Quantitative tracer test (2010)

A natural-gradient, quantitative dye tracer test was conducted from July 13 until July 29, 2010 (collection of trench samples stopped on July 20). The hydraulic connections between the tracer injection and resurgence points were established by a previous qualitative dye tracer test (Laincz, 2007).

The tracer introduction point consisted of two trenches located in the mid-section of an instrumented research plot established on the pasture by previous studies (Figure 4-4). The trenches (each 4x0.75x1m, LxWxD) were dug down to resistant layers of the epikarst and are oriented perpendicular to the slope/flow lines.

The sampling stations downgradient from the injection trenches included an interceptor trench and five epikarstic springs. The interceptor trench (10x1x1.5m, LxWxD) is located on the pasture about 66 m down the slope from the injection trenches. It is dug down to compact epikarst, roughly perpendicular to the flow lines, and features a French drain. It intercepts the epikarst throughflow midway along the studied flowpath. The epikarstic springs are located on the side slope downgradient from the interceptor trench and about 69 to 137 meters from the

injection trenches (Figure 4-1). The springs represent the terminal points of the flowpaths within the studied section of the epikarst.

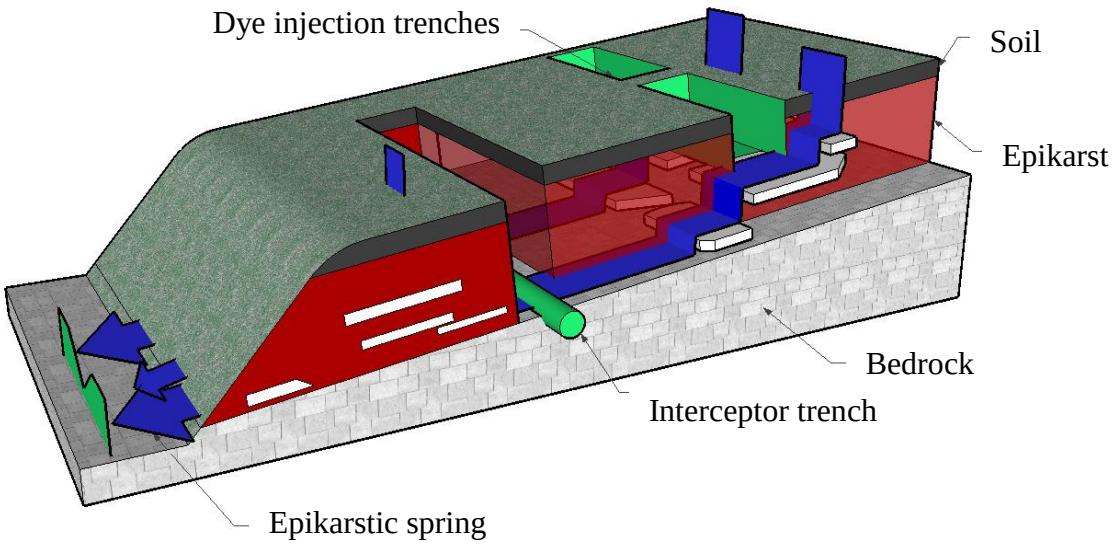

Figure 4-4 Conceptual model of the epikarst site featuring injection and sampling points

Uranine was used as the tracer dye. This dye was selected due to low sorption and high chemical stability making it suitable for use in epikarst conditions (Aley, 1997). A solution of 3 kg of the dye in 8 l of water was poured into the trenches on the morning of July 13 (Figure 4-5). The preceding night (July 12) saw a 10 cm rainfall (Figure 4-6) which filled the trenches with water which served as carrier or chaser water helping to move the tracer through the system. The initial concentration of the tracer slug of dye solution mixed with trench water was around 500 ppm. A second rainfall of 11.4 cm occurred in the late evening of July 15. This storm re-filled half-empty trenches and provided additional chaser water. A third rainfall came on July 26 and was of negligible magnitude of 0.7 cm.

Samples were collected using automatic portable samplers (Hach Sigma 900MAX). The sampling interval varied from 3 hours to 24 hours (except for one 5-day interval prior to the last

Figure 4-5 Dye injected into trenches situated on the pasture inside the instrumented plot. The trench in the upper photograph is on the east side of the plot, the other trench is on the west side. (Photo by author)

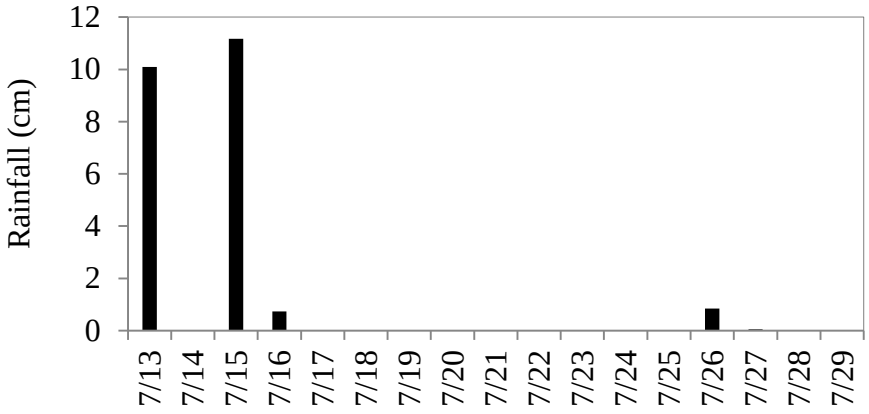

Figure 4-6 Total daily precipitation during the experiment

sample), with shorter intervals during rain events. Discharge from the springs was determined from stage levels of ponds created by the v-notch weirs. The stage data and water temperature were measured every 15 minutes using pressure transducers. Discharge and temperature at the trench were measured manually at selected times during the test. Specific conductance of the samples was determined in the lab using a conductivity meter (VWR Symphony SP80PC). Uranine concentration was also determined in the lab using a scanning spectrofluorophotometer (Shimadzu RF 5000). The analytical procedure generally followed the guidelines in Wilson and others (1986). The optimal emission and excitation wavelengths for the uranine dye as determined by synchronous scan were 508.8 and 489.6 nm, respectively. The instrument's detection limit for this dye in water is 0.0005 ppb (Aley, 1998).

The results were analyzed using the Qtracer2 program for the analysis of tracer-breakthrough curves from tracer studies in karstic aquifers (Field, 2002). The program generates tracer breakthrough curves and automatically calculates parameters such as total quantity of tracer recovered, mean tracer velocity, aquifer volume, and others. Definitions and equations for

calculating these parameters can be found in the respective reference. The parameters are listed in Table 4-2; those relevant to this study are discussed below.

RESULTS AND DISCUSSION

Qualitative tracer tests (2005-2007)

Four preliminary qualitative tracer tests had been conducted at the site between 2005 and 2007 aiming to determine hydraulic connections and tracer travel times between the plot area and downgradient discharge points.

The first three of these failed; no tracer came through likely due to an insufficient amount of the tracer used, persistent dry conditions, or an insufficient volume of chaser water, or a combination of these. The first two tests were performed simultaneously on July 30, 2005, and both failed likely due to insufficient tracer quantities. One of these used 0.5 kg of fluorescein introduced as a solution into three 10 cm wide boreholes at the upper boundary of the plot (Figure 4-1) and chased by 1,000 gallons of water. The other one used 1.8 kg of bromide dissolved in 2,000 gallons of water and sprayed over the plot area, chased by another 6,000 gallons delivered from a fire tanker truck. The third tracer test was conducted in June 2006 and failed likely as a result of insufficient rainfall which was relied on as chaser water. The test applied 50 kg of sodium bromide sprinkled on the plot in the middle of a 1.9 cm storm. During the next five months with the average monthly precipitation of approximately 9.1 cm, the tracer was detected only in lysimeters sampling soil water from the upper 85 cm of soil inside the plot. The low amount of rainfall combined with high evapotranspiration rates during the summer months may have been the reason why the tracer did not move past the soil horizon (Dr. Kris Brye, personal communication, March 2007).

The fourth test was conducted in January 2007. A solution made from 1.5 kg of sodium fluorescein dye was poured into two trenches dug in the middle section of the plot (Figure 4-1). Activated charcoal packets were placed and regularly replaced at monitoring points which included J1, J2, J2B (a spring immediately adjacent to J2, which later dried out), J3, J4, J5, and trench (Figure 4-1). Subsequent elution of the packets and visual assessment of fluorescence revealed that the tracer arrived at J2, J2B, J3, J4, and J5 within 10 hours after injection. The tracer reached the trench at a later time, during the subsequent 30-hour sampling interval, and also continued to appear at the springs. It continued to arrive at all of the points for the remainder of the test (7 days), although concentration steadily decreased, as indicated by decreasing amounts of dye in the elutants (Figure 4-7). No dye was detected at J1; extremely weak fluorescence in two J1 samples was deemed to be caused by organic matter. Visual qualitative comparison of fluorescence of the elutants under UV light indicated that J3 and J4 tended to have to have the most amount of dye; the trench had an intermediate amount; J2/J2B, J5 the least amount (Figure 4-7). These amounts could indicate dye concentration and hence the degree of hydraulic connection between the discharge point and the plot given that all of the aspects of sampling, preparation and analysis (e.g., quality/quantity of charcoal, placement conditions of the packets in the springs, elutriation process, reagents, fluorescence evaluation) were consistent for all samples in order to achieve equivalent adsorption or elutriation efficiency and detection characteristics. Overall, the relatively close travel times in spite of the varying travel distances and the apparent variable concentration of dye at different springs indicate a heterogeneous character of the epikarst, which is consistent with varying solute transport velocities and non-linear character of flowpaths observed in the local epikarst by Al-Qinna (2003). In addition, the tracer arrival times of up to 40 hours indicated a faster solute transport than can be ascribed to

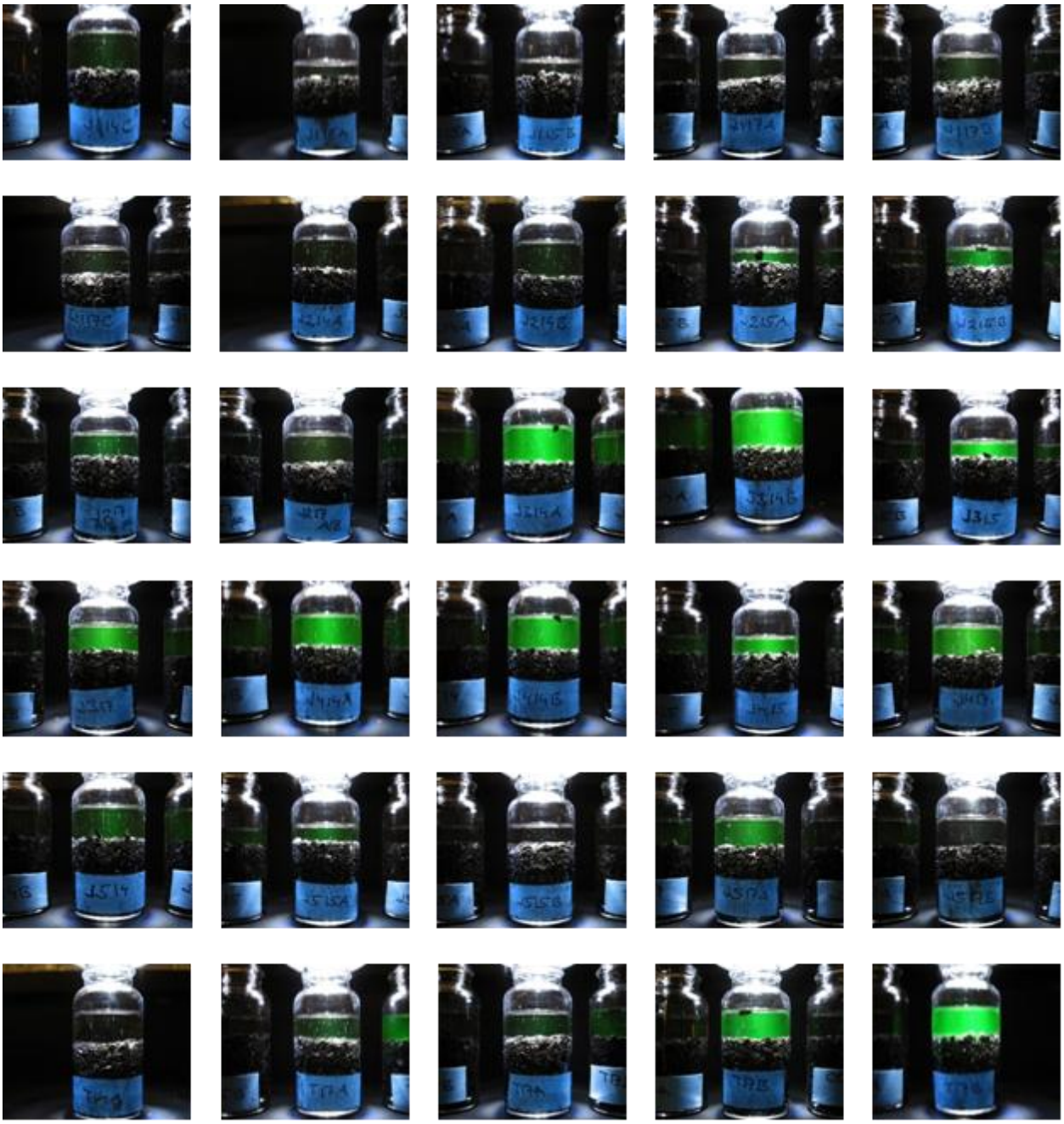

Figure 4-7 Elutants of charcoal samples from 2007 tracer test showing the presence of fluorescein at the monitored springs and trench. Samples are grouped by sampling site, arranged from J1 through J5 and trench. Within sites, 14, 15, 17 represent successive collection batches (sampling periods). (Photo by author)

matrix flow, suggesting the presence of preferential flowpaths also noted in previous research (Al-Qinna, 2003; Brahana and others, 2005; Leh and others, 2008). Most importantly, recovery

of the dye confirmed the existence of viable lateral flowpaths through the epikarst acting to divert some of the flow away from conduits in the bedrock. Finally, no detection of dye at J1 suggested lack of hydraulic connection to the plot (based on this, J1 was selected to represent off-plot water in a 2-component mixing model in Chapter 3).

Quantitative tracer test (2010)

Hydraulic response to storms

The quantitative tracer test was conducted from July 13 until July 29, 2010. This period saw a total of three storm events; only the first two were strong enough to significantly affect the discharge, as is reflected in the hydrographs (Figure 4-8).

During the first storm of July 13 (10 cm), the discharge of all of the springs except for J4 increased within an hour from the beginning of the storm, then fluctuated with changing rain intensity, and reached its maximum about three hours into the storm in all springs simultaneously. On average, the springs peaked at 60 times their average discharge rate during baseflow (Figure 4-8). Discharge returned to baseflow levels in about 1-2 hours except for J1 where it took about 6 hours. During the second storm of July 15 (11.4 cm), which unlike the first one did not have fluctuating intensity but one period of relatively intense rainfall, discharge at the springs rapidly increased about 90 minutes into the storm as rainfall increased, leading half an hour later to culmination at about 200 times the baseflow level on average (Figure 4-8). The return to baseflow levels occurred within 1-4 hours.

Both the first and the second storm hydrographs thus show a relatively rapid and strong discharge response to rainfall recharge. A quick and pronounced hydraulic response to recharge is typically encountered in conduit-dominated karst systems; however, according to Klimchouk (2004), many epikarst systems exhibit a similar behavior. Peaky hydrographs with steep rising

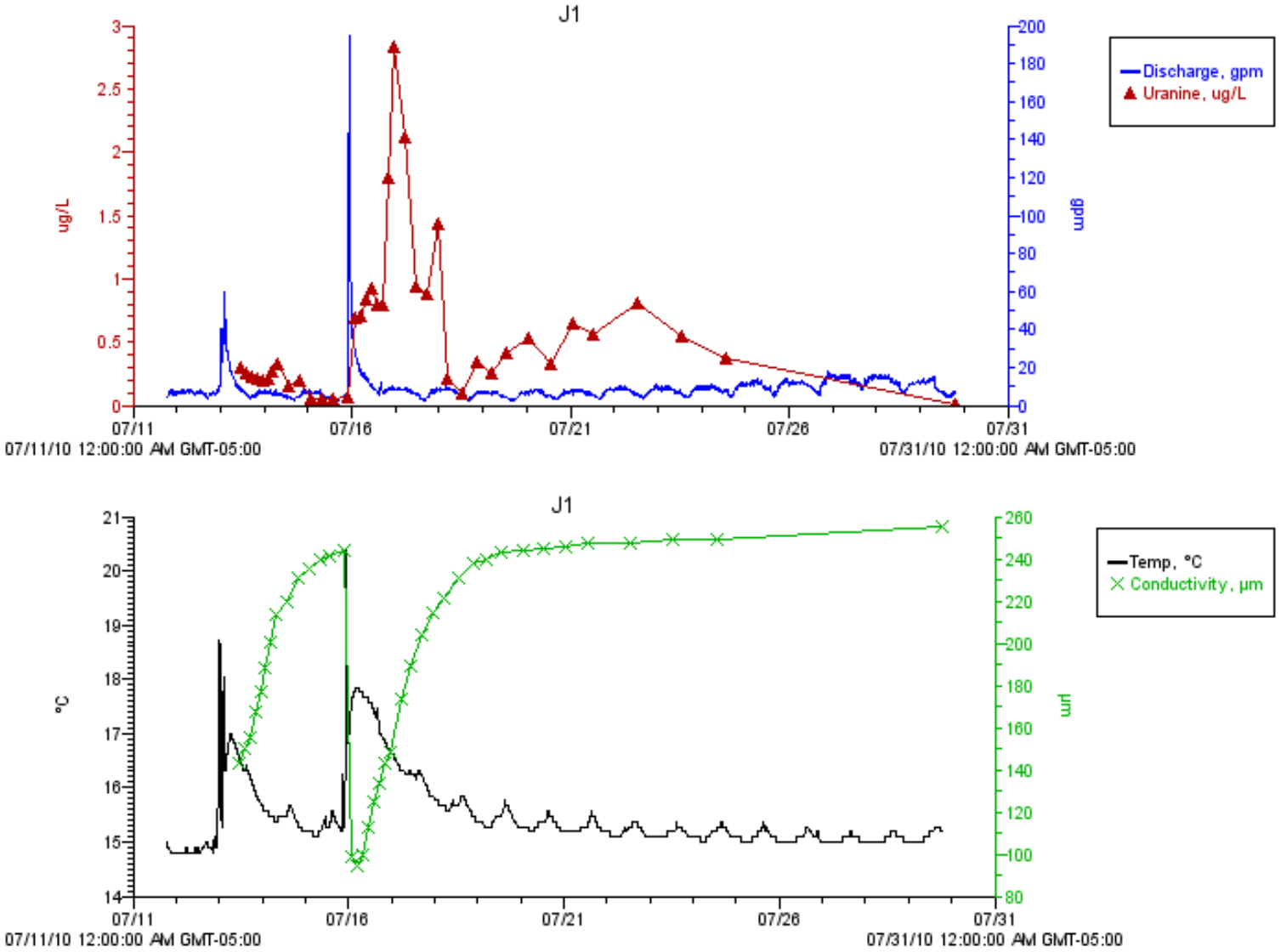

Figure 4-8 Hydrograph, tracer breakthrough curve, spec. conductance and temperature for the sampled springs and trench

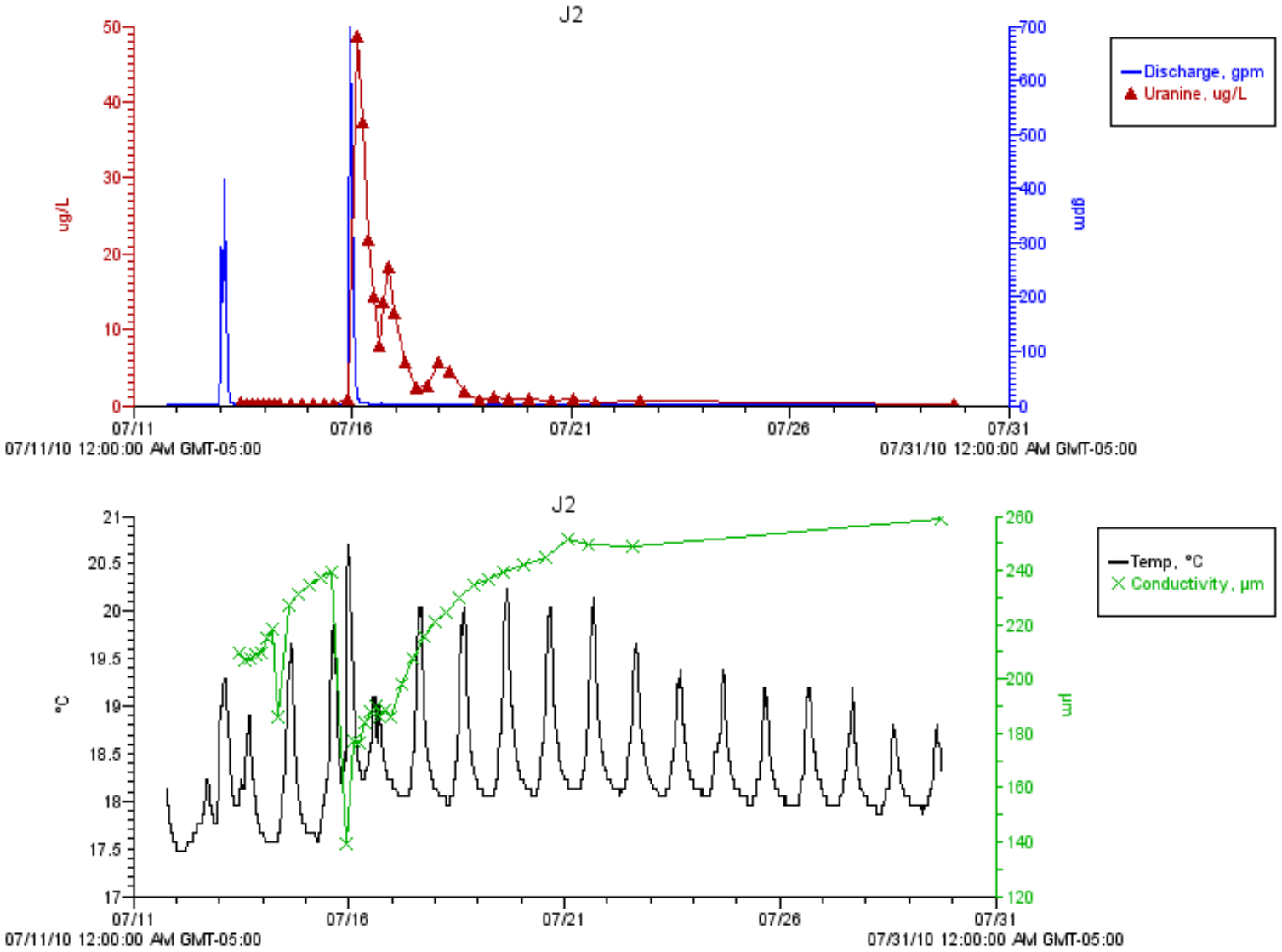

Figure 4-8 Cont. Hydrograph, tracer breakthrough curve, spec. conductance and temperature for the sampled springs and trench

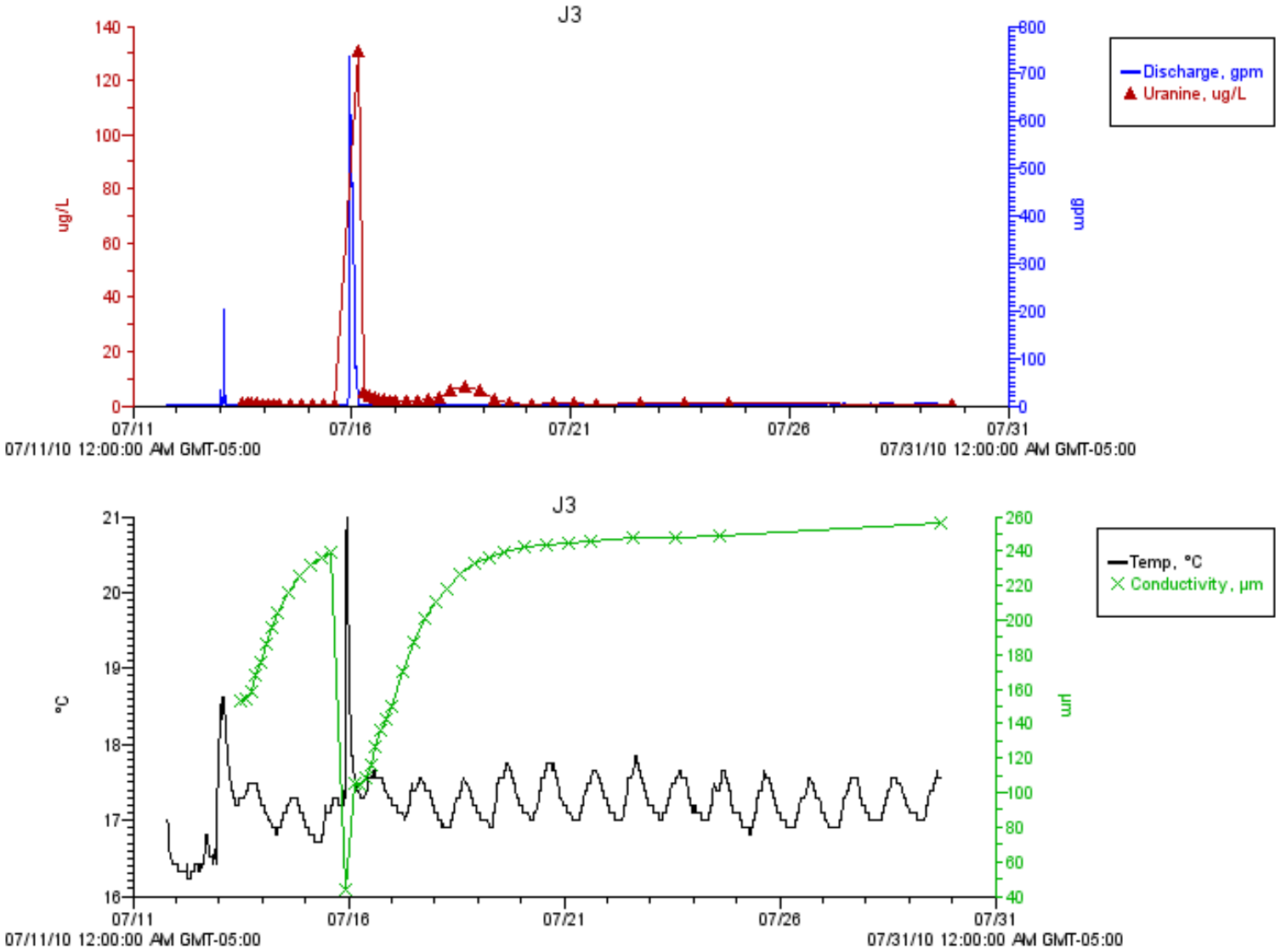

Figure 4-8 Cont. Hydrograph, tracer breakthrough curve, spec. conductance and temperature for the sampled springs and trench

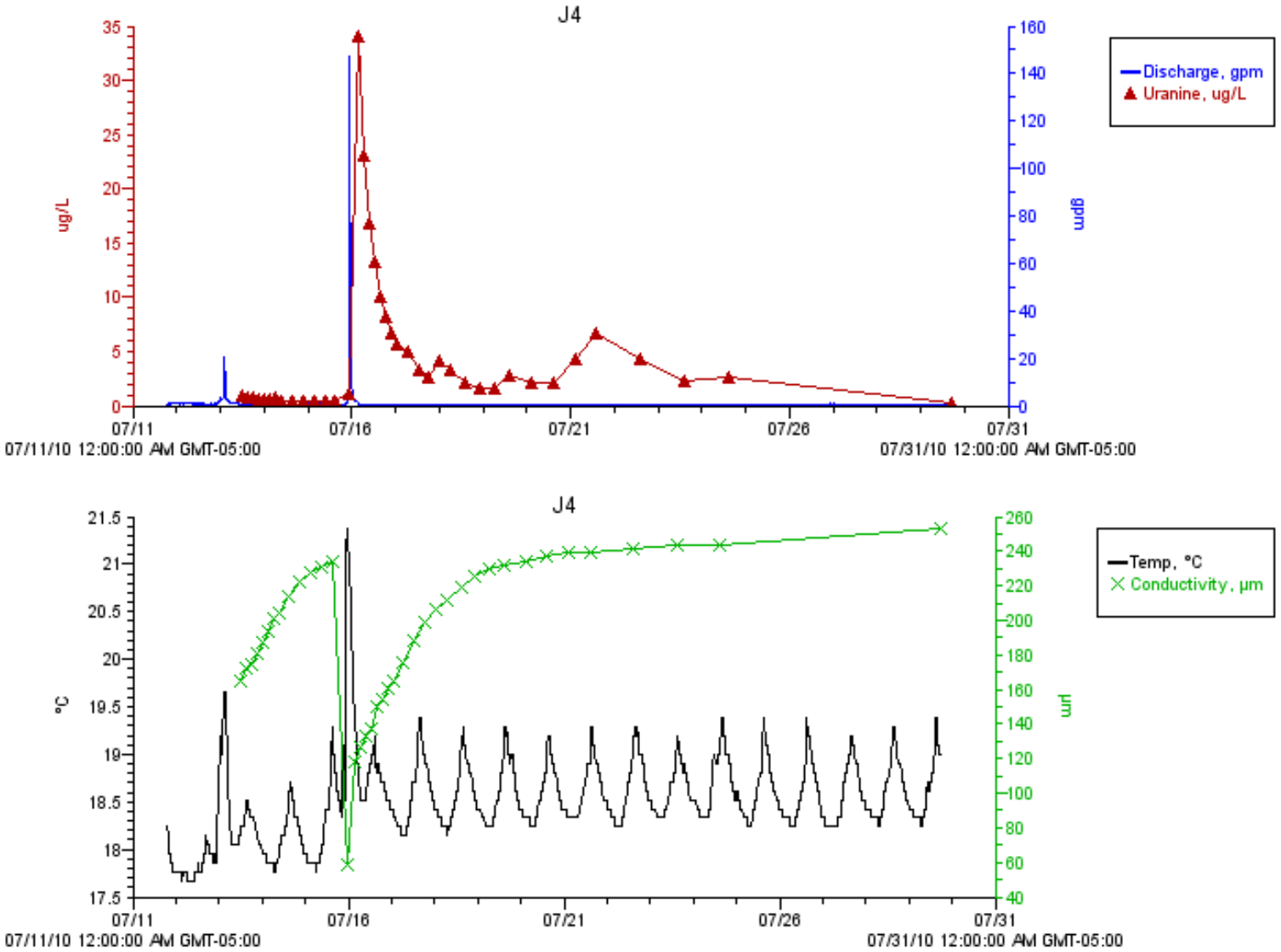

Figure 4-8 Cont. Hydrograph, tracer breakthrough curve, spec. conductance and temperature for the sampled springs and trench

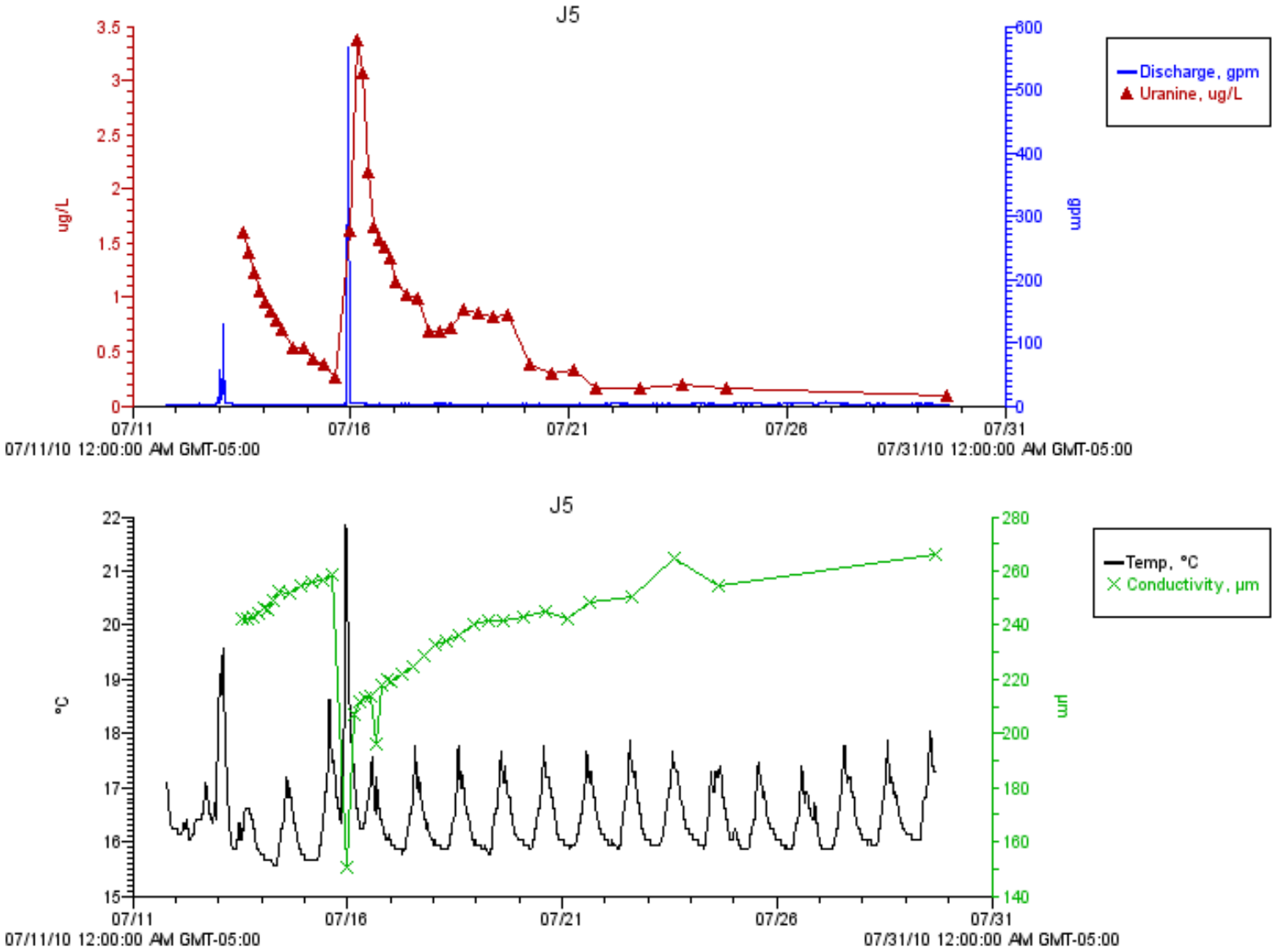

Figure 4-8 Cont. Hydrograph, tracer breakthrough curve, spec. conductance and temperature for the sampled springs and trench

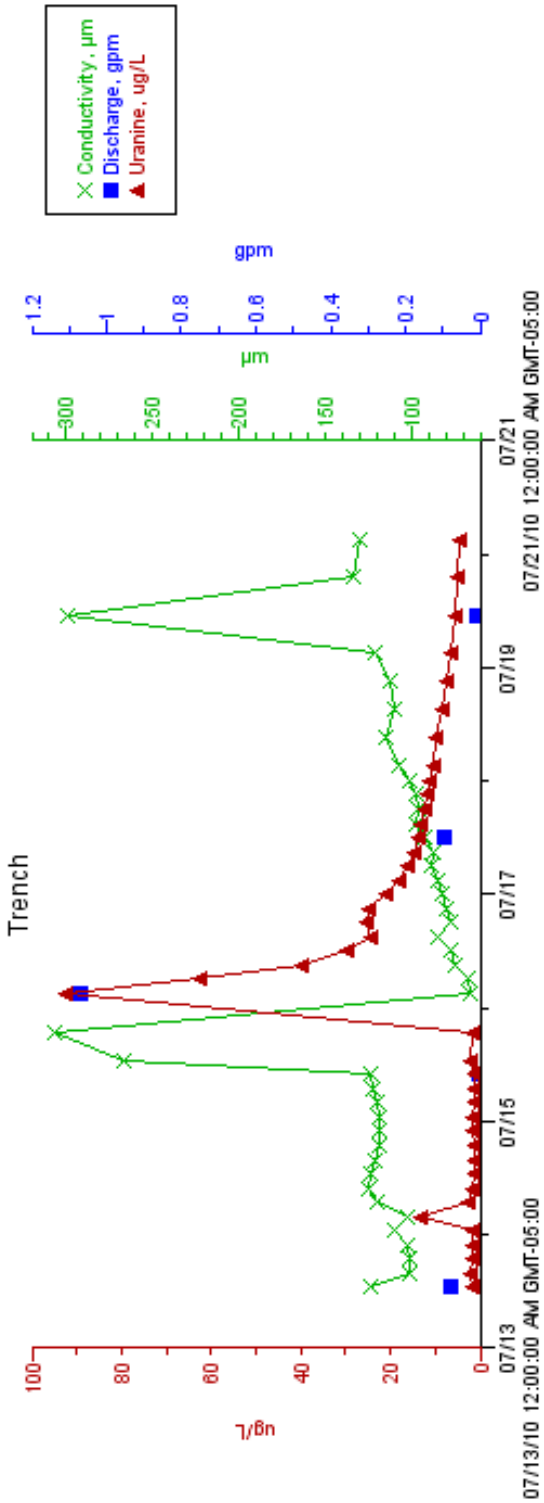

Figure 4-8 Cont. Hydrograph, tracer breakthrough curve, spec. conductance and temperature for the sampled springs and trench

and recessional curves imply that the aquifer lacks the ability to buffer recharge pulses and are characteristic of karst aquifers where conduit flow dominates over diffuse flow (Bonacci, 1993). In the context of the studied epikarst system, the un-muted response likely indicates flow through various macrostructures present throughout the epikarst profile. In the upper epikarst, which is dominated by soil matrix and where most of the volume of the injection trenches lies, Al-Qinna (2003) identified macropores at a nearby epikarst site in the form of root holes, worm holes and loose contact between rock fragments and the matrix. Al-Qinna (2003) also found that these macropores convey flow only in conditions of saturation during storm events, such as those during the test. In the lower epikarst, which consists mostly of compact carbonate which also forms the bottom of the injection trenches, Al-Rashidy (1999) documented abundant dissolutional voids, fissures and joints.

Tracer breakthrough

The dye breakthrough curves and hydrographs show (Figure 4-8) that the dye breakthrough at every monitoring site as well as almost all of its mass discharged during the experiment are associated with the second storm event on the night of July 15 and the resultant hydraulic pulse. The storm started at 8:30 pm and lasted for about 6 hours, with the intense rainfall period ending at around midnight. Within about 8 hours from the start, the dye both arrived and reached peak concentration at all monitoring sites except for J1 (J1 had a weak fluorescence signal of ambiguous origin during this interval, with a stronger peak occurring about 20 hours later as discussed below). The storm with the associated discharge pulse therefore appears to be the critical factor that expedited and facilitated the dye breakthrough; while the dye front may have moved some distance down the epikarst flowpaths already before the storm, it is not possible to

tell how far. Thus, all findings regarding the epikarst water and solute transport discussed below reflect these specific hydrologic conditions.

The arrival of the tracer was registered between 59 and 64 hours after the injection. The tracer arrival times are normally given as travel times to the leading edge of the tracer breakthrough curve, that is, to the last sample with non-elevated concentration before concentration increases (Kilpatrick and Wilson Jr, 1989). However, in this case, the tracer travel times were determined based on the first samples with elevated concentration (the first point on the rising limb) since the leading edge samples were followed by a 4-8 hour long sampling gap and the storm pulse, which is believed to be the driving force behind the breakthrough, did not occur until immediately (about 30-60 min.) prior to collection time of the elevated concentration samples; these samples, therefore, are likely a truer and more accurate mark of the tracer arrival time.

The corresponding travel rates or flow velocities calculated based on the arrival times and the sampling site-injection point distances were between 1 and 2.2 m per hour (Table 4-1). These values are greater than some reported for natural gradient traces with no irrigation, e.g., 0.2 m per hour for less karstified and 0.6 m per hour for more karstified epikarst (Petrella, Falasca, and Celico, 2008). On the other hand, traces conducted under irrigation conditions found rates ranging from 3.6 (Kogovsek, 1997) to more than 10 m per hour (Sinreich and Flynn, 2011). Given that the calculation of the travel rates for Savoy epikarst is based on the time period from the moment of dye introduction, which includes both the roughly 2-day-long base-flow period and the 8 hours of stormflow before the breakthrough, it is reasonable that the values fall between those reported for wet and those for dry conditions, and closer to the latter. If the travel rate calculation would only use the stormflow period before the breakthrough, i.e. approximately

5 hours on average (assuming that the tracer movement began with the storm), the travel rate for the average distance from a spring to the injection point (about 100 m) would be 20 m per hour, which is consistent with the range reported for wet conditions by Sinreich & Flynn (2011).

Table 4-1 Summary of dye breakthrough characteristics

	Site						
Characteristic	**J1**	**J2**	**J3**	**J4**	**J5**	**Trench**	**Aver.**
Distance from injection point (m)	69	81	94	116	137	66	99
Time to arrival (hours)	63	59	64	60	61	64	62
Time to peak conc. (hours)	84	64	64	65	65	64	68
Velocity, arrival time-based (m/h)	1.1	1.4	1.5	1.9	2.2	1.0	1.6
Velocity, peak conc. time-based (m/h)	0.8	1.3	1.5	1.8	2.1	1.0	1.5

The obtained arrival times and corresponding velocities are another indication of the involvement of preferential flowpaths or macropores in the transport of water and dye through the epikarst. Had the transport occurred entirely through the soil matrix, which constitutes about 50 percent by volume of the upper portion of the epikarst where the injection trenches are constructed (and progressively thins out with depth), the arrival times would be considerably longer – on the order of weeks – based on hydraulic conductivity of the matrix at the site, approximately 90 mm/h (Sauer and Logsdon, 2002). The preferential flowpaths therefore likely served to significantly expedite flow through the epikarst.

Peak concentrations

The peak concentrations at J3, J4, J5 and the trench occurred around 6 hours into the storm (approx. 64-65 hours after dye injection) (Table 4-1, Figure 4-9); however, as with the dye arrival, the peak concentrations at these sites may have occurred up to about 3 hours earlier but

may have not been detected due to large time gaps between the samples during this time. At spring J1, the concentration peaked at around 84 hours after dye injection, that is, 20 hours later than at the other springs. The peak concentration arrival times indicate dominant flow velocities in the range of 0.8-2.1 m per hour.

The peak concentrations ranged from 0.7 to 131.2 µg/l (Figure 4-9). The peak concentrations were notably lower at springs J1 and J5 compared to the other sites. Spring J1 peaked at 9.6 times of its background concentration and J5 at only 2.1 times. A common practice in dye-tracing data analysis is to regard concentrations below 10 times of the background concentration as false hits since background fluorescence (e.g., from organic matter) may be highly variable and difficult to assess accurately. Based on this criterion, then, these two springs would have no or very limited hydraulic connection with the tracer injection area. However, other evidence suggests that this may be the case only for J1. Apart from the low peak concentration of dye at J1, this concentration occurred with a significant delay as already noted, and the rise toward this peak was less steep and less even compared to the other sites. In addition, the results of the earlier qualitative tracing experiment also indicated that J1 has no or very limited hydraulic connection with the tracer injection area. On the other hand, J5 was shown by the earlier test to have such connection. The low peak concentration at J5 could result from a combination of dispersion and lateral mixing. The spring is located further from the injection site than the other monitoring sites and is also situated furthest to the side (westward) in the string of the epikarst springs on the pasture side slope; this flowpath may therefore be experiencing greater dispersion and dilution than the other ones.

Following the concentration peak at the sites, the concentrations gradually decreased to near-background levels within approximately 30 hours for J1, J2, J3 and J4 and 100 hours for J5.

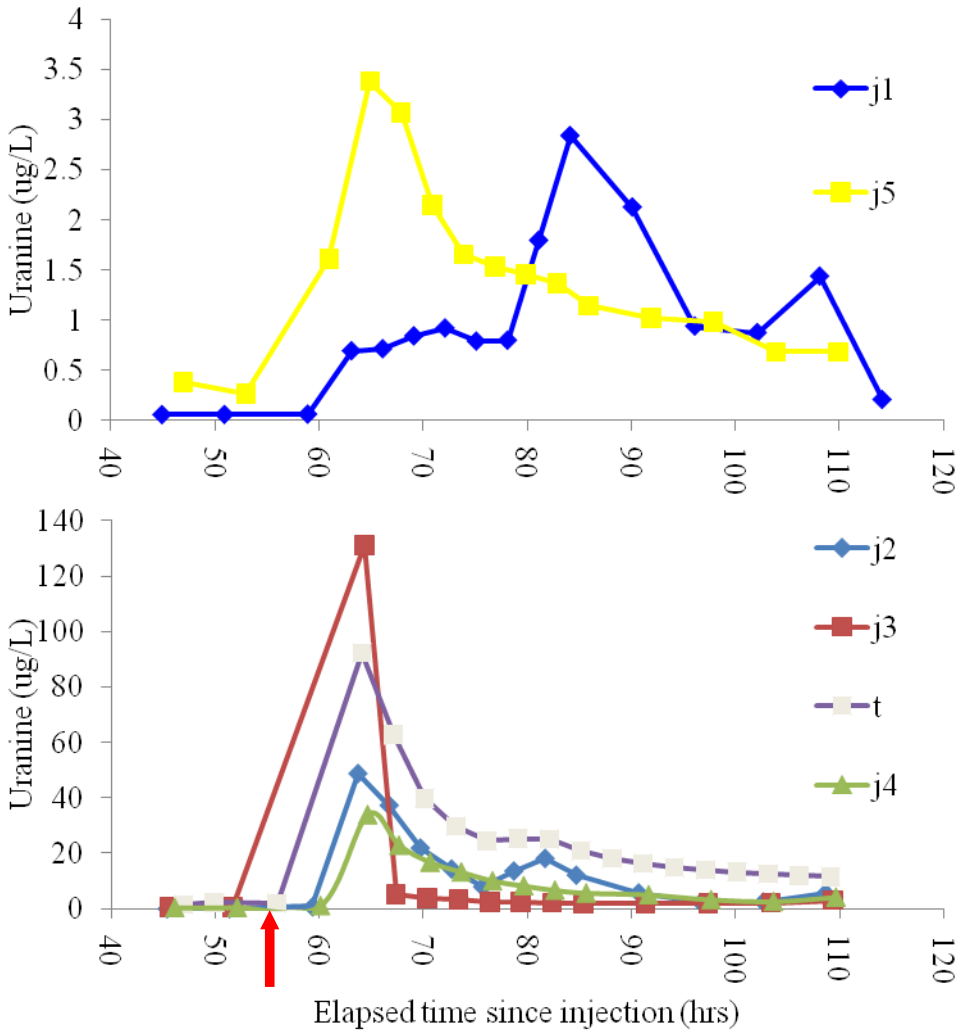

Figure 4-9 Variation in uranine concentration during the breakthrough period. The arrow indicates the onset of rainfall.

Concentration at the trench also decreased, but remained above the background level throughout the sample-collection period which at this sampling site stopped on July 20. The resulting long tails of the tracer breakthrough curves (skeweness to the right) are typical and can be caused by several factors including dispersion, non-steady flow conditions and dead zones, e.g., storage of tracer in very slow-moving water of small voids with later release (Atkinson, 1987). The first two factors were certainly involved in this case as dispersion takes place in every dye-tracing situation and the flow conditions during the test were in fact changing. The third factor, however,

may have also played a role since detainment (storage) and later release of recharge or a particle or solute tracer is a common behavior of the epikarst (Perrin, Jeannin, and Zwahlen, 2003; Aquilina, Ladouche, and Dörfliger, 2006; Sinreich and Flynn, 2011). Ting (2005) documented this mechanism locally at another epikarst site at Savoy using solute, bacteria and clay tracers.

Tracer recovery load

The tracer recovery load or the total quantity of recovered tracer as calculated by Qtracer2 was approximately 25 grams which represents 0.82% of the injected mass of the tracer (Table 4-2). This rate is considerably lower than the 20 to 50% recovery rates which are common for tracer studies in karst terrains; however, Aley (1997) reports that the epikarst generally has lower recovery rates than conduit-dominate karst and that rates around one percent are typical for epikarstic systems such as the one in this study in which dissolutional voids are filled with fine sediments. The sediments decrease hydraulic conductivity and increase water retention ability and, consequently, significant amounts of the tracer may be held up in these systems and be only gradually flushed out over prolonged periods of time. This time may be on the order of months (Bottrell and Atkinson, 1992; Kogovšek and Šebela, 2004), and in certain settings, a complete recovery may take more than a decade (Kogovšek and Šebela, 2004). A simple calculation shows that in this case, at a mass-flux rate characteristic of the peak-flux period of the second storm (calculated as the sum of average fluxes at springs during the 6-hour long hydraulic pulse), a complete recovery would occur in a little over 3 months (13 weeks). Calculated with the combined average flux rate of the entire period of dye passage including the tail end low-flux period (about 50 hours), the recovery would take about 7 months. Finally, at the combined average flux rate of the entire test period, a 100% recovery would occur in about 10 years. Another factor responsible for the low recovery rate appears to be the rainfall activity limited to

Table 4-2 Selected Qtracer2 output data for the sampling stations

Parameter	**Units**	**Site**		
		J1	**J2**	**J3**
Limits to integration for the data file:				
Lower integration limit	hrs	0	0	0
Upper integration limit	hrs	391.97	390.55	389.82
The quantity of tracer recovered	kg	1.54E-04	1.91E-03	2.22E-02
	g	0.15426	1.9096	22.192
	mg	154.26	1909.6	22192
	µg	1.54E+05	1.91E+06	2.22E+07
Distance from input to outflow point	m	69.375	80.625	93.75
Corrected for sinuosity = 1.50X				
Time to leading edge (first arrival)	hrs	21	59	63.7
Time to peak tracer concentration	hrs	84.2	63.367	63.7
For a peak tracer concentration		2.542	48.403	130.04
Upper Limit to integration				
Lower integration limit	hrs	0	0	0
Upper integration limit	hrs	84.2	63.367	63.7
The mean tracer transit time	d	3.2231	2.5673	2.2646
	hrs	77.354	61.615	54.35
	min	4641.2	3696.9	3261
Variance for mean tracer time	d^2	0.13381	6.03E-03	0.15178
	hrs^2	77.073	3.4756	87.422
	min^2	2.77E+05	12512	3.15E+05
Standard deviation for tracer time	d	0.3658	7.77E-02	0.38958
	hrs	8.7791	1.8643	9.35
	min	526.75	111.86	561
The mean tracer velocity	m/d	21.524	31.405	41.398
	m/hr	0.89685	1.3085	1.7249
	m/s	2.49E-04	3.63E-04	4.79E-04
Dispersion coefficient	m^2/s	1.11E-04	1.34E-05	2.56E-02
Longitudinal dispersivity	m	0.4468	3.69E-02	53.348
Dispersion estimate is probably too		yes	yes	yes
Peclet number		155.27	2184.6	1.7573
		Adve>Diff	Adve>Diff	Diff=Adve
Peclet estimate is probably too small		yes	yes	yes
The maximum tracer velocity	m/d	79.286	32.797	35.322
	m/hr	3.3036	1.3665	1.4717
	m/s	9.18E-04	3.80E-04	4.09E-04
Transport zone volume estimate	m^3	131.24	335.84	39.468
Transport zone cross-sectional area	m^2	1.8918	4.1655	0.42099
Hydraulic head loss along channel	m	6.00E-05	1.02E-04	1.56E-04

Parameter	Units	Site		
		J1	J2	J3
Estimated Reynolds number		1.2644	1.8448	2.4319
Molecular mass transport parameters				
Estimated Schmidt number		1140	1140	1140
Estimated Sherwood number		7.7998	9.4214	10.817
Percent recovery of tracer injected	%	5.14E-03	6.37E-02	0.73974
Accuracy index (0.0 = Perfect		0.9999	0.9994	0.9926

Table 4-2 Cont. Selected Qtracer2 output data for the sampling stations

Parameter	Units	Site		
		J4	J5	T
Limits to integration for the data file: J1.DAT				
Lower integration limit	hrs	0	0	0
Upper integration limit	hrs	389.12	387.48	158.22
The quantity of tracer recovered	kg	8.47E-05	8.83E-06	2.52E-04
	g	8.47E-02	8.83E-03	0.25163
	mg	84.735	8.8333	251.63
	µg	84735	8833.3	2.52E+05
Distance from input to outflow point	m	116.25	136.88	65.625
Corrected for sinuosity = 1.50X				
Time to leading edge (first arrival)	hrs	59	59	3
Time to peak tracer concentration	hrs	63.533	62.917	62.2
For a peak tracer concentration		33.103	1.787	90.449
Upper Limit to integration necessarily changed!				
Lower integration limit	hrs	0	0	0
Upper integration limit	hrs	63.533	62.917	62.2
The mean tracer transit time	d	2.5727	2.556	2.4474
	hrs	61.745	61.344	58.737
	min	3704.7	3680.7	3524.2
Variance for mean tracer time	d^2	6.17E-03	8.08E-03	4.07E-02
	hrs^2	3.5519	4.656	23.426
	min^2	12787	16761	84335
Standard deviation for tracer time	d	7.85E-02	8.99E-02	0.20167
	hrs	1.8846	2.1578	4.8401
	min	113.08	129.47	290.4

Parameter	Units	Site		
		J4	J5	T
The mean tracer velocity	m/d	45.186	53.55	26.815
	m/hr	1.8827	2.2313	1.1173
	m/s	5.23E-04	6.20E-04	3.10E-04
Dispersion coefficient	m^2/s	2.83E-05	5.25E-05	6.91E-05
Longitudinal dispersivity	m	5.41E-02	8.47E-02	0.22281
Dispersion estimate is probably too large		yes	yes	yes
Peclet number		2146.9	1616.6	294.54
		Adve>Diff	Adve>Diff	Adve>Diff
Peclet estimate is probably too small		yes	yes	yes
The maximum tracer velocity	m/d	47.288	55.678	525
	m/hr	1.9703	2.3199	21.875
	m/s	5.47E-04	6.44E-04	6.08E-03
Transport zone volume estimate	m^3	144.64	44.76	2.1851
Transport zone cross-sectional area	m^2	1.2442	0.32702	3.33E-02
Hydraulic head loss along channel	m	2.11E-04	2.95E-04	7.07E-05
Estimated Reynolds number		2.6543	3.1457	1.5752
Molecular mass transport parameters				
Estimated Schmidt number		1140	1140	1140
Estimated Sherwood number		11.301	12.303	8.7057
Percent recovery of tracer injected	%	2.82E-03	2.94E-04	8.39E-03
Accuracy index (0.0 = Perfect Recov.)		1	1	0.9999

****

Total quantity of tracer recovered	2.46E-02	kg
	24.601	g
Total aquifer volume estimate	698.14	m^3

****

ALL PRELIMINARY SORPTION COEFFICIENT ESTIMATES ARE INVALID BECAUSE TRACER MASS WAS RECOVERED AT MORE THAN ONE LOCATION!!! ONLY FINAL SORPTION COEFFICIENT ESTIMATE SHOULD BE CONSIDERED

****

Percent recovery of tracer injected	0.82004	%
Accuracy index (0.0 = Perfect Recov.)	0.9918	

one major storm event during the test. The association of the breakthrough curves with the hydraulic pulse of the second storm (Figure 4-8) suggests that dye transport occurred chiefly because of this pulse. This would be consistent with the observation of Williams (2008) that transfer of water in the epikarst tends to occur in response to a pressure pulse produced by increase in hydraulic head during storm events. A major role in this transfer was likely played by the already mentioned preferential flowpaths present throughout the epikarst profile, which have been found to convey flow during saturated conditions (Al-Qinna, 2003). Therefore, rainfall sufficient to cause epikarst saturation appears to be of critical importance for effective solute transport through the epikarst. After the storm, saturation of the epikarst decreases, and the macropore flow along with solute transport in the upper epikarst ceases.

A third factor in the small recovery could be a small footprint of the injection trenches within the studied segment of the epikarst. If the trenches had been larger, more trench wall area would have provided greater coverage of the macropore network for tracer infiltration.

Finally, the recovered rate could be somewhat underestimated due to the fact that uranine concentration data are not available for several hours of the period of peak discharge (discharge was measured independently every 15 min). Qtracer2 filled this gap by extrapolating both concentration and discharge data, which discounted several measured discharge values that were larger than the extrapolated values and possibly also underestimated concentration, thus lowering the estimate for total mass recovery.

After the end of the 16-day experiment period, a portion of the tracer was remaining in the trenches and in trace amounts was visible there even after a year. Over time, some of the tracer likely gradually seeped into the epikarst, especially during rain events, while some part could

have been removed by microbial and chemical/UV decomposition. Similar processes of retention and decomposition likely occurred in the subsurface.

Temperature

The high-resolution temperature data (Figure 4-8) show expected diurnal fluctuation as well as highs associated with the storm, produced by the influx of warmer precipitation water. Time-series temperature data for the sites reveal that the diurnal fluctuation during base-flow periods was generally within approximately 2°C. Spring J1, however, fluctuated within only approximately 0.5°C, suggesting integration of deeper flowpaths, better insulated from atmospheric temperature changes. This observation is in agreement with an earlier study indicating deeper and unique flowpaths for J1, with certain groundwater geochemical parameters such as DOC bioavailability being markedly different from the other sites (Winston, 2006). Additionally, site J1 had the lowest average temperature, averaging about 2-3°C less than the other sites, which also suggests integration of deeper flowpaths. Temperature was not measured in the trench, but since the trench intercepts the shallowest epikarst flowpaths, water temperature at the trench was likely warmer than at the other sites.

Specific conductance

Specific conductance values ranged from 60 to 307 uS/cm (Figure 4-8), which is a typical range for the site. The values exhibited a pattern of variation with hydrologic conditions that is characteristic of karst springs (Toran and others, 2006), with large dips due to influx of low conductivity water during precipitation events – in this case with a greater dip during the second, larger rain event – and gradual leveling off to the base level in between.

Epikarst discharge can be conceptualized as a mixture of two types of water whose proportions vary over time as hydrologic conditions change: relatively low-conductivity, short-residence-time water derived from an ongoing or recent storm (event water) and relatively high-conductivity, long-residence-time water sourced from epikarst storage (pre-event water). The event water infiltrates and for a limited time saturates the upper epikarst during storm events, a state marked by discharge from the interceptor trench constructed mostly in the upper epikarst. The pre-event water provides for the perennial saturation of the lower epikarst; this water should be the sole component of the epikarst discharge during baseflow periods when the upper epikarst is dry.

The variation of proportions of these two types of water over time was quantified on the basis of specific conductance for each site using a binary mixing equation (stormflow endmember value used was local precipitation = 5.2 uS/cm, the baseflow endmember was each site's average specific conductance during baseflow). The proportion of the event water ranged between 0.4 and 85 percent (Figure 4-10). The event-water proportion was the highest during the second storm, reaching from 45 to about 85 percent during the storm, and gradually declined to minimum values approaching zero percent during baseflow (the proportion of the pre-event water is the complement to 100). This calculation thus shows that the storm recharge contributes significant volumes to the total epikarst discharge during stormflow periods while the storm recharge essentially decreases to zero during baseflow when the epikarst storage becomes the only source of discharge. At the same time, the changing proportions indicate the changing flow status of the upper epikarst as hydrologic conditions change: transmitting flow primarily during storms and gradually "drying up" in between.

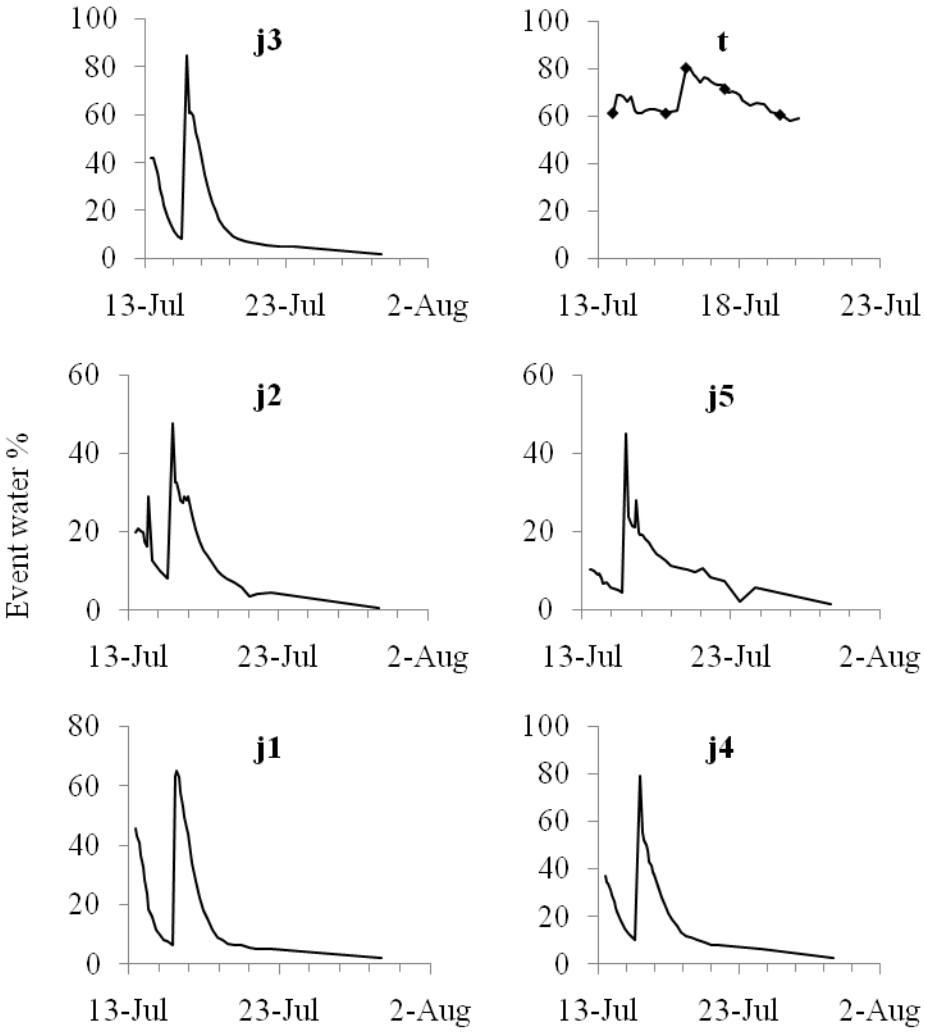

Figure 4-10 Percentage of event water (storm recharge) in discharge of the monitored springs (J1-J5) and trench (t) determined on the basis of specific conductance

CONCLUSIONS

This study aimed to characterize the epikarstic flow at the Savoy Experimental Watershed using dye tracing.

In general terms, the experiments demonstrate that dye tracing is a viable method for studying water and solute movement in the epikarst, but success is dependent on sufficient tracer

quantities, chaser water quantities, and epikarst saturation as dictated by hydrologic conditions. The latter appears to be the most critical factor; the successful traces occurred only when storms created enough saturation to induce flow in the upper epikarst. However, seasonality is also a factor. During summer months, even with rain, high evapotranspiration may reverse the hydraulic gradient and effectively stop drainage from the soil, thus hampering tracer tests in which the tracer is applied to the surface.

The quantitative tracer test showed that the epikarst is a dynamic hydrologic system which responds to recharge events with great rapidity and magnitude. During the first and the second storm events, discharge increased almost instantaneously, changed according to rainfall intensity and peaked at average levels of 60 and 200 times the baseflow level, respectively. Discharge returned to baseflow levels within approximately 2-4 hours after the storms ended.

The tracer dye was positively detected at springs J2, J3, J4, and J5, and at the trench, confirming the existence of viable flowpaths between these points and the plot. The dye breakthrough at these sites was associated with the July 15 storm and was likely initiated by the resulting hydraulic pulse. The breakthrough at the springs occurred roughly around the time of peak discharge, approximately 60 hours since dye injection (trench was not sampled during this time). Peak concentrations at various levels were detected at all of the sites about 4-5 hours later, although they could have occurred earlier and not been registered due to low sampling frequency. The rates of travel were in the range of 1.0 to 2.2 m/h, which falls in between the rates for wet and dry conditions reported by other studies and reasonably reflects the mixed hydrologic conditions since the tracer injection. The total mass of dye recovered during the test was 0.82 %, which reflects the low permeability of the epikarst caused by clay sediments, prevailing hydrologic conditions with only one hydraulic pulse event (critical to solute transport

in the upper epikarst), and possibly a small footprint of the injection trenches within the studied area.

Short tracer arrival times and peaky hydrographs indicated flow through preferential flowpaths. These are an abundant feature of the epikarst and convey flow only during saturated conditions created by storm events (Al-Qinna, 2003). After the storm, the epikarst saturation decreases and the macropore flow along with solute transport in the upper epikarst ceases.

Data further indicate spring J1 as having unique flowpaths as compared to the other springs; low dye concentrations indiscernible from background suggest lack of hydraulic connection to the plot/injection site (or greater dilution) while more uniform and lower temperature data indicate deeper, better thermally insulated flowpaths.

The analysis of specific conductance data showed that the event water can dominate the epikarst discharge during storm events, constituting up to 85%, while the event water proportion steadily decreases to below 1% after the storm when the pre-event water becomes dominant. This variation points to changing flow status of the upper epikarst: transmitting flow primarily during storm events and gradually "drying up" between the storms while flow in the lower epikarst continues.

The great spatial variation in all of the measured variables including discharge response, travel rates, peak concentrations, recovery loads, temperature and specific conductance indicate a great degree of hydrologic heterogeneity that is characteristic of the epikarst.

Overall, the study confirms that the epikarst is a unique subsystem of karst with unique water and solute transport attributes. From a contaminant transport standpoint, a point-source solute in the upper epikarst can be transported rapidly via macropore flow; however, the transport is limited by the duration of epikarst saturation and the transported mass is likely to be

negligible in the short term under the normal weather pattern. In contrast to conduit-dominated karst, as long as the solute source does not reach into the deeper, perennially saturated zone, the epikarst seems to have a good ability to retard contaminant movement.

REFERENCES

Adamski, J., 1997, Nutrients and Pesticides in Ground Water of the Ozark Plateaus in Arkansas, Kansas, Missouri, and Oklahoma: 96-4313

Aley, T., 1997, Groundwater tracing in the epikarst: The Engineering Geology and Hydrogeology of Karst Terranes—Proceedings of the 6th multidisciplinary conference on sinkholes and the engineering and environmental impacts of karst, Springfield, MO, April 6-9, 1997, p. 6-9.

Aley, T., 1998, Procedures and criteria analysis of fluorescein, eosine, rhodamine WT, sulforhodamine B, and pyranine dyes in water and charcoal samplers: Protem, MO, Ozark Underground Laboratory

Al-Qinna, M.I., 2003, Measuring and modeling soil water and solute transport with emphasis on physical mechanisms in karst topography: Fayetteville, University of Arkansas, Ph.D. Dissertation, 273 p.

Al-Rashidy, S.M., 1999, Hydrogeologic controls of groundwater in the shallow mantled karst aquifer, Copperhead Spring, Savoy Experimental Watershed, northwest Arkansas: Fayetteville, University of Arkansas, M.S. Thesis, p.96

Aquilina, L., Ladouche, B., and Dörfliger, N., 2006, Water storage and transfer in the epikarst of karstic systems during high flow periods: Journal of Hydrology, v. 327, no. 3-4, p. 472-485.

Atkinson, T., 1987, Karst Hydrology Course Manual. Karst Field Studies at Mammoth Cave, Center for Cave and Karst Studies. Western Kentucky University and Mammoth Cave National Park

Bakalowicz, M., 1995, La zone d'infiltration des aquifères karstiques. Méthodes d'étude: Structure et fonctionnement.Hydrogéologie, v. 4, p. 3-21.

Bonacci, O., 1993, Karst springs hydrographs as indicators of karst aquifers: Hydrological Sciences Journal, v. 38, no. 1, p. 51-62.

Bottrell, S.H., and Atkinson, T.C., 1992, Tracer study of flow and storage in the unsaturated zone of a karstic limestone aquifer: Tracer hydrology: Rotterdam, Balkema, p. 207-211.

Boyer, D.G., and Pasquarell, G.C., 1996, Agricultural land use effects on nitrate concentrations in a mature karst aquifer: Journal of the American Water Resources Association, v. 32, no. 3, p. 565-573.

Brahana, J.V., Killingbeck, J.J., Stielstra, C., Leh, M.D.K., Murdoch, J.F., and Chaubey, I., 2006, Elucidating flow characteristics of epikarst springs using long-term records that encompass extreme hydrogeologic stresses: Geological Society of America Abstracts with Programs, Philadelphia, Pennsylvania, v. 38, p. 196.

Brahana, J.V., Ting, T.E., Al-Qinna, M., Murdoch, J.F., Davis, R.K., Laincz, J., Killingbeck, J.J., Szilvagyi, E., Doheny-Skubic, M., Chaubey, I., Hays, P.D., and Thoma, G., 2005, Quantification of hydrologic budget parameters for the vadose zone and epikarst in mantled karst: U. S. Geological Survey Karst Interest Group Proceedings, Rapid City, South Dakota, September 12-15, 2005, September 12-15, 2005, v. U.S. Geological Survey Scientific Investigations Report 2005-5160, p. 144-152.

Davis, R.K., Brahana, J.V., and Johnston, J.S., 2000, Groundwater in Northwest Arkansas: Minimizing Nutrient Contamination From Non-Point Sources in Karst Terrane. MSC-288, 69 p.

Einsiedl, F., 2005, Flow system dynamics and water storage of a fissured-porous karst aquifer characterized by artificial and environmental tracers: Journal of Hydrology, v. 312, no. 1, p. 312-321.

Ernenwein, E.G., and Kvamme, K.L., 2004, Geophysical Investigations For Subsurface Fracture Detection In The Savoy Experimental Watershed, Arkansas: Unpublished report, Department of Biological and Agricultural Engineering, University of Arkansas, 24 p.

Field, M.S., 2002, The QTRACER2 program for tracer-breakthrough curve analysis for tracer tests in karstic aquifers and other hydrologic systems, National Center for Environmental Assessment--Washington Office, Office of Research and Development, US Environmental Protection Agency

Flury, M., and Wai, N.N., 2003, Dyes as tracers for vadose zone hydrology: Reviews of Geophysics, v. 41, no. 1, p. 1002.

Ford, D.C., and Williams, P.W., 2007, Karst hydrogeology and geomorphology: Chichester, England, John Wiley & Sons, 576 p.

Friederich, H., and Smart, P.L., 1981, Dye tracer studies of the unsaturated zone: recharge of the Carboniferous Limestone aquifer of the Mendip Hills, England: Proceeding of the 8th International Speleological Congress, Bowling Green, Kentucky, USA, p. 283-286.

Gillieson, D., 1996, Caves: Processes, Development, Management: Oxford, Blackwell, 324 p.

Green, M.B., Wollheim, W.M., Basu, N.B., Gettel, G., Rao, P.S., Morse, N., and Stewart, R., 2009, Effective denitrification scales predictably with water residence time across diverse systems: Nature Precedings, accessed June 15, 2013, http://precedings.nature.com/documents/3520/version/1/html.

Kilpatrick, F., and Wilson Jr, J., 1989, Measurement of time of travel in streams by dye tracing: 3-A9

Klimchouk, A., 2004, Towards defining, delimiting and classifying epikarst: Its origin, processes and variants of geomorphic evolution: Speleogenesis and Evolution of Karst Aquifers, v. 2, no. 1, p. 1-13,

Klimchouk, A., 2000, The formation of epikarst and its role in vadose speleogenesis: Speleogenesis: Evolution of Karst Aquifers, National Speleological Society: Huntsville, p. 91-99.

Kogovšek, J., and Šebela, S., 2004, Water tracing through the vadose zone above Postojnska Jama, Slovenia: Environmental Geology, v. 45, no. 7, p. 992-1001.

Kogovsek, J., 1997, Water tracing tests in the vadose zone, *in* Kranjc ed. Tracer Hydrology 97: Roterdam, Balkema, p. 167-172.

Kogovšek, J., and Šebela, S., 2004, Water tracing through the vadose zone above Postojnska Jama, Slovenia: Environmental Geology, v. 45, no. 7, p. 992-1001.

Laincz, J., 2011, Investigation of Nitrate Processing in the Interflow Zone of Mantled Karst, NW Arkansas: U.S. Geological Survey Karst Interest Group Proceedings, Fayetteville, Arkansas, April 26-29, 2011, April 26-29, 2011, v. U.S. Geological Survey Scientific Investigations Report 2011–5031, p. 75-83.

Laincz, J., Hays, P.D., Winston, B., and Ziegler, S., 2009, BIOGEOCHEMICAL/HYDROLOGICAL INVESTIGATION OF THE FATE OF NITRATE IN THE INTERFLOW ZONE OF MANTLED KARST: 2009 Portland GSA Annual Meeting

Laincz, J., 2007, Qualitative dye tracer test at the Savoy Experimental Watershed plot: Unpublished Report.

Laubhan, A.C., 2007, A hydrogeologic and water-quality evaluation of the Springfield aquifer in the vicinity of North-Central Washington County, Arkansas: Fayetteville, University of Arkansas, M.S. Thesis, 182 p.

Lee, E.S., and Krothe, N.C., 2001, A four-component mixing model for water in a karst terrain in south-central Indiana, USA. Using solute concentration and stable isotopes as tracers: Chemical Geology, v. 179, no. 1, p. 129-143.

Leh, M., Chaubey, I., Murdoch, J., Brahana, J., and Haggard, B., 2008, Delineating runoff processes and critical runoff source areas in a pasture hillslope of the Ozark Highlands: Hydrological Processes, v. 22, no. 21, p. 4190-4204.

Mangin, A., 1975, Contribution à l'étude hydrodynamique des aquifères karstiques: Dijon, France, Université de Dijon, Ph.D., p.124

Mull, D.S., Liebermann, T.D., Snoot, J.L., and Woosley, L.H., 1988, Application of dye-tracing techniques for determining solute transport characteristics of ground water in karst terranes: Atlanta, GA, US EPA, EPA904/6-88-001

Owenby, J.R., and Ezell, D.S., 1992, Monthly station normals of temperature, precipitation, and heating and cooling degree days, 1961-1990, Arkansas. Climatography of the United States No. 81:

Perrin, J., Jeannin, P., and Zwahlen, F., 2003, Epikarst storage in a karst aquifer: a conceptual model based on isotopic data, Milandre test site, Switzerland: Journal of Hydrology, v. 279, no. 1, p. 106-124.

Petrella, E., Falasca, A., and Celico, F., 2008, Natural-gradient tracer experiments in epikarst: a test study in the Acqua dei Faggi experimental site, southern Italy: Geofluids, v. 8, no. 3, p. 159-166.

Power, J., and Schepers, J., 1989, Nitrate contamination of groundwater in North America: Agriculture, Ecosystems & Environment, v. 26, no. 3, p. 165-187.

Sauer, T.J., and Logsdon, S.D., 2002, Hydraulic and Physical Properties of Stony Soils in a Small Watershed: Soil Science Society of America Journal, v. 66, no. 6, p. 1947-1956.

Seitzinger, S., Harrison, J.A., Bohlke, J.K., Bouwman, A.F., Lowrance, R., Peterson, B., Tobias, C., and Van Drecht, G., 2006, Denitrification across landscapes and waterscapes: a synthesis. Ecological Applications, v. 16, no. 6, p. 2064-2090.

Sinreich, M., and Flynn, R., 2011, Comparative tracing experiments to investigate epikarst structural and compositional heterogeneity: Speleogenesis and Evolution of Karst Aquifers, no. 10, p. 253-258,

Steele, K.F., and McCalister, W.K., 1990, Nitrate concentrations of ground water from limestone and dolomitic aquifers in the Northeastern Washington County area, Arkansas: MSC-68

Stone, P.R.I., William C. Nelson, Dennis Bowser, Thomas J. Aley, Thomas R. Tibbs, Rusi B. Charna, Edward M. Kellar, and and Gerald J. Murphy, 1995, Defining Contaminant Flow Pathways in a Complex Geologic Terrain Using Dye Tracer Studies: Proceedings of the Petroleum Hydrocarbons and Organic Chemicals in GroundWater: Prevention, Detection, and Remediation Conference. National Ground Water Association and the American Petroleum Institute, Houston, TX, Nov 29-Dec 1, 1995, p. 239-253.

Ting, T., 2005, Assessing bacterial transport, storage and viability in mantled Karst of northwest Arkansas using clay and Escherichia coli labeled with lanthanide series metals: Fayetteville, University of Arkansas, Ph.D. Dissertation, p.279

Toran, L., Tancredi, J.H., Herman, E.K., and White, W.B., 2006, Conductivity and sediment variation during storms as evidence of pathways to karst springs: SPECIAL PAPERS-GEOLOGICAL SOCIETY OF AMERICA, v. 404, p. 169.

Veni, G., DuChene, H., Crawford, N.C., Groves, C.G., Huppert, G.H., Kastning, E.H., Olson, R., and Wheeler, B.J., 2001, Living with Karst: A Fragile Foundation (Environmental Awareness Series ed.), American Geological Institute, 64 p.

Williams, P.W., 2008, The role of the epikarst in karst and cave hydrogeology: a review: International Journal of Speleology, v. 37, no. 1, p. 1-10.

Wilson Jr, J., Cobb, E.D., and Kilpatrick, F.A., 1986, Fluorometric procedures for dye tracing: 3-A12

Winston, B.A., 2006, The biogeochemical cycling of nitrogen in a mantled karst watershed: Fayetteville, University of Arkansas, M.S. Thesis, p.88

5. GEOCHEMICAL EVIDENCE FOR DENITRIFICATION IN THE EPIKARST AT THE SAVOY EXPERIMENTAL WATERSHED, NORTHWEST ARKANSAS

ABSTRACT

Karst aquifers are highly vulnerable to agricultural NO_3^- contamination due thin soils and rapid conduit flow characteristic of karst geology; however, many karst regions contain epikarst, an upper weathered layer of carbonate bedrock, which, owing to hydrologic properties that are distinctly different from the underlying karst could support a higher degree of denitrification. This study aimed to identify denitrification and characterize controls on denitrification in a well delineated epikarst system in NW Arkansas. Water samples were collected from an interceptor trench and from epikarst springs downgradient from the trench after four storm events in the spring 2011 and analyzed for NO_3^- concentration, NO_3^--$\delta^{15}N$ and NO_3^--$\delta^{18}O$, dissolved organic/inorganic carbon concentration and $\delta^{13}C$, and dissolved gas concentration (N_2, O_2, Ar). Denitrification was indicated by an average NO_3^- decrease of 50% along the trench-spring flowpaths and, for the flowpaths upgradient from the trench, by simultaneous isotopic enrichment in NO_3^--^{15}N and ^{18}O and by the trend of increasing DIC concentration with decreasing $\delta^{13}C$ of DIC detected in the trench samples. The occurrence of denitrification in the system was corroborated by dissolved N_2 measurements which showed supersaturation of up to 106% in all except for three samples. Consistent with environmental requirements of denitrifiers, N_2 saturation negatively correlated with O_2 saturation ($r^2 = 0.600802$; $p = 0.0007$) and positively correlated with DOC concentration at the springs ($r^2 = 0.686494$; $p < 0.0001$), with the latter suggesting a limiting role of DOC on denitrification in the epikarst. The results also suggest that hydrology (epikarst saturation) plays an important indirect role in controlling denitrification:

more saturated conditions likely deliver more DOC substrate and more restrict O_2 diffusion into the epikarst helping to create anoxic environment suitable for denitrification. In conclusion, this study successfully identified denitrification and several of its controls in the studied epikarst system, and its findings can serve as a foundation for future, quantitative studies.

INTRODUCTION

High nitrate (NO_3^-) concentrations in water are detrimental to man and the environment alike. Intake of NO_3^- may result in formation of potentially carcinogenic compounds in the human gastric system (Tenovuo, 1986) as well as low oxygen levels in infant blood (methemoglobinemia), a potentially fatal condition and the reason for the U.S. Environmental Protection Agency to set the maximum contaminant level for NO_3^- in drinking water at 10 mg/L NO_3^--N (Fan and Steinberg, 1996). In aquatic ecosystems excess nitrate concentrations create ecological imbalances. For example, large amounts of NO_3^- discharging from agricultural watersheds have been implicated in the development of hypoxic zones around the world threatening marine biota (Rabalais and others, 1996; Goolsby and Battaglin, 2001).

The problem of groundwater NO_3^- contamination is most often associated with agricultural activity, and one type of landscape especially vulnerable to such contamination is karst (Power and Schepers, 1989; Boyer and Pasquarell, 1996). Here, the typically thin or missing soil cover, direct point-recharge via sinkholes, and rapid, concentrated flow in the conduit network with little microbial remediation and high rates of dispersion offer little protection of aquifers from contamination originating at the surface. A case in point is the area under study, the karst region of northwest Arkansas, where intense animal production and excess nutrient generation have been linked to elevated NO_3^- concentrations in local springs and wells (Steele and McCalister, 1990; Adamski, 1997; Davis, Brahana, and Johnston, 2000; Laubhan, 2007). Protection of these

systems is paramount as karst aquifers are important sources of drinking water; as much as one quarter of the world's population obtains its drinking water from karst aquifers (Ford and Williams, 2007).

Many karst systems are mantled by a layer known as regolith or epikarst, generally defined as the dissolutionally weathered, typically 3-15 m thick, upper portion of the carbonate bedrock (Ford and Williams, 2007). The U.S. karst map (Veni and others, 2001) classifies in excess of 50% of U.S. karst as buried, i.e., covered by the epikarst.

Epikarst hydrology is distinctly different from that in the underlying bedrock and could be conducive to significant microbial activity including denitrification, which is the most important NO_3^- attenuation process removing NO_3^- from watersheds in the form of gaseous nitrogen. For example, as porosity and permeability diminish with depth, the epikarst has a tendency to detain and delay recharge (Bakalowicz, 1995; Einsiedl, 2005; Aquilina, Ladouche, and Dörfliger, 2006), which translates into increase in residence time, an important factor facilitating denitrification (Seitzinger and others, 2006; Green and others, 2009). The decrease in permeability also induces lateral flow (Klimchouk, 2004) which acts to route the flow away from vertical shafts and conduits leading to the phreatic zone in the deeper bedrock. Studies have documented that the epikarst is a chemically reactive zone changing the chemistry of recharging water with respect to Cl^-, Br^-, oxygen-18 and deuterium (Aquilina, Ladouche, and Dörfliger, 2006) as well as attenuating organic dye and phosphate tracers (Sinreich and Flynn, 2011).

At the same time, the epikarst discharge has been found to constitute a significant part of the total discharge of springs or small catchments. During high flow conditions, this contribution can be in the range of 30-35% (Einsiedl, 2005; Perrin, Jeannin, and Zwahlen, 2003), but it can be as high as 55% (Lee and Krothe, 2001). The quality of waters discharging out of karst

watersheds is therefore likely to a great degree dictated by biogeochemical processes taking place in the epikarst. This emphasizes the importance of understanding of biogeochemical functioning of the epikarst.

While various aspects of the epikarst hydrology have been well established, the understanding of its biogeochemical functioning, including the processes of nitrate attenuation, is lacking. A number of studies on this topic have characterized karst systems where the epikarst was present (Einsiedl, 2005; Lee and Krothe, 2001; Panno and others, 2001), but none focused solely on the epikarst itself.

The purpose of our investigation was to add to the knowledge of the biogeochemical functioning of the epikarst and, more specifically, to identify denitrification and its spatial or temporal variation as well as any controlling factors in an epikarst system with well-delineated hydrology. Methodology-wise, this study relied on a complex geochemical characterization involving measuring concentration and stable isotopes of all of the key reactants and products of the denitrification reaction, including NO_3^-, dissolved organic/inorganic carbon (DOC/DIC), and dissolved dinitrogen (N_2). We hypothesized that denitrification occurs in the epikarst, supported by favorable hydrologic properties such as increased residence time, and that this denitrification causes detectable decrease in concentration of NO_3^- as the reactant chemical species and increase in concentration of DIC and N_2 as the products of denitrification, with enrichment of the remnant NO_3^- in the heavy isotopes ($\delta^{15}N$, $\delta^{18}O$) and of the DIC pool in the light carbon isotope (^{13}C).

A somewhat novel element in this study is the application of the direct denitrification detection technique of dissolved dinitrogen to the epikarst. This technique, while commonly applied to aquatic and marine systems, has been rarely used in unsaturated terrestrial systems due to challenges posed by high N_2 background and its rapid exchange with air (Groffman and

others, 2006); furthermore, there appears to be no study that has employed this technique specifically in the epikarst.

METHODOLOGY

Site description

The study site is located at the Savoy Experimental Watershed (SEW) near the town of Savoy in northwest Arkansas. The landscape of SEW is characterized by steep-sided valleys cut into a highly dissected plateau formed on impure, chert-rich limestone. Land use is dictated by the topography, with the steep side slopes and narrow ridge tops in hardwood forest and the broader ridge tops and valley bottoms in permanent pasture characteristic of the Illinois River Watershed. Geologically, the SEW represents the regolith-mantled karst setting of the Ozark Highlands, and is a geologic setting typical of approximately 15% of the eastern U.S., in which the karstified carbonate bedrock is overlaid by a variable thickness of erosional residuum (regolith or epikarst) composed mainly of clay and rock fragments of silicic carbonate. The epikarst at the site is from 3 to 12 feet thick. The soil at the top consists of up to 60% of rock fragments which with depth become more abundant and also progressively turn into more continuous and less weathered rock ledges. A detailed pedologic characterization of the site can be found in Sauer and Logsdon (2002) and a structural description of the epikarst based on subsurface geophysics in Ernenwein and Kvamme (2004).

Sampling strategy

Denitrification was studied in a section of the epikarst in Basin 1 of the Savoy facility. Samples were collected at two stages of the hydrologic gradient of the epikarst section: an interceptor trench located on a sloping (15%) ridge-top pasture and five epikarst springs (J1-J5)

located on the side slope from 69 to 137 meters downgradient from the trench (Figure 5-1). The trench was constructed according to the trench design in Smettem and others (1991), with its central feature being a French drain. The trench is about 5' deep and dug down to relatively solid carbonate bedrock. The trench serves to intercept waters representative of epikarst through flow.

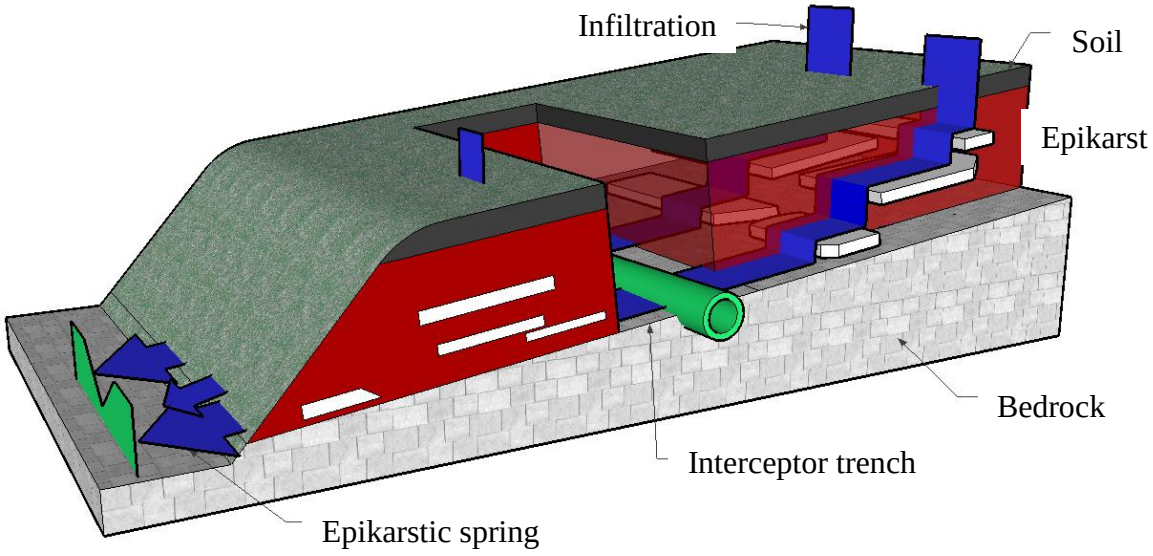

Figure 5-1 Conceptual model of the epikarst illustrating the lateral flow and sampling points along the flowpath

The springs are natural, terminal drainage points of the epikarst flowpaths and thus provide samples representing the final geochemical signature of waters leaving the epikarst. The springs were fitted with V-notch weirs for accurate discharge measurement. The hydrologic connections between the trench and each of the springs had previously been established by dye tracing (Laincz, 2007). Amendment of chicken litter was applied to the area upgradient from the trench prior to sampling in March 2011 at a rate of 5 tons per acre to simulate common NO_3^- loading practices in Arkansas and also to increase NO_3^- signal.

Samples were collected following each of four consecutive storm events from May 2011 until July 2011 in conditions of increased saturation and flow. The trench and all of the springs were sampled for each event. Samples were collected for each type of chemical and isotopic analysis into appropriate containers, filtered and preserved in accordance with guidelines from the analyzing lab. For anion (NO_3^-, Cl^-) and NO_3^- stable isotope ($\delta^{15}N$ and $\delta^{18}O$) analyses, samples were collected without filtration or preservation. For DIC/DOC concentration and ^{13}C stable isotope analysis, samples were filtered on-site (0.7 μm Whatman GF/F filters in a Millipore 47-mm syringe filter assembly), and those for DOC-^{13}C isotopic analysis were also acidified with 85% H_3PO_4. For dissolved gas analyses, samples were collected via a portable sampler (Masterflex E/S, Cole-Parmer, Vernon Hills, IL) directly from the point of emergence of water from the ground to minimize contact with air. The pump outflow tubing was inserted all the way to the bottom of a sample vial, with 234 μl of 50% $ZnCl_2$ preservative solution (1.2% final conc., v/v) pre-dosed in each vial (18 ml Kimax test tube with a ground glass stopper), and water was pumped in at a slow rate to prevent bubble formation before the vial was stoppered, sealed with Parafilm and carefully checked to ascertain that no air bubbles were present. Collected samples were placed on ice and transported into laboratory where they were stored in the dark at 4°C until analysis. In addition, during collection, several field and environmental parameters were measured with dedicated meters: pH, electrical conductivity and temperature (sympHony SP80PC handheld multimeter, VWR, Radnor, PA), dissolved oxygen (DO meter, YSI, Yellowsprings, OH) and barometric pressure required for dissolved gas calculations (Thommen altimeter/barometer, Model 2000, Waldenburg, Switzerland).

Chemical analyses

Chemical analysis of samples for major anions and cations was conducted at the Arkansas Department of Environmental Quality Water Quality Lab using ion chromatography (EPA method 300.0) and ICP (EPA method 200.7), respectively. Stable isotopes of NO_3^- ($\delta^{15}N$ and $\delta^{18}O$) were analyzed at the University of Arkansas Stable Isotope Lab using the denitrifier method (Sigman and others, 2001; Casciotti and others, 2002) involving the use of genetically modified denitrifier to quantitatively convert sample NO_3^- to N_2O, with adaptations described in Winston (2006). The analysis was performed using a GasBench II system with a CO_2 trap made up of stainless steel and organics and a water trap consisting of isopropanol-dry ice slush, connected to a continuous flow isotope ratio mass spectrometer (XP, ThermoFinnigan, Bremen, Germany). The method precision for $\delta^{15}N$ and $\delta^{18}O$ was ±0.46 and ±0.49‰, respectively. DOC and DIC stable isotopes (^{13}C) and concentration (ppm C) were analyzed at the Colorado Plateau Stable Isotope Lab, Flagstaff, AZ, using an O.I. Analytical Model 1010 TOC analyzer (OI Analytical, College Station, TX) interfaced to a Finnigan Delta+ XL isotope ratio mass spectrometer (Finnigan-MAT, San Jose, CA) (St-Jean, 2003). The DIC and DOC measurements had an error margin of ±0.03 and ±0.13‰, respectively.

The results of stable isotope analyses are expressed in the text below in δ notation defined as:

$$\delta X\ (‰) = (R_s/R_{st} - 1) * 1000$$

where X is ^{15}N, ^{18}O, or ^{13}C, and R is the $^{15}N/^{14}N$, $^{18}O/^{16}O$, $^{13}C/^{12}C$ ratios of the sample (s) and reference standard (st), respectively. The reference standards are Air for $\delta^{15}N$, Vienna Standard Mean Ocean Water (VSMOW) for $\delta^{18}O$, and Vienna Pee Dee belemnite (VPDB) for ^{13}C.

MIMS

Dissolved gas samples were analyzed within four weeks after the last collection for their O_2:Ar and N_2:Ar ratios using a membrane inlet mass spectrometry (MIMS) setup consisting of a Pfeiffer Prisma mass spectrometer and a Bay Instruments DGA membrane inlet S-25-75. The MIMS setup is described in detail in Kana and others (1994). Potential instrument-specific O_2 interference in N_2:Ar determination was previously ruled out by comparing the N_2-N concentration of replicate (oxic) samples measured both with and without O_2 removal using a copper-reduction column heated to 600°C (Eyre and others, 2002). Measured N_2-N concentrations in replicates treated for O_2 interference were not consistently lower than in untreated replicates, as would occur in the case of O_2 interference.

Prior to MIMS analysis, sample temperature was brought back to in situ temperature, and the temperature of the MIMS standard solution was adjusted to match each sample. The MIMS method assumes 100% Ar saturation, which varies with temperature and salinity but not due to biological production or consumption. Biological effects on the O_2 and N_2 pool of samples were separated from physical effects using the Ar signal. Sample N_2 concentration ($[N_2]_{sample}$) was defined as:

$$[N_2]_{sample} = (N_2 : Ar_{sample} \times [Ar]_{exp}) ([N_2] : [Ar]_{exp} / N_2 : Ar_{standard})$$

where N_2 : Ar sample is the measured sample signal and N_2 : Ar standard is the measured signal for well-mixed deionized water open to the atmosphere at the same temperature as the samples. The terms $[Ar]_{exp}$ and $[N_2] : [Ar]_{exp}$ were the theoretical saturated concentration or ratio, respectively, calculated for each in situ sample temperature using gas solubility tables (Weiss, 1970). A similar equation was used to calculate sample O_2 concentrations. Subsequently, N_2 saturation ($N_2\%_{sat}$) was calculated as:

$$N_2\%_{sat} = ([N_2]_{sample} / [N_2]_{exp}) \times 100$$

where $[N_2]_{exp}$ is the saturated N_2 concentration at a given temperature (Weiss, 1970). A few $[N_2]$ sample measurements were less than $[N_2]_{exp}$, yielding N_2 saturation less than 100%. Apparent undersaturation of these samples was attributed to matrix differences between the deionized standard and environmental samples containing dissolved and suspended solids, the presence of which likely lowered equilibrium N_2 concentration in the epikarst waters. O_2 saturation was calculated in a similar way. The precision of the MIMS analysis was ±0.3%.

Data analysis including analysis of variance, correlation and linear regression were performed using JMP version 10 (SAS Institute Inc., Cary, NC).

RESULTS

Nitrate concentration and $\delta^{15}N$ and $\delta^{18}O$

Nitrate concentrations ranged from 1.5 to 7.6 mg/L (Table 5-1), with an average of around 3 mg/L. These concentrations are similar to those reported for the watershed by other authors (Winston, 2006; Sauer and others, 2008). The NO3- concentration did not seem to have been significantly affected by the application of chicken litter two months prior to the test. The average concentration of the trench samples was 4.7 mg/L. The average concentration of the spring samples was 2.6 mg/L. The NO_3^--$\delta^{18}O$ values ranged between 1.3 and 4.6‰. The trench average was higher than the springs average (5.2 and 3.7‰, respectively). The NO_3^--$\delta^{15}N$ values varied between 2.5 and 5.8‰. The trench average was around 2‰ while the springs averaged 3.6‰. The measured NO_3^--$\delta^{15}N$ and -$\delta^{18}O$ values are consistent with NO_3^- originating from soil organic matter and animal waste (i.e., manure, chicken litter) (Kendall and McDonnell, 1998).

The indicated origin is accurate as soil and animal waste were in fact the primary potential sources of NO_3^- at the site.

Table 5-1 Chemical analysis of the samples and field parameters

Date	Site	Cl^- (mg/l)	SO_4^- (mg/l)	NO_3^- (mg/l)	NO_3^--$d^{15}N$ (‰)	NO_3^--$d^{18}O$ (‰)	DIC (mg C/l)	DIC (mg $CaCO_3$/l)	DIC-$d^{13}C$ (‰)	DOC (mg C/l)	DIC-$d^{13}C$ (‰)
4/15	J1	4.3	1.1	3.4	3.34	2.24	34.1	284.2	-13.34	0.3	-25.31
4/15	J2	4.5	1.2	2.9	4.10	2.58	35.5	295.5	-13.64	0.4	-25.20
4/15	J3	4.1	1.0	3.1	3.48	2.32	33.8	281.9	-14.05	0.5	-26.28
4/15	J4	4.7	1.3	3.1	4.49	4.50	33.6	280.0	-14.11	0.3	-26.39
4/15	J5	4.4	1.3	3.0	4.04	4.47	34.9	290.8	-13.56	0.4	-26.12
4/15	T1	3.4	24.2	-	-	-	7.2	59.8	-14.34	4.0	-25.99
4/15	T2	3.4	24.5	7.6	4.00	1.34	-	-	-	-	-
4/28	j1	4.1	3.8	3.1	2.69	3.65	21.5	178.7	-15.96	1.8	-26.09
4/28	J2	3.9	4.6	2.8	3.76	2.93	24.3	202.8	-16.71	1.5	-26.31
4/28	J3	3.7	4.0	2.8	2.66	3.64	18.0	150.0	-14.60	1.7	-26.54
4/28	J4	3.6	4.2	2.5	2.52	3.16	20.3	169.0	-16.51	1.6	-26.48
4/28	J5	3.1	2.9	2.2	3.64	4.59	29.4	244.9	-14.60	0.6	-26.55
4/28	T	1.5	11.5	4.6	5.26	1.81	10.8	89.8	-21.25	3.4	-24.95
5/4	J1	4.2	2.7	2.8	3.35	4.18	28.9	241.2	-14.29	0.9	-25.74
5/4	J2	4.3	3.5	2.5	4.29	4.57	27.9	232.6	-15.42	1.0	-25.81
5/4	J3	4.4	2.8	2.5	3.14	2.78	23.5	195.4	-13.41	1.1	-25.58
5/4	J4	4.3	3.2	2.3	3.22	2.84	25.7	214.1	-15.21	1.1	-25.92
5/4	J5	3.4	2.5	1.5	2.90	4.39	29.9	249.5	-14.63	0.5	-25.26
5/4	T	1.7	14.2	4.0	5.48	2.13	10.2	85.2	-19.60	3.5	-25.28
5/29	J1	4.7	1.8	2.9	3.24	2.35	30.0	250.2	-13.29	0.3	-26.65
5/29	J2	4.8	2.3	2.5	4.09	2.36	32.0	266.7	-14.61	0.5	-26.80
5/29	J3	5.1	1.9	2.0	7.58	7.48	28.5	237.2	-13.80	0.6	-26.83
5/29	J4	4.9	2.0	2.6	3.81	2.59	29.5	245.7	-14.17	0.5	-26.59
5/29	J5	3.8	1.9	1.9	3.53	4.23	30.7	255.8	-14.51	0.4	-26.52
5/28	T	1.3	18.4	2.8	5.78	2.54	12.5	104.3	-18.88	4.8	-25.44

Table 5-1 Cont. Chemical analysis of the samples and field parameters

Q (l/min)	DO (mg/l)	pH	Temp. (°C)	Cond. (uS/cm)	N2 (uM)	O_2 (uM)	N_2 (mg/l)	O_2 (mg/l)	N_2 Sat. (%)	O_2 Sat. (%)
14.510	8.4	7.28	13.6	262.7	-	-	-	-	-	-
8.579	7.48	7.5	12.4	263.5	-	-	-	-	-	-
1.352	8.78	7.59	11.8	264	592.4	220.6	16.5885	7.0599	99.4	68.3
1.410	8.42	7.58	12.6	263.8	-	-	-	-	-	-
9.981	7.41	7.41	12.2	283.2	-	-	-	-	-	-
0.041	-	-	-	-	-	-	-	-	-	-
0.041	-	-	-	-	-	-	-	-	-	-
50.352	7.87	6.86	14.8	138.8	591.5	211.6	16.5621	6.7697	105.5	70.0
13.964	5.86	6.91	13.4	171.3	608.6	148.0	17.0417	4.7355	104.3	46.9
2.841	7.86	7.21	14.3	152.6	592.8	252.4	16.5981	8.0759	103.7	81.7
4.480	6.95	6.95	14.3	145.3	594.5	189.6	16.6457	6.0657	104.0	61.4
19.495	7.15	7.09	12.9	212	594.9	175.4	16.6581	5.6114	101.9	55.5
0.940	8.58	6.48	14.1	94.4	597.0	236.6	16.7151	7.5728	104.4	76.6
49.675	8.39	7.25	14.0	203.1	588.1	235.0	16.4675	7.5215	102.8	76.1
10.888	6.33	7.02	13.3	204.7	596.6	174.6	16.7060	5.5875	102.2	55.3
2.652	7.6	7.49	13.3	233.2	590.2	173.7	16.5247	5.5586	101.1	55.0
4.021	7.87	7.11	13.0	189.3	586.9	209.7	16.4319	6.7094	100.6	66.4
17.822	7.8	7.14	13.1	238.1	584.5	198.0	16.3652	6.3369	100.1	62.7
0.524	9.14	6.76	13.6	117.8	583.9	239.9	16.3490	7.6754	102.1	77.7
49.622	8.84	7.31	14.6	225.9	559.7	236.1	78.1481	7.5551	99.8	78.1
9.714	5.76	6.95	14.7	219.3	567.1	159.6	15.8791	5.1074	101.2	52.8
1.235	8.17	7.31	15.4	162.8	575.6	169.9	16.1167	5.4357	102.7	56.2
3.036	7.1	7.3	15.6	197.3	547.6	206.7	15.3330	6.6158	99.6	69.9
16.841	7.32	7.23	14.0	210.8	574.2	202.7	16.0764	6.4864	100.4	65.6
0.139	7.98	6.77	18.2	134.2	540.1	256.7	15.1225	8.2151	102.1	90.6

DIC, DOC concentration and $\delta^{13}C$

DIC varied from 7.2 to 35.5 mg C/l (Table 5-1), with an average of 25.5 mg C/l. The average concentration in the trench samples was 28.6 mg C/l and in the spring samples 10.1 mg C/l. Isotope analyses showed the DIC $\delta^{13}C$ values between around -13 and -21‰. The springs averaged at about -15‰ while the trench average was lower (-19‰). DOC concentration varied between 0.3 and 4.8 mg C/l. The springs averaged 0.8 mg C/l, which is typical for groundwater,

while the trench average was higher, at 3.9 mg C/l, possibly as a result of being situated closer to the organics-rich soil zone than the former. DOC $\delta^{13}C$ values were within a relatively narrow range of about -25 to -27‰. This is an expected range which accurately pinpoints the origin of this DOC in the local vegetation dominated by C-3 plants.

Dissolved N_2 and O_2

Dissolved N_2 concentration ranged from 15.1 to 17.2 mg/L (Table 5-1). The concentration data varied in both time and space. Spatially, on average, the highest concentration was in J2 (103 mg/L) while the lowest was in J5 samples (100.8 mg/L). Temporally, samples collected on April 28 tended to have the highest concentration (104.2 mg/L) while the lowest concentration was found in the only sample of April 15 (99.4 mg/L). N_2 saturation levels calculated from N_2:Ar ratios and Ar concentrations ranged from 99.4 to 105.6%, with an average of 102.2%. All but three samples were supersaturated with respect to N_2, i.e., their N_2 content exceeded the equilibrium-with-air concentration or 100% saturation. Dissolved oxygen concentration (DO) was between 4.9 and 8.2 mg/L and averaged 6.5 mg/L. On average, the highest DO concentration was in the trench (7.9 mg/L), the lowest in J2 (5.1 mg/L). Temporally, the variation in DO was small, with the highest value at 7.1 mg/L on 4/15 (only one sample from J3) and the lowest average at 6.2 mg/L on 4/28. Calculated O_2 saturation ranged between 46.9 and 90.5% and averaged 65.9%. The trends of temporal and spatial averages were similar to those for DO concentration.

DISCUSSION

Denitrification is a biological reduction of NO_3^- to nitrogen oxides, principally N_2 and N_2O, which in most cases is mediated by widely common soil bacterium Thiobacilus

denitrificans. Denitrification generally requires anoxic conditions and an accessible organic substrate serving as an electron donor, represented in the following as generic DOC:

$$NO_3^- + 5/4CH_2O \rightarrow 1/2N_2 + 5/4\ HCO^{3-} + 1/4H + 1/2H_2O$$

The reaction manifests itself by changes in the geochemistry of the studied environment. These changes include decrease in NO_3^-, increase in DIC as well as isotopic effects imparted on the respective chemical species: enrichment of the residual NO_3^- fraction in ^{15}N and ^{18}O and progressive depletion of the product DIC in ^{13}C (Groffman and others, 2006). In addition, denitrification produces several N gaseous species including the major denitrification end product N_2 (Kendall and McDonnell, 1998). Detection of N_2 is a direct measure of net denitrification (difference between gross denitrification and gross N fixation) with interferences in closed systems limited only to biological N fixation (Groffman and others, 2006). The following discussion focuses on these geochemical indicators and trends inherent to the denitrification process as discernable in the obtained dataset.

Nitrate concentration and $\delta^{15}N$ and $\delta^{18}O$

The NO_3^- concentration data show a pattern of decrease in concentration between the trench and the springs (Table 5-1). The concentration of the former was on average two times higher than of the latter. The processes that in subsurface situations can cause decreases in NO_3^- concentration are dilution and denitrification (Clark and Fritz, 1997). Dilution did not appear to be the cause since chloride concentration between these two points of the flowpath did not decrease. Consequently, the likely process responsible for the NO_3^- depletion was denitrification.

Denitrification, as noted above, causes an isotopic enrichment in both ^{15}N and ^{18}O of the remnant NO_3^-, with the ^{15}N enrichment approximately twice that of ^{18}O (Mariotti, Landreau, and

Simon, 1988; Bottcher and others, 1990). This phenomenon shows on a $\delta^{15}N$ vs. $\delta^{18}O$ plot as a line with a positive slope of 0.5. While all of the samples analyzed together do not produce such trend, the trench samples $\delta^{15}N$ and $\delta^{18}O$ exhibit a strong positive correlation with a slope of 0.6 ($r^2 = 0.8779$; $p = 0.0630$) (Figure 5-2). In spite of the relatively high p-value resulting from the small sample size, it is considered to be a valid indication of denitrification in the upper compartment of the epikarst drained by the trench. Further down the flowpath, the spring samples do not show any definite $\delta^{15}N$-$\delta^{18}O$ relationship ($r^2 = 0.019629$; $p = 0.5673$). Denitrification could occur on the flow path to the springs as well, but the remnant NO_3^- could mix with NO_3^- from extraneous sources (e.g. decomposition of organic matter) concealing the isotopic signature of denitrification.

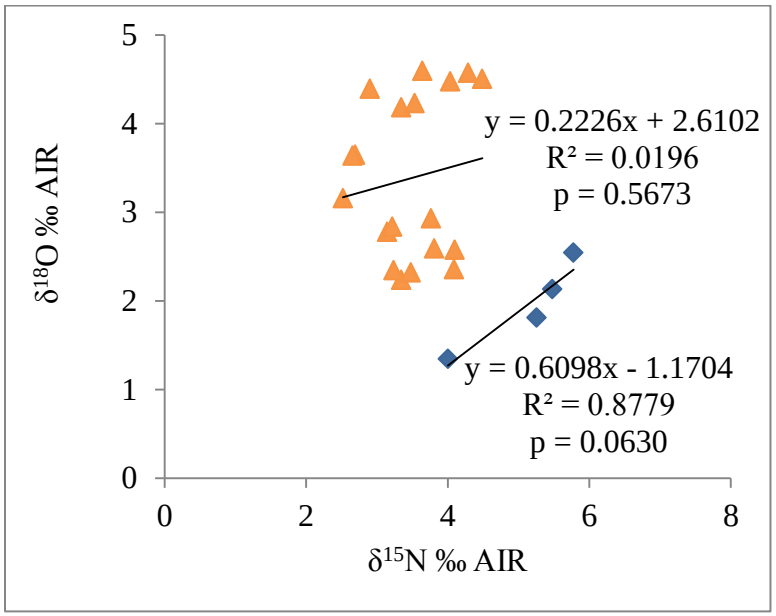

Figure 5-2 Isotopic composition of nitrate in trench samples (squares) and spring samples (triangles)

DIC concentration and $\delta^{13}C$

The denitrification reaction is also known to increase DIC concentration (Aravena and Robertson, 1998) as well as to impart ^{13}C depletion to the DIC through the addition of ^{13}C-depleted organic carbon participating in the reaction (Fritz and others, 1976). Among the analyzed samples, the spring samples indeed had significantly higher DIC compared to the trench samples, with the average concentration in the springs about 3 times higher than in the trench. This DIC, however, was not depleted in ^{13}C relative to the trench values. A likely reason for that is addition of DIC via carbonate dissolution along the flowpath. If the only DIC source was denitrification, DIC in the samples would have a $\delta^{13}C$ in the range of its source organic matter (Aravena and Robertson, 1998). In this case, the $\delta^{13}C$ of DOM of all samples ranged 25-27‰. However, if the aquifer is a carbonate aquifer, dissolution of carbonate minerals ($\delta^{13}C$ ~ 0‰) will buffer the input of the depleted ^{13}C generated by denitrification. Mixing equal amounts of organic ($\delta^{13}C$ = -26‰) and inorganic ($\delta^{13}C$ = 0‰) carbon would generate DIC with a $\delta^{13}C$ value of -13‰. A calculation using a binary mixing equation shows that DIC with the same $\delta^{13}C$ value as the average for the springs (-15‰) would be produced by mixing of about 42% of inorganic and 58% of organic carbon. Thus, denitrification may have been occurring along the trench-to-spring flowpaths and is responsible for the NO_3^- depletion observed at the springs, but the expected DIC $\delta^{13}C$ response was masked by DIC from calcite dissolution.

Applying the same approach as with NO_3^- isotopes and separately analyzing for trends in the spring samples and trends in the trench samples shows a positive relation between DIC and $\delta^{13}C$ in the trench samples (r^2 = 0.583848; p = 0.2359) (Figure 5-3). As in the case of the $\delta^{15}N$ and $\delta^{18}O$ relationship, a major factor responsible for the high p-value of this relationship is the limited number of trench samples and as such, the correlation is viewed as a valid indication that denitrification may be occurring in the upper epikarst compartment drained by the trench (Figure

5-3). This is consistent with the NO_3^- $\delta^{15}N$ and $NO_3^-\delta^{18}O$ data which also indicated denitrification in the trench samples. On the other hand, the spring samples exhibited a positive trend for DIC vs. $\delta^{13}C$, which does not support an interpretation of denitrification; however, as shown by the above mixing calculation, mixing in the epikarst may have occurred and could be masking the effect of denitrification on the DIC and $\delta^{13}C$ composition of the samples.

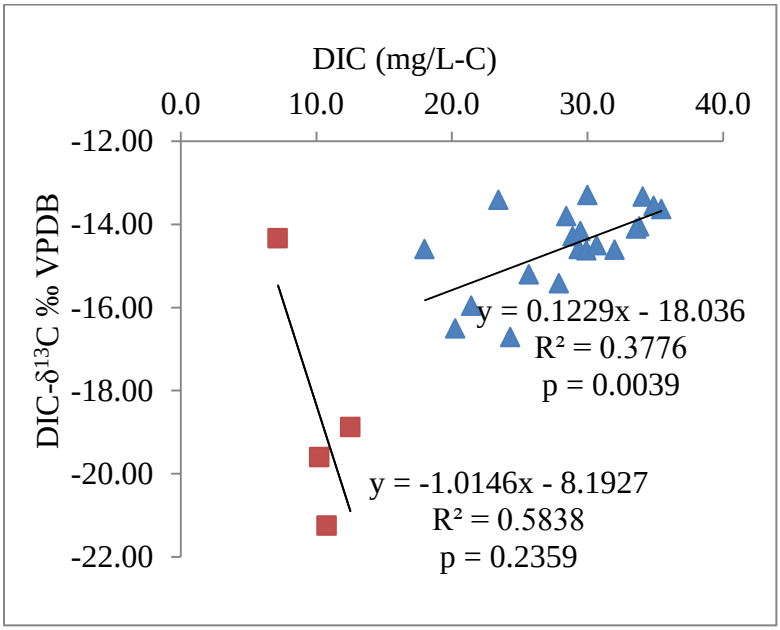

Figure 5-3 Relationship between DIC concentration and del13C in trench samples (squares) and spring samples (triangles)

Dissolved N_2 and O_2

The most significant observation that can be made from the data is that 18 out of the total of 21 analyzed samples were supersaturated with respect to N_2. This supersaturation is most probably the footprint of denitrification because virtually no other process apart from denitrification that could feasibly occur in the system would cause dissolved N_2 to increase

beyond saturation levels. The only other possible process would be the incorporation of excess air, i.e., the dissolution of air bubbles entrapped in capillary-sized pore spaces by downward migrating waters. This mechanism, however, is only feasible at sufficient depth and hydrostatic pressure below the water table, with about 10 m depth required for complete dissolution of the air bubbles (Heaton and Vogel, 1981). The thin (generally <2 m) and transiently saturated epikarst does not offer conditions for the occurrence of this process. Denitrification as the cause of N_2 supersaturation is corroborated by multiple lines of evidence already presented – NO_3^- and DIC concentrations as well as the corresponding isotopic data. Hence, denitrification is the most plausible cause of N_2 supersaturation.

Very little in the way of denitrification research measuring N_2 supersaturation in the epikarst or in groundwater systems in general has been conducted, making comparison of these data with other example studies difficult; however, studies conducted in deep sea waters that determined N_2 supersaturation linked to denitrification tend to report values in the range between 101% and 108% (Rönner and Sörensson, 1985; Quinones-Rivera and others, 2007), which is similar to the obtained values.

Most denitrifiers are facultative anaerobes and, consequently, denitrification requires anoxic or very low oxygen conditions – generally below 0.2 mg/L (Tiedje, 1988). The measured O_2 concentration, however, was in the range of 4.7-8.2 mg/L and therefore, any denitrification activity in the epikarst would have to be restricted to anoxic mircroenvironments such as those described by Sexstone and others (1985) or Koba and others (1997). Such microsites could exist in the studied epikarst, indeed; pockets of grayish colors indicative of reducing conditions were observed in abundance throughout the epikarst profile during excavation works at the site.

Concentration of O_2 within these microsites would probably be affected by O_2 concentration in the surrounding matrix; the lower the latter, the lower the former. As a result, granted that all other requirements for denitrification are met, one could expect to see that the less O_2 is in the system as a whole, the more denitrification will occur in these micro sites. This phenomenon would then manifest itself as a negative correlation between the measured N_2 and O_2 saturation levels. While such correlation is found to be only negligible for the entire dataset, correlation is relatively strong when the highest O_2 saturation sites – the trench and J1 site – are excluded from the analysis ($r^2 = 0.600802$; $p = 0.0007$) (Figure 5-4). The exclusion seems justified since the relatively high O_2 content of waters from these two sites could well be due to the distinct physical hydrologic character of these flowpaths as opposed to being a reflection of some intrinsic biogeochemical process affecting the O_2 content in the epikarst (e.g., aerobic or anaerobic respiration consuming O_2 along the other flowpaths). This is especially true for the trench waters which could be oxygenated in the final, pipe segment of the installed collector (French drain) of this flowpath. The J1 flowpath, as suggested by discharge and specific conductance (this study data) as well as DOC bioavailability (Winston, 2006), is dominated by focused flow, a more turbulent type of flow characterized by increased potential for aeration and oxygenation. Thus, a combined analysis of N_2 and O_2 data indicates denitrification occurring along the J2-J5 flowpaths of the epikarst. Dissolved O_2, or lack thereof, appears to play a role in enabling this denitrification.

The effect of O_2 saturation on denitrification suggested by the data invites the question as to exactly what mechanism could enable the further drawdown of O_2 concentration, creating anaerobic conditions within the microsites. While, in general, dissolved O_2 is consumed by aerobic or anaerobic microbial activity and geochemical reactions, the key mechanism enabling

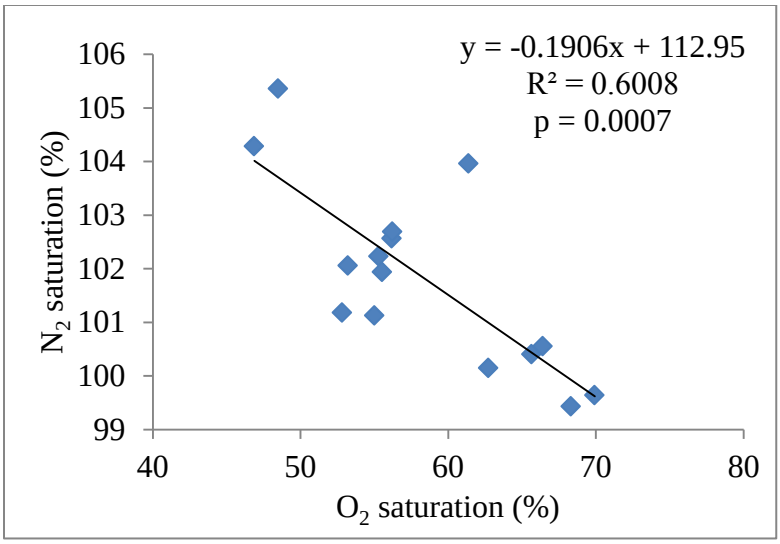

Figure 5-4 Relationship between dissolved oxygen and nitrogen saturation in J2-J5 spring samples (Samples from J1 and trench are excluded)

the development of anoxic conditions in the microsites could be the blocking of access of O_2 by waterlogging. The phenomenon of waterlogging causing an increase in denitrification and consequently loss of soil nitrogen by restricting oxygen diffusion to the soil is widely known among agronomists and soil scientists. Under certain conditions, even a small percentage increase in soil saturation can initiate denitrification by sealing off a sufficient soil volume from diffusion of atmospheric O_2 (Craswell, 1978). Similarly, according to Sylvia and others (1999), rates of denitrification are generally greatest in wet soils where more than 80% of pore space is saturated and respiratory activity is reasonably high. The data in this study provide some evidence for the occurrence of this mechanism in the epikarst. Assuming the average discharge for a sampling event to be a measure of epikarst saturation, the highest epikarst saturation event (4/28) had the lowest average O_2 saturation (and the highest average N_2 saturation), the lowest epikarst saturation event (4/15) had the highest O_2 saturation (and the lowest N_2 saturation), and the two intermediate epikarst saturation events had proportionally inverse intermediate O_2

saturation (and intermediate N_2 saturation) (Figure 5-5). When the analysis is conducted for the sites individually instead of averaging the sites for each event, the trend of increasing discharge with decreasing O_2 saturation is present in all of the sites except for trench. This inconsistency could be again caused by aeration effects of the collector elevating the O_2 content of trench waters, particularly at higher discharge rates. The evidence overall thus indicates that physical hydrology of the epikarst has control on its geochemistry, specifically, O_2 concentration and subsequently denitrification. The analysis, however, relies on only four events and uses discharge to assess water saturation. The trend therefore should be confirmed with an analysis involving more measurements and perhaps some more direct method of measuring water saturation (e.g., the electrical resistivity method).

DOC

One of the reactants of denitrification is organic carbon which the microbes use as an electron donor. Denitrifying activity has been found to be related to organic carbon contents in a wide range of environments, including sediments (Van Kessel, 1978), soils (Bremner and Shaw, 1958; Burford and Bremner, 1975), riparian zones (Vidon and Hill, 2005), shallow aquifers (Starr and Gillham, 1993) as well as oxic surface waters and pore waters (Sobczak and Findlay, 2002). The data from this study suggest this to also be the case in the epikarst; for the spring samples, N_2 saturation, which can be taken as a proxy measure of denitrification, was positively correlated with DOC concentration ($r^2 = 0.686494$; $p < 0.0001$) (Figure 5-6). This correlation does not hold when the trench samples are included in the analysis due to their abnormally high DOC levels, on average about 5 times higher than those in the springs. These are suspected to be caused by contamination of C compounds leaching from surface-derived organic detritus accumulated in the French drain gravel pack and pipe. The trench samples, therefore, were

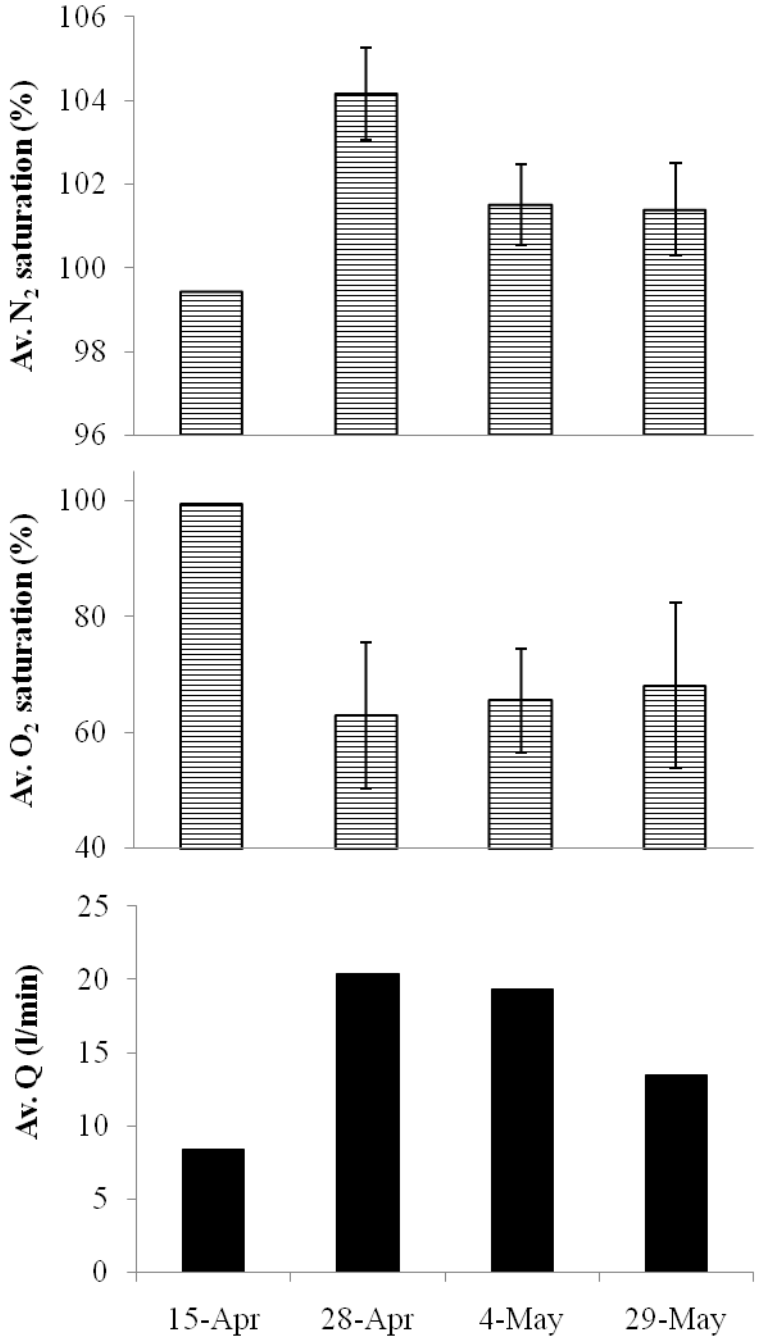

Figure 5-5 Average discharge, O_2 saturation, and N_2 saturation for four sampling events (error bars represent mean +/- 1 SD)

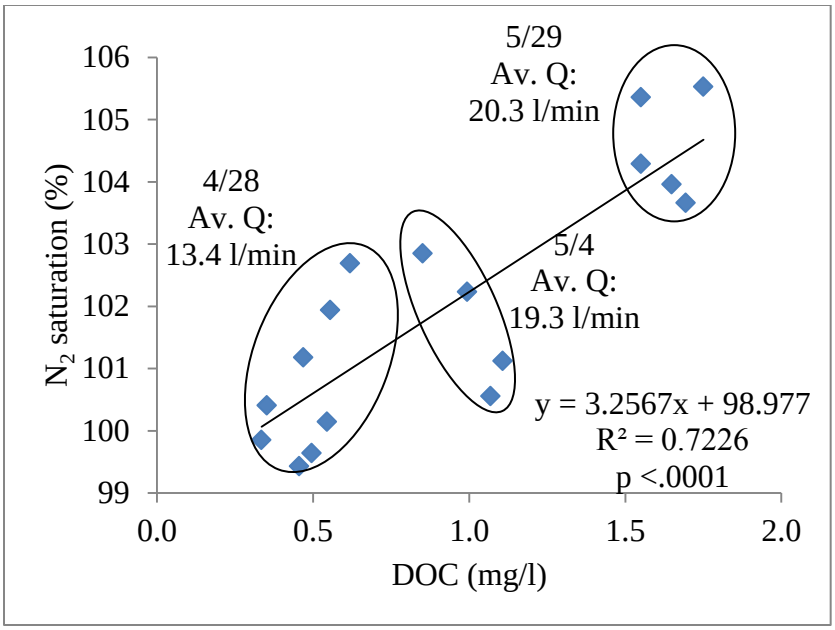

Figure 5-6 Relationship between DOC concentration and N_2 saturation of spring samples (trench samples are excluded). Circles enclose datapoint clusters corresponding with sampling dates with varying hydrologic conditions (saturation) as indicated by average discharge (Av. Q).

excluded. In addition, the utilization of DOC by denitrifiers also depends on quality or bioavailability of this DOC. While this parameter was not assessed, the positive relation between DOC and N_2 saturation suggests that this DOC was sufficiently labile for denitrifiers.

The relation thus indicates that carbon availability has a limiting effect on denitrification in the epikarst, and two reasons may explain why this perhaps should be the case in the epikarst even more than in other environments: Firstly, in general, in environments that are not completely anaerobic such as the epikarst, denitrifiers have to compete for carbon with obligately aerobic heterotrophs which in these environments make up the bulk of the microbial biomass (Sylvia and others, 1999). Secondly, organic carbon in the system is already a limited resource due to the fact that karst groundwater systems do not have significant autotrophic sources of organic C (Susan Ziegler, personal comm.)

The correlation also shows data points clustered according to event date, with the higher discharge events having higher N_2 saturation and DOC concentration (Figure 5-6). This indicates that hydrology (epikarst saturation) not only impacts O_2 concentrations and subsequently denitrification in the epikarst as noted before, but epikarst saturation also seems to exert control on denitrification by controlling DOC availability. Higher discharge events likely mobilize and deliver more DOC than lower discharge events. The greater supply of DOC then likely translates into a greater denitrification potential during storm events. This dynamic makes the epikarst different from surface systems where storm flow events are typically thought of as events where more refractory C is delivered (Susan Ziegler, personal comm.). The lack of significant autotrophic sources of C means that the epikarst system depends upon the pulse of C from storm events.

CONCLUSIONS

This study examined the geochemistry of the epikarst waters for evidence of denitrification.

The occurrence of denitrification along the flowpaths between the trench and the epikarst springs was indicated by the general trend of NO_3^- depletion, which in the absence of dilution could only be caused by denitrification. Additional geochemical indicators, including relations between nitrate $\delta^{15}N$ and $\delta^{18}O$ as well as DIC concentration and DIC $\delta^{13}C$, did not corroborate this evidence, although it is possible that the positive signature of denitrification had been masked – in the case of NO_3^- isotopic composition by mixing in of extraneous NO_3^- and in the case of DIC $\delta^{13}C$ by dissolution of calcite.

Denitrification was also detected in the epikarst upgradient from the trench. The evidence includes the trend of simultaneous enrichment in nitrate ^{15}N and ^{18}O and another trend of

increasing depletion in ^{13}C of DIC as DIC concentration in the trench samples increased. The trench waters also had higher concentration of DOC relative to the epikarst springs, being closer to the soil zone DOC source, which would give the former a greater potential for denitrification.

The most significant finding of this study is the dissolved N_2 supersaturation detected in all except for three samples, strongly signaling denitrification in the epikarst. Negative correlation between N_2 and O_2 saturation suggested that the magnitude of denitrification is controlled by oxygenation levels of the epikarst waters. Oxygen concentration, in turn, seemed to have been affected by the wetness or saturation level of the epikarst as suggested by negative correlation between discharge and O_2 saturation. Thus, as is the case in soils, hydrology (waterlogging) appears to be an important control on denitrification in the epikarst.

Further, N_2 saturation was positively correlated with DOC concentration indicating a limiting role of carbon in denitrification in this system. Such a situation would be expected given the lack of autotrophic sources in karst and the dominant presence of obligately aerobic heterotrophs which compete with denitrifiers for carbon. As with the O_2 content, hydrologic conditions also appear to affect DOC: higher discharge events tended to have higher DOC concentrations. The greater storm pulses likely are able to mobilize and deliver more C which then drives denitrification activity.

Thus, the measured geochemical parameters altogether indicate denitrification occurring in this epikarst system. While the experimental approach did not allow for quantitative evaluation of denitrification or its controlling variables, it managed to identify their occurrence which is a valuable contribution to understanding the biogeochemical functioning of the epikarst. These findings also reaffirm the concept that within karst systems with their limited soil development and lack of bioremediation capacity, the epikarst is a potentially important zone of attenuation of

leaching nitrate. They can serve as a foundation for future, more quantitative investigations of these phenomena in the epikarst including their response to specific nutrient management practices to ultimately optimize these to reflect the ecological limitations of vulnerable karst landscapes.

REFERENCES

Adamski, J., 1997, Nutrients and Pesticides in Ground Water of the Ozark Plateaus in Arkansas, Kansas, Missouri, and Oklahoma: 96-4313

Aquilina, L., Ladouche, B., and Dörfliger, N., 2006, Water storage and transfer in the epikarst of karstic systems during high flow periods: Journal of Hydrology, v. 327, no. 3-4, p. 472-485.

Aravena, R., and Robertson, W.D., 1998, Use of Multiple Isotope Tracers to Evaluate Denitrification in Ground Water: Study of Nitrate from a Large-Flux Septic System Plume: Ground Water, v. 36, no. 6, p. 975-982.

Bakalowicz, M., 1995, La zone d'infiltration des aquifères karstiques. Méthodes d'étude: Structure et fonctionnement.Hydrogéologie, v. 4, p. 3-21.

Bottcher, J., Strebel, O., Voerkelius, S., and Schmidt, H.L., 1990, Using isotope fractionation of nitrate-nitrogen and nitrate-oxygen for evaluation of microbial denitrification in a sandy aquifer: Journal of Hydrology, v. 114, no. 3-4, p. 413-424.

Boyer, D.G., and Pasquarell, G.C., 1996, Agricultural land use effects on nitrate concentrations in a mature karst aquifer: Journal of the American Water Resources Association, v. 32, no. 3, p. 565-573.

Bremner, J., and Shaw, K., 1958, Denitrification in soil. II. Factors affecting denitrification: The Journal of Agricultural Science, v. 51, no. 01, p. 40-52.

Burford, J., and Bremner, J., 1975, Relationships between the denitrification capacities of soils and total, water-soluble and readily decomposable soil organic matter: Soil Biology and Biochemistry, v. 7, no. 6, p. 389-394.

Casciotti, K.L., Sigman, D.M., Hastings, G.M., Bohlke, J.K., and Hilkert, A., 2002, Measurement of the Oxygen Isotopic Composition of Nitrate in Seawater and Freshwater Using the Denitrifier Method: Analytical Chemistry, v. 74, no. 19, p. 4905-4912.

Clark, I.D., and Fritz, P., 1997, Environmental Isotopes in Hydrogeology: Boca Raton, Florida, CRC Press LLC, 328 p.

Craswell, E., 1978, Some factors influencing denitrification and nitrogen immobilization in a clay soil: Soil Biology and Biochemistry, v. 10, no. 3, p. 241-245.

Davis, R.K., Brahana, J.V., and Johnston, J.S., 2000, Groundwater in Northwest Arkansas: Minimizing Nutrient Contamination From Non-Point Sources in Karst Terrane. MSC-288, 69 p.

Einsiedl, F., 2005, Flow system dynamics and water storage of a fissured-porous karst aquifer characterized by artificial and environmental tracers: Journal of Hydrology, v. 312, no. 1, p. 312-321.

Ernenwein, E.G., and Kvamme, K.L., 2004, Geophysical Investigations For Subsurface Fracture Detection In The Savoy Experimental Watershed, Arkansas: Unpublished report, Department of Biological and Agricultural Engineering, University of Arkansas, 24 p.

Eyre, B.D., Rysgaard, S., Dalsgaard, T., and Christensen, P.B., 2002, Comparison of isotope pairing and N_2:Ar methods for measuring sediment denitrification—Assumption, modifications, and implications: Estuaries, v. 25, no. 6, p. 1077-1087.

Fan, A.M., and Steinberg, V.E., 1996, Health Implications of Nitrate and Nitrite in Drinking Water: An Update on Methemoglobinemia Occurrence and Reproductive and Developmental Toxicity: Regulatory Toxicology and Pharmacology, v. 23, no. 1, p. 35-43.

Ford, D.C., and Williams, P.W., 2007, Karst hydrogeology and geomorphology: Chichester, England, John Wiley & Sons, 576 p.

Fritz, P., Cherry, J.A., Weyer, K.V., and Sklash, M.G., 1976, Storm runoff analysis using environmental isotopes and major ions, *in* Interpretation of Environmental Isotopes and Hydrochemical Data in Groundwater Hydrology. Panel Proceedings Series - International Atomic Energy Agency 108: Vienna, IAEA, p. 111-130.

Goolsby, D.A., and Battaglin, W.A., 2001, Long-term changes in concentrations and flux of nitrogen in the Mississippi River Basin, USA: Hydrological Processes, v. 15, no. 7, p. 1209-1226.

Green, M.B., Wollheim, W.M., Basu, N.B., Gettel, G., Rao, P.S., Morse, N., and Stewart, R., 2009, Effective denitrification scales predictably with water residence time across diverse systems: Nature Precedings, accessed June 15, 2013, *http://precedings.nature.com/documents/3520/version/1/html*.

Groffman, P.M., Alatabet, M.A., Bohlke, J.K., Butterbach-Bahl, K., David, M.B., Firestone, M.K., Giblin, A.E., Kana, T.M., Nielsen, L.P., and Voytek, M.A., 2006, Methods For Measuring Denitrification: Diverse Approaches To a Difficult Problem: Ecological Applications, v. 16, no. 6, p. 2091-2122.

Heaton, T.H.E., and Vogel, J.C., 1981, "Excess air" in groundwater: Journal of Hydrology, v. 50, p. 201-216.

Kana, T.M., Darkangelo, C., Hunt, M.D., Oldham, J.B., Bennett, G.E., and Cornwell, J.C., 1994, Membrane inlet mass spectrometer for rapid high-precision determination of N2, O2, and Ar in environmental water samples: Analytical Chemistry, v. 66, no. 23, p. 4166-4170.

Kendall, C., and McDonnell, J.J., 1998, Isotope Tracers in Catchment Hydrology: Amsterdam, Elsevier Science B.V., 839 p.

Klimchouk, A., 2004, Towards defining, delimiting and classifying epikarst: Its origin, processes and variants of geomorphic evolution: Speleogenesis and Evolution of Karst Aquifers, v. 2, no. 1, p. 1-13,

Koba, K., Tokuchi, N., Wada, E., Nakajima, T., and Iwatsubo, G., 1997, Intermittent denitrification: The application of a 15N natural abundance method to a forested ecosystem: Geochimica et Cosmochimica Acta, v. 61, no. 23, p. 5043-5050.

Laincz, J., 2007, Qualitative dye tracer test at the Savoy Experimental Watershed plot:

Laubhan, A.C., 2007, A hydrogeologic and water-quality evaluation of the Springfield aquifer in the vicinity of North-Central Washington County, Arkansas: Fayetteville, University of Arkansas, M.S. Thesis, 182 p.

Lee, E.S., and Krothe, N.C., 2001, A four-component mixing model for water in a karst terrain in south-central Indiana, USA. Using solute concentration and stable isotopes as tracers: Chemical Geology, v. 179, no. 1, p. 129-143.

Mariotti, A., Landreau, A., and Simon, B., 1988, N-15 isotope biogeochemistry and natural denitrificatiion process in groundwater: Application to the chalk aquifer in Northern France: Geochimica et Cosmochimica Acta, v. 52, p. 1869-1878.

Panno, S.V., Hackley, K.C., Hwang, H.H., and Kelly, W.R., 2001, Determination of the sources of nitrate contamination in karst springs using isotopic and chemical indicators: Chemical Geology, v. 179, no. 1-4, p. 113-128.

Perrin, J., Jeannin, P., and Zwahlen, F., 2003, Epikarst storage in a karst aquifer: a conceptual model based on isotopic data, Milandre test site, Switzerland: Journal of Hydrology, v. 279, no. 1, p. 106-124.

Power, J., and Schepers, J., 1989, Nitrate contamination of groundwater in North America: Agriculture, Ecosystems & Environment, v. 26, no. 3, p. 165-187.

Quinones-Rivera, Z.J., Wissel, B., Justic, D., and Fry, B., 2007, Partitioning oxygen sources and sinks in a stratified, eutrophic coastal ecosystem using stable oxygen isotopes: Marine Ecology Progress Series, v. 342, p. 69-83.

Rabalais, N.N., Turner, R.E., Justic, D., Dortch, Q., Wiseman, W.J., and Sen Gupta, B.K., 1996, Nutrient changes in the Mississippi River and System Responses on the Adjacent Continental Shelf: Estuaries and Coasts, v. 19, no. 2, p. 386-407.

Rönner, U., and Sörensson, F., 1985, Denitrification rates in the low-oxygen waters of the stratified Baltic proper: Applied and Environmental Microbiology, v. 50, no. 4, p. 801-806.

Sauer, T., Alexander, R., Brahana, J., and Smith, R., 2008, . The Importance and Role of Watersheds in the Transport of Nitrogen: Nitrogen in the Environment, p. 203.

Sauer, T.J., and Logsdon, S.D., 2002, Hydraulic and Physical Properties of Stony Soils in a Small Watershed: Soil Science Society of America Journal, v. 66, no. 6, p. 1947-1956.

Seitzinger, S., Harrison, J.A., Bohlke, J.K., Bouwman, A.F., Lowrance, R., Peterson, B., Tobias, C., and Van Drecht, G., 2006, Denitrification across landscapes and waterscapes: a synthesis. Ecological Applications, v. 16, no. 6, p. 2064-2090.

Sexstone, A.J., Revsbech, N.P., Parkin, T.B., and Tiedje, J.M., 1985, Direct Measurement of Oxygen Profiles and Denitrification Rates in Soil Aggregates: Soil Science Society of America Journal, v. 49, no. 3, p. 645.

Sigman, D.M., Casciotti, K.L., Andreani, M., Barford, C., Galanter, M., and Bohlke, J.K., 2001, A Bacterial Method for the Nitrogen Isotopic Analysis of Nitrate in Seawater and Freshwater: Analytical Chemistry, v. 73, p. 4145-4153.

Sinreich, M., and Flynn, R., 2011, Comparative tracing experiments to investigate epikarst structural and compositional heterogeneity: Speleogenesis and Evolution of Karst Aquifers, no. 10, p. 253-258,

Smettem, K.R.J., Chittleborough, D.J., Richards, B.G., and Leaney, F.W., 1991, The influence of macropores on runoff generation from a hillslope soil with a contrasting textural class: Journal of Hydrology, v. 122, no. 1-4, p. 235-252.

Sobczak, W.V., and Findlay, S., 2002, Variation in bioavailability of dissolved organic carbon among stream hyporheic flowpaths: Ecology, v. 83, no. 11, p. 3194-3209.

Starr, R.C., and Gillham, R.W., 1993, Denitrification and Organic Carbon Availability in Two Aquifers: Ground Water, v. 31, no. 6, p. 934-947.

Steele, K.F., and McCalister, W.K., 1990, Nitrate concentrations of ground water from limestone and dolomitic aquifers in the Northeastern Washington County area, Arkansas: MSC-68

St-Jean, G., 2003, Automated quantitative and isotopic (^{13}C) analysis of dissolved inorganic carbon and dissolved organic carbon in continuous-flow using a total organic carbon analyser: Rapid Communications in Mass Spectrometry, v. 17, no. 5, p. 419-428.

Sylvia, D.M., Fuhrmann, J.J., Hartel, P.G., and Zuberer, D.A., 1999, Principles and Applications of Soil Microbiology: Upper Saddle River, New Jersey, Prentice Hall, 550 p.

Tenovuo, J., 1986, The biochemistry of nitrates, nitrites, nitrosamines and other potential carcinogens in human saliva: Journal of oral pathology, v. 15, no. 6, p. 303-307.

Tiedje, J.M., 1988, Ecology of denitrification and dissimilatory nitrate reduction to ammonium: Biology of anaerobic microorganisms, v. 717, p. 179-244.

Van Kessel, J., 1978, Gas production in aquatic sediments in the presence and absence of nitrate: Water research, v. 12, no. 5, p. 291-297.

Veni, G., DuChene, H., Crawford, N.C., Groves, C.G., Huppert, G.H., Kastning, E.H., Olson, R., and Wheeler, B.J., 2001, Living with Karst: A Fragile Foundation (Environmental Awareness Series ed.), American Geological Institute, 64 p.

Vidon, P., and Hill, A.R., 2005, Denitrification and patterns of electron donors and acceptors in eight riparian zones with contrasting hydrogeology: Biogeochemistry, v. 71, no. 2, p. 259-283.

Weiss, R., 1970, The solubility of nitrogen, oxygen and argon in water and seawater: Deep Sea Research and Oceanographic Abstracts, v. 17, no. 4, p. 721-735.

Winston, B.A., 2006, The biogeochemical cycling of nitrogen in a mantled karst watershed: Fayetteville, University of Arkansas, M.S. Thesis, p.88

6. CONCLUSIONS

This dissertation investigated the biogeochemical processes and hydrologic properties affecting NO_3^- transport in the epikarst.

The initial biogeochemical study provided evidence for NO_3^- processing in the studied karst system and identified some factors affecting this processing, including dissolved organic carbon availability, seasonality and type of flow (diffuse or interflow vs. focused flow). Mass-balance calculations indicated that although mixing was the primary mechanism decreasing NO_3^- concentration along the epikarst (in the corresponding chapter referred to as the interflow zone) flowpaths, up to 33 percent of NO_3^- may have been removed through microbial processing. The magnitude of this processing varied spatially and temporally. Dissolved organic carbon bioavailability was elevated in the epikarst relative to the focused-flow zone while dissolved organic carbon concentration was lower in the epikarst than in the focused flow zone. This suggests that, compared to the focused-flow zone, the epikarst has a greater quality and greater utilization of carbon substrate, and consequently greater potential for denitrification.

The second geochemical study narrowed the focus of investigation to the epikarst flowpaths, corroborated the early evidence of NO_3^- processing, and identified denitrification and some of its key controls. Denitrification was indicated by an average NO_3^- decrease of 50% along the epikarst (trench-spring) flowpaths and, for the flowpaths upgradient from the trench, by simultaneous isotopic enrichment in NO_3^--^{15}N and NO_3^--^{18}O and by the trend of increasing DIC concentration with decreasing $\delta^{13}C$ of DIC detected in the trench samples. The occurrence of denitrification in the system was corroborated by dissolved N_2 measurements which showed supersaturation of up to 106% in all except for three samples. Consistent with environmental

requirements of denitrifiers, N_2 saturation negatively correlated with O_2 saturation and positively correlated with DOC concentration at the springs, with the latter suggesting a limiting role of DOC on denitrification in the epikarst. The results also suggest that hydrology (epikarst saturation) plays an important indirect role in controlling denitrification: more saturated conditions likely deliver more DOC substrate and more restrict O_2 diffusion into the epikarst helping to create anoxic environment suitable for denitrification.

The hydrologic study focused on the flow, solute transport and aquifer characteristics of the studied epikarst system. The epikarst exhibited a dynamic response to recharge events, with a nearly instantaneous discharge increase, culmination at 60 and 200 times the baseflow level on average, and return to baseflow level in 2-4 hours after rainfall cessation. Dye was positively detected at all of the sites except for one (J1). The breakthrough occurred about 60 hours after injection and was associated with a storm-induced flow pulse. Travel velocities ranged from 1.0 to 2.2 m/h. Both the dynamic hydraulic response and the velocities exceeding the hydraulic conductivity of the epikarst matrix indicated flow through preferential flowpaths. Dye recovery rate was 0.82%. Relatively low temperature indicated deeper flowpaths for J1. Event water dominated the epikarst storm discharge (45-85% of discharge) and steadily decreased to >1% after the storm. All of the measured parameters varied greatly in space indicating heterogeneity of the system. Overall, the results confirm that the epikarst is a subsystem of karst with unique hydrologic properties. From a contaminant transport standpoint, epikarst transport of a point-source solute can be relatively rapid; however transport is dependent on saturation (flow pulse). Under the normal weather pattern and as long as the solute source does not reach into the deeper, perennially saturated zone, the epikarst appears to have a good ability to contain a point-source contaminant.

In conclusion, the investigation found evidence of denitrification in the epikarst system and identified several denitrification controls. While the experimental approach did not allow for quantitative evaluation of denitrification or its controls, it succeeded in identifying their occurrence which is a valuable contribution to understanding the biogeochemical functioning of the epikarst. The study also found that, although the epikarst is a dynamic hydrologic system in which water and solutes can move rapidly, the epikarst has a good ability to retard contaminant movement under the normal weather pattern.

The findings reaffirm the concept that within karst systems characterized by limited soil development and lack of bioremediation capacity, the epikarst can be an important buffer against potential groundwater contaminants. The findings can serve as a foundation for future, more quantitative investigations of NO_3^- attenuation mechanisms and of their response to specific nutrient management practices so that these may be optimized to reflect the ecological limitations of vulnerable karst landscapes.